8-2019

The Influence Of The Pep-Pts And Other Metabolic Systems On The Master Virulence Regulator Atxa And Toxin Gene Expression In Bacillus Anthracis

Naomi Bier-Reizes

The Influence of the PEP-PTS and Other Metabolic Systems on the Master Virulence Regulator AtxA and Toxin Gene Expression in *Bacillus anthracis*

by

Naomi Bier-Reizes, B.S.

APPROVED:

_____

Theresa M. Koehler, Ph.D.
Advisory Professor

_____

Zheng (Jake) Chen, Ph.D.

_____

Nicholas DeLay, Ph.D.

_____

Heidi B. Kaplan, Ph.D.

_____

Hung Ton-That, Ph.D.

APPROVED:

_____

Dean, The University of Texas
MD Anderson Cancer Center UTHealth Graduate School of Biomedical Sciences

The Influence of the PEP-PTS and Other Metabolic Systems on the Master Virulence Regulator AtxA and Toxin Gene Expression in *Bacillus anthracis*

A

DISSERTATION

Presented to the Faculty of

The University of Texas

MD Anderson Cancer Center UTHealth

Graduate School of Biomedical Sciences

in Partial Fulfillment

of the Requirements

for the Degree of

DOCTOR OF PHILOSOPHY

by

Naomi Bier-Reizes, B.S.

Houston, Texas

Date of Graduation August 2019

Acknowledgements

I'd like to thank my advisor, Theresa M Koehler, Ph.D. for helping me develop my scientific and communication skills. Terri demonstrated patience and commitment to helping me improve my presentation skills over the years with great results.

My committee has been very helpful in making sure I progressed in my dissertation research and for that I am grateful. They have been instrumental in helping me troubleshoot techniques and critique my experimental designs.

I am grateful to my lab mates in the Koehlertarian Army for their support in both my research and my personal development. A big shout out to Malik Raynor for being a huge part of my graduate school experience. I couldn't have done it without Malik!

I could not have made it through this journey of graduate school and this dissertation research without the support of my Houston family and friends. They have been instrumental in carrying me through the toughest times and for that I am eternally grateful.

I'd like to thank my family, and WhatsApp for keeping me connected to my family, for listening to my sorrows and frustrations throughout this process. They exerted peer pressure at its greatest and I think it paid off. Thanks guys!

Saving the best for last, a special thank you to my husband Elchonon who has been my rock in finishing this journey. Finishing projects hasn't always been my strong suit, but with

Elchonon I can do anything. His patience, support, ideas, and general attitude have helped me make it through and successfully write this dissertation.

THE INFLUENCE OF THE PEP-PTS AND OTHER METABOLIC SYSTEMS ON THE MASTER VIRULENCE REGULATOR ATXA AND TOXIN GENE EXPRESSION IN *BACILLUS ANTHRACIS*

Naomi Bier-Reizes, B.S.

Advisory Professor: Theresa M. Koehler, Ph.D.

AtxA, the master virulence gene regulator in *Bacillus anthracis,* is a PRD-containing virulence regulator (PCVR) as indicated by the crystal structure, post-translational modifications, and activity of the protein. PCVRs are transcriptional regulators, named for the regulatory domains subject to phosphorylation by the phosphoenolpyruvate phosphotransferase system (PEP-PTS), termed PTS Regulatory Domains (PRD), and for their impact on virulence gene expression. Generally, the phosphorylation of a PCVR regulates protein activity and multimerization. AtxA is phosphorylated at two histidine residues - one in each of its two PRDs. Phosphorylation at position 199 allows for AtxA to positively affect expression of virulence genes, whereas phosphorylation at position 379 prevents or destabilizes dimerization, and therefore ablates activity of AtxA. Interestingly, current data from experiments employing physiological, genetic, and biochemical approaches do not support the predominant model of PCVR function in which the PTS proteins HPr and EI are responsible for phosphorylation of AtxA. Rather, we have determined that HPr and EI are required for transcription of the *atxA* gene. Assessment of *atxA* transcript levels using a transcriptional reporter assay revealed that transcript levels were 2.5-fold lower in a mutant lacking HPr and EI compared to the parent strain, and that this change is enough to affect toxin production. Mutants harboring HPr proteins altered for phosphotransfer activity were unable to restore *atxA* transcription to wild-type levels, suggesting that phosphotransfer activity of HPr and EI is important in the regulation of

atxA gene production. In a mouse model of late-stage anthrax disease the PTS double mutant ($HPr^{-}EI^{-}$) was attenuated for virulence. Virulence was restored by expressing *atxA* from an alternative, PTS-independent promoter region indicating the PTS influences virulence through control of *atxA* expression. These findings are intriguing; the proteins (HPr and EI) that were hypothesized to regulate protein (AtxA) activity are in fact involved in regulating transcription of the gene encoding AtxA. HPr is a phosphotransfer protein and is not predicted to bind DNA. Thus, we hypothesize that HPr transfers a phosphate to a downstream transcriptional regulator to influence *atxA* gene transcription. Future studies aim to identify the transcriptional regulator involved in this process.

Table of Contents

List of Figures

List of Tables

Chapter I

Introduction

1.1 Metabolism and Virulence

When scientists first started studying pathogenesis and identifying genes necessary for virulence they created a category of genes known as virulence factors that typically included genes encoding toxins, capsules, invasins, and other secreted factors. This category of virulence factors did not include genes products necessary for basic cell physiology, such as housekeeping genes involved in cell division and metabolism. With the advent of *in vivo* expression technology (IVET), signature-tagged mutagenesis (STM), and differential PCR analyses, scientists identified housekeeping genes and basic physiological processes necessary for successful colonization and/or dissemination and survival in the host (Rediers *et al.*, 2005). Regulation of physiological processes and virulence are interrelated for many pathogenic organisms and key metabolic regulators including CcpA and CodY, and metabolite import systems, such as the phosphoenolpyruvate phosphotransferase system (PTS), have been identified as important players in virulence factor production and pathogenicity in many Gram-positive organisms (Poncet *et al.*, 2009a, Stenz *et al.*, 2011).

Bacteria often find themselves in environments with multiple carbon sources. In order to conserve resources and optimize growth, bacteria have developed a mechanism for utilizing one preferred carbon source first and later metabolize secondary or less preferred carbon sources. This is accomplished through repression of the gene expression necessary for using secondary carbon sources when the preferred carbon source is available, known as carbon catabolite

repression (CCR). In Gram-positive bacteria CCR is carried out by the catabolite control protein A, CcpA, together with HPr, a general protein of the PTS (Deutscher *et al.*, 2014).

CcpA has been implicated in virulence factor production for many Gram-positive bacteria. In *Bacillus anthracis* and *Streptococcus pyogenes* CcpA positively affects expression of the master virulence regulators AtxA and Mga (Chiang *et al.*, 2011, Almengor *et al.*, 2007a). In *Streptococcus pneumoniae*, bacteria deficient in CcpA have reduced expression of the capsular polysaccharide and are attenuated for mouse nasopharyngeal and lung infection (Iyer *et al.*, 2005). In *Enterococcus faecalis and Enterococcus faecium*, CcpA positively affects expression of collagen binding factor and full virulence in animal models of infection (Somarajan *et al.*, 2014, Gao *et al.*, 2013). For some Gram-positive pathogens, CcpA plays an inhibitory role to suppress virulence factor production. For instance, in *Streptococcus gordonii* and *Streptococcus sanguis* CcpA represses H_2O_2 production in carbon rich environments, and in *Streptococcus mutans* a *ccpA* mutant produces more acid than the parent, grows better at low pH, and excretes acid more rapidly (Richardson *et al.*, 2015).

Another global regulator involved in both central metabolism and virulence is the metabolite-responsive global regulator CodY. CodY regulates primary metabolic genes in response to nutrient availability and starvation in low G+C content Gram-positive organisms. During nutrient replete conditions CodY binds activating ligands branched chain amino acids (BCAAs) and in some organisms GTP. When bound to ligands, CodY is active in binding target sequences on DNA to repress transcription of target genes. During the transition to stationary

phase when nutrients become limited and BCAA and GTP levels drop, CodY releases from DNA and repression of target genes is alleviated. Genes regulated by CodY mediate adaptation of the bacteria to nutrient limitation via a number of mechanisms including increased secretion of proteases and production of amino acid transporters, promotion of sporulation and/or biofilm formation. For a number of pathogenic bacteria CodY also regulates key virulence factors that facilitate invasion, dissemination, and survival in the host (Stenz *et al.*, 2011).

The role of CodY in virulence factor regulation and pathogenesis has been explored for a number of pathogens including *B. anthracis*, *Clostridum difficile*, *Listeria monocytogenes*, *Staphylococcus aureus*, *S. pneumoniae*, and *S. pyogenes* (Stenz *et al.*, 2011, Richardson *et al.*, 2015). CodY was found to be important in a subcutaneous model for anthrax infection. Though the mechanism has not yet been elucidated, toxin production in *B. anthracis* is abrogated in a *codY*-null mutant due to the effect of CodY on post-translational accumulation of AtxA, the regulator of toxin in *B. anthracis* (van Schaik *et al.*, 2009). In *C. difficile*, CodY represses the expression of the toxin genes responsible for the development of gastrointestinal damage and antibiotic-associated pseudomembranous colitis through the direct binding of CodY to the promoter of the toxin gene regulator *tcdR*. Binding of CodY to the promoter of *tcdR* is enhanced *in vitro* in the presence of BCAA and GTP linking nutrient deprivation with toxin expression in *C. difficile* (Dineen *et al.*, 2007). In *S. aureus* the quorum sensing *agr* system, responsible for regulating a number of virulence factors including the including haemolytic α-toxin (hla) and δ-toxin (hld), is a target for CodY repression. A *codY*-null mutant has increased hemolytic activity toward rabbit erythrocytes due to activation of the Agr system and toxin genes (Majerczyk *et al.*,

2008). The general trend among these organisms is for CodY to repress genes involved in virulence during exponential growth and release repression as nutrients become scarce, conditions often encountered in the host.

In recent years, the PTS, depicted schematically in Figure 1-1, has been implicated in virulence regulation as well. The PTS plays regulatory roles through the interaction HPr with CcpA, and in a CcpA-independent manner through the control of transcriptional regulators with PTS regulatory domains, known as PRD-containing regulators. The PEP-PTS is an energy dependent sugar import system used across bacterial species. It is made up of two general components, Enzyme I (EI) and HPr, and sugar-specific Enzyme II (EII) proteins. EI autophosphorylates using a phosphate from the end product of glycolysis phosphoenol pyruvate (PEP) (Deutscher *et al.*, 2014). The high energy phosphate is transferred to HPr on a conserved histidine residue, and then relayed to an EIIA protein. EIIB phosphorylates the incoming sugar transported by EIIC. This phosphorylation event serves to prevent efflux from the cell as EIIC has a low affinity for phosphorylated sugars and charge the sugar to enter glycolysis. In addition to phosphorylating EII proteins, HPr transfers the phosphate from its histidine residue to transcriptional regulators at conserved domains, known as PTS regulatory domains (Deutscher *et al.*, 2014). These regulators, known as PRD-containing regulators because they are subject to phosphorylation by the PTS, generally control transcription of genes involved in sugar transport and utilization.

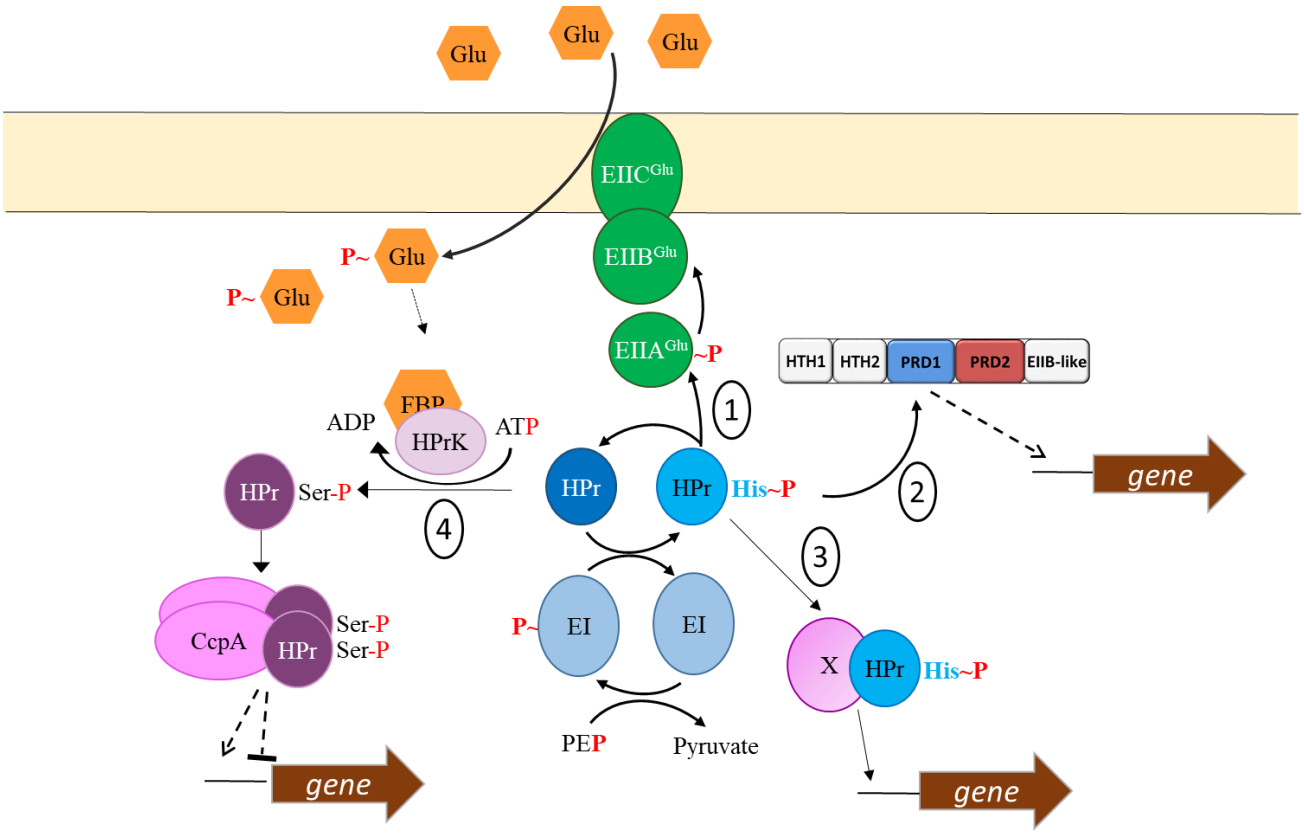

Figure 1-1 HPr phosphorylation and transcriptional control. EnzymeI (EI) autophosphorylates using phosphate from PEP and transfers the phosphate to the Histidine containing protein (HPr) on a conserved histidine residue. HPr-H15-P can transfer the phosphate to EIIA components of sugar-specific EII protein complexes (1), or to PRD-containing transcriptional regulators (2). After the enzyme IIA receives the phosphate group, it relays the P to EIIB which delivers the phosphate to the incoming sugar transported by the transmembrane protein EIIC. HPr in its histidine phosphoarylated form can also interact with transcriptional regulators to act as a co-effector and activate the regulator activity at target promoters (3). In the presence of readily metabolizable sugars, glycolytic intermediates, such as glucose-6-P and fructose-bis-P, as well as energy in the form of ATP, are at high concentrations and stimulate HPrKinase/Phosphorylase (HPrK/P). HPrK/P phosphorylates HPr at a conserved serine residue (S46) (4). In this Ser46P form, HPr interacts with the catabolite control protein, CcpA, to activate CcpA as a transcriptional regulator.

1.2 PRD-containing Virulence Regulators

PRD-containing transcriptional activators have a general protein organization as follows (Fig1-2). At the N-terminus of the proteins are DNA binding regions followed by PRDs. The PRD closer to the N-terminus is called PRDI, the PRD proximal to the C-terminus is called PRDII. At the C-terminus of the proteins are two domains resembling EII proteins of the PTS, an EIIA-like domain and an EIIB-like domain. Phosphorylation to control the PRD-containing regulators may occur at histidine residues in the PRDs or EIIA-like domain, or at a cysteine residue in the EIIB-like domain (Stulke *et al.*, 1998). The outcomes of the phosphorylation events at specific sites differs for each protein. In the absence of a cognate sugar, the EII proteins of a specific system are found in their phosphorylated form and may phosphorylate the PRD-containing regulator to inactivate the regulator activity. Alternatively, when the substrate is present, the EII proteins transfer phosphate to the substrate and do not phosphorylate the PRD-containing regulator, thereby relieving the repressive phosphorylation on regulator activity. When HPr is phosphorylated at His15 (*B. subtilis* numeration), it can transfer the phosphate to PRD-containing regulators, thereby activating their activity. The presence of PTS substrates influences the phosphorylation state of the various components of the system, and therefore influence the system's ability to phosphorylate and control PRD-containing regulators (Deutscher *et al.*, 2014).

Within the last ten years a group of PRD-containing regulators, primarily in Gram-positive pathogens, has been associated with virulence. In *B. anthracis*, AtxA, AcpA, and AcpB are required for immune evasion, colonization, and dissemination within the host. In *S. pyogenes*, a Group A *Streptococcus* that can cause throat and skin infections, Mga is required for biofilm formation,

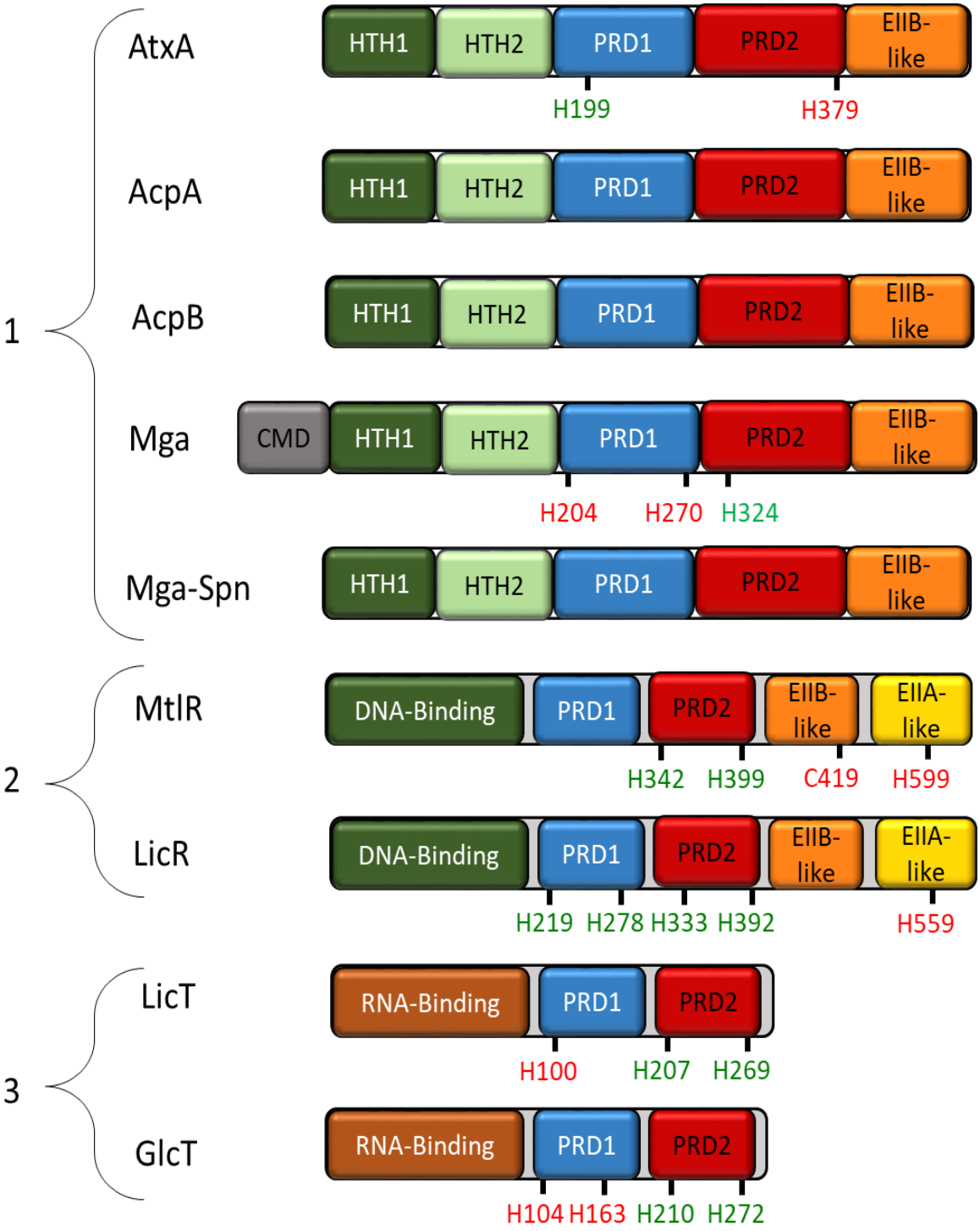
1
AtxA
HTH1
HTH2
PRD1
PRD2
EIIB-like
H199
H379
AcpA
HTH1
HTH2
PRD1
PRD2
EIIB-like
AcpB
HTH1
HTH2
PRD1
PRD2
EIIB-like
Mga
CMD
HTH1
HTH2
PRD1
PRD2
EIIB-like
H204
H270
H324
Mga-Spn
HTH1
HTH2
PRD1
PRD2
EIIB-like
2
MtlR
DNA-Binding
PRD1
PRD2
EIIB-like
EIIA-like
H342
H399
C419
H599
LicR
DNA-Binding
PRD1
PRD2
EIIB-like
EIIA-like
H219
H278
H333
H392
H559
3
LicT
RNA-Binding
PRD1
PRD2
H100
H207
H269
GlcT
RNA-Binding
PRD1
PRD2
H104
H163
H210
H272

Figure 1-2. Comparison of AtxA and PRD-containing proteins.
The structural organization of PRD-containing regulators and PRD containing virulence regulators is depicted above (drawings are not drawn to scale). AtxA contains five domains; two DNA-binding domains, two PTS regulation domains, and a domain resembling EIIB of the PTS. Other PRD-containing regulators are shown for comparison. Group 1 are some of the PCVRs in Gram-positive pathogens. Group 2 are transcriptional activators from *B. subtilis.* Group 3 are transcriptional antiterminators from *B. subtilis.* Phosphorylation sites that have been identified are highlighted in green and red. Green indicates phosphorylation at this residue increases regulator activity. Red indicates phosphorylation at the site decreases or inhibits activity of the regulator. An alignment of the PRDs of these regulators and a few others is presented in figure 7-1.

growth in whole blood, and resistance to phagocytosis (Hondorp, et al., 2013). Although in the same organism, RivR, another PRD-containing transcriptional regulator, negatively regulates capsule production and protease inhibitors that act on host proteases (Trevino *et al.*, 2013). *S. pneumoniae* expresses a PCVR, known as MgaSpn, which has been found to play a significant role in infection in a murine model of infection (Solano-Collado *et al.*, 2013). A PRD-containing regulator in a Gram-negative bacterium, uropathogenic *Escherichia coli*, named PafR was shown to be required for urinary tract colonization in a murine UTI model, as well as playing a role in biofilm formation (Baum *et al.*, 2014).

Like other, general PRD-containing regulators, PCVRs are also subject to phosphorylation at histidine residues with the PRDs. AtxA from *B. anthracis* is subject to phosphorylation at H199 in PRDI and H379 in PRDII. Phosphorylation at H199 allows for AtxA activity, whereas phosphorylation at H379 inhibits AtxA activity and dimerization (Hondorp *et al.*, 2013, Raynor *et al.*, 2018). Mga from *S. pyogenes* is subject to phosphorylation as well. Phosphorylation at positions H204 and H270 within PRDI inhibits Mga activity and phosphorylation at H324 in PRDII activates Mga (Hondorp *et al.*, 2013). Direct phosphorylation of Mga by the PTS proteins HPr and EI has been demonstrated, and mimicking phosphorylation affects the affinity of Mga binding to Mga-regulated promoters (Hondorp *et al.*, 2013).

1.3 *Bacillus anthracis* and Anthrax Disease

B. anthracis is unique among PCVR-expressing pathogens studied thus far in that it expresses three PCVRs; AtxA, AcpA, and AcpB (Raynor *et al.*, 2018). *B. anthracis,* the causative

agent of anthrax disease, is a low G+C content bacterium and part of the *B. cereus* group. The genome of the bacterium consists of three genetic elements; the chromosome (5.3 Mb) and two virulence plasmids pXO1 (182 kb) and pXO2 (96 kb) (Kaspar & Robertson, 1987). The structural genes for the well-studied anthrax toxin, *pagA*, *lef,* and *cya*, are on pXO1, and the capsule biosynthesis operon (*capBCADE*) is on pXO2 (Makino *et al.*, 1988, Tippetts & Robertson, 1988, Koehler, 2009, Schuch *et al.*, 2010).

B. anthracis like other *Bacillus* species has a developmental lifestyle with two life stages: vegetative cells and dormant spores (Koehler, 2009). The bacterium is most commonly found in its spore form in the environment, however studies have shown it can grow in the rhizospheres of plants and the intestines of earthworms (Schuch *et al.*, 2010, Saile & Koehler, 2006). Due to the prevalence of the spores in the soil, anthrax infection typically affects grazing animals, which leads to infection of humans and other mammals through food and textile production (Dixon *et al.*, 1999). Upon entry into a host the spores germinate and vegetative cells disseminate and replicate, sometimes reaching concentrations of 10^{-8} colony forming units (CFU) per ml in the blood (Lyons *et al.*, 2004). Septicemia can lead to host death. Once the host dies cells are exposed to increased levels of O_2 which leads to sporulation, completing the developmental cycle (Dixon *et al.*, 1999).

The first step in the infection process is entry of dormant spores into a host. The three natural routes of infection are inhalation, ingestion, and entry of spores into a preexisting cutaneous lesion (Koehler, 2002). The well-studied form of anthrax is inhalational anthrax. Upon

entry into the host spores are engulfed by alveolar macrophages and transported to regional lymph nodes from which they can spread systemically. Within the macrophages, germination occurs and vegetative cells start to produce virulence factors (Guidi-Rontani *et al.*, 1999, Lyons *et al.*, 2004).

Two of the most important and well-studied virulence factors expressed soon after germination are the tripartite anthrax toxin and the poly-d-glutamic acid (PDGA) capsule. These virulence factors are essential for virulence in some animal models as they assist in survival and dissemination within the host (Lyons *et al.*, 2004, Levy *et al.*, 2014). The anthrax toxin is a variation of the classic A-B type toxin. There are two enzymatic A portions, edema factor (EF, 89 kDa) and lethal factor (LF, 90 kDa) and one binding/translocating moiety, protective antigen (PA, 83 kDa). PA binds the host cell receptors tumor endothelial marker 8 (TEM8, ANTXR1) and capillary morphogenesis gene 2 (CMG2, ANTXR2). Once bound PA oligomerizes into heptamers or octomers, and in this form LF and EF may bind the PA complex. The receptor-toxin oligomers are endocytosed, and a drop in pH in the endosome triggers a conformational change in PA leading to pore formation and translocation of the toxin effectors into the host cell cytoplasm (Friebe *et al.*, 2016). The poly-d-glutamic acid capsule of *B. anthracis* is unique among bacteria as it is composed of polymers of a single amino acid as opposed to typical polysaccharide capsules. The capsule is weakly immunogenic and serves to inhibit host defenses through inhibiting host-immune detection and phagocytosis (Ezzell & Welkos, 1999). Recent evidence suggests free capsule also acts to alter the maturation of host immune cells (Jelacic *et al.*, 2014).

1.4 The Anthrax Toxin Activator, AtxA

The toxin genes (pXO1) and the PDGA capsule (pXO2) are both positively regulated by the *trans*-acting transcriptional regulator, AtxA. *atxA* is encoded on a pathogenicity island on pXO1. AtxA was first identified as a positive regulator of toxin production and therefore was named anthrax toxin activator (Dai *et al.*, 1995). *atxA*-null mutants have severely reduced, or completely abrogated, toxin and capsule production, and are attenuated for virulence in animal models for infection (Fouet & Mock, 1996, Dai *et al.*, 1995, Uchida *et al.*, 1997, Hadjifrangiskou & Koehler, 2008). The transcripts of 145 genes are affected by AtxA at least 4-fold or greater (Dale *et al.*, 2018). Although no consensus regulatory sequences have been observed upstream of AtxA regulated genes, the toxin gene promoters display structure similarity (Hadjifrangiskou & Koehler, 2008).

The importance of AtxA is demonstrated by the attenuation of virulence of an *atxA*-null mutant, and underscored by the numerous levels of regulation exerted on transcription of *atxA*. Transcription of *atxA* is initiated from two promoters. The predominant promoter, P1, is proximal to the translation start site, and the much weaker, less active promoter, P2 is located approximately 600 bp upstream from P1 (depicted in Fig 1-3) (Dai *et al.*, 1995, Bongiorni *et al.*, 2008). In addition to the influence of CcpA on *atxA* transcription, and CodY on AtxA stability, there is a complex regulatory network of environmentally responsive regulators in place to further modulate transcription of *atxA*. The mechanisms of control for most of the regulation, however, remain largely unclear. In agreement with its role in pathogenesis in mammalian hosts,

atxA transcript levels are increased 5-6 fold when cells are grown in culture at 37 °C compared to 28 °C (Dai & Koehler, 1997). PagR affects *atxA* expression two-fold (Hoffmaster & Koehler, 1999). AbrB, a transition state regulator that controls growth-phase specific genes, represses *atxA* transcription in early exponential phase, and is the only identified *trans*-acting factor reported so far to bind directly to the *atxA* promoter region (Saile & Koehler, 2002, Strauch *et al.*, 2005). A second repressor binding site was identified just downstream of the P1 transcriptional start site, however, the protein has not yet been identified (Dale *et al.*, 2012). In accordance with these observations *atxA* transcription appears to be low in early phases of growth and peaks around transition phase. When the repressor binding site in the *atxA* promoter was mutated, activity from a P*atxA*-*lacZ* reporter was detectable in lysates earlier and at higher levels than in the parent strain (Dale *et al.*, 2012). The redox potential of cells seems to play a role in *atxA* transcription as well. In cells deficient in cytochrome C, a sensor of the cell's redox state, *atxA* transcription was increased in early exponential phase in rich medium, indicating cytochrome C may repress *atxA* transcription in response to the cellular redox state (Wilson *et al.*, 2009).

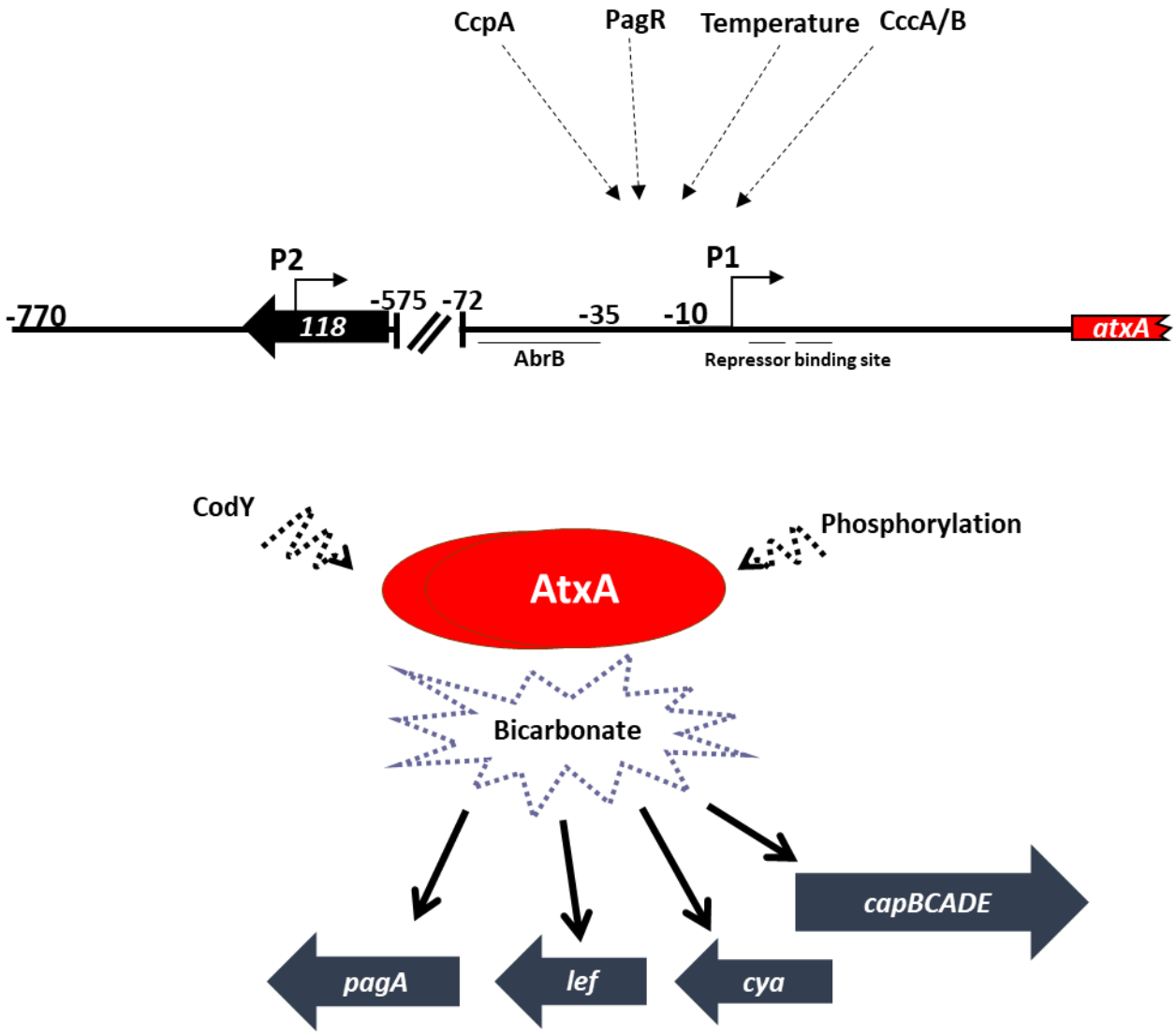

Figure 1-3. Regulation of AtxA in *B. anthracis.* The multiple levels of AtxA regulation are depicted. Many factors have been shown to affect *atxA* transcription and post-translational stability and activity, but most of the mechanisms have not yet been defined (demonstrated by dotted arrows).

Environmental signals also play a role in modulating AtxA once the protein has been synthesized. CodY affects AtxA protein stability through an unknown mechanism (van Schaik *et al.*, 2009). CO_2 and bicarbonate appear to play a role in enhancing AtxA homomultimerization and activity (Hammerstrom *et al.*, 2011). The high resolution crystal structure of AtxA revealed a structure similar to PRD-containing regulators, typically regulated by the PTS. At the N-terminus of the protein are two helix-turn-helix domains, indicative of DNA binding. In the center of the protein are two PRDs, used to regulate AtxA activity via phosphorylation. The C-terminus of AtxA has a domain resembling an EIIB of the PTS, involved in multimerization of the protein. AtxA crystalized as a homodimer with the PRDII and EIIB-like domains of chain A interacting with the PRDII and EIIB-like domain of chain B (Hammerstrom *et al.*, 2015).

Phosphorylation and homomultimerization of AtxA is important for regulator activity. AtxA is phosphorylated at position H199 in the PRDI, proximal to the DNA binding region, and at H379 in PRDII proximal to the EIIB-like domain (Tsvetanova *et al.*, 2007). Phosphorylation at H199 allows for AtxA activity to positively affect toxin production, and phosphorylation at H379 inhibits AtxA activity and dimerization (Tsvetanova *et al.*, 2007, Hammerstrom *et al.*, 2015).

1.5 Gaps in knowledge and significance of this work

AtxA, the master virulence regulator of the important pathogen *B. anthracis* has been studied for many years for its role in pathogenesis. Much of the work has focused on understanding the mechanism of AtxA activity and the regulation governing the production and activity of AtxA. There still exists gaps in knowledge regarding the mechanism by which AtxA is

phosphorylated, how AtxA positively affects transcription of target genes, and as the work in this thesis describes, many levels of transcriptional regulation.

In this work I found that AtxA, a PRD-containing regulator hypothesized to be controlled post-translationally by the PTS, is in fact controlled by the PTS at the level of transcription. I also explored further the effects phosphorylation of AtxA has on protein-protein interactions and solubility. Although many studies of PRD-containing proteins have focused on protein function and regulation of activity, relatively little is known regarding the potential influence of carbohydrate metabolism and signaling on transcription of the genes encoding these regulators. My data supports a model in which HPr transfers phosphate to a transcriptional regulator that regulates the transcription of a PRD-containing regulator, *atxA*. Future studies will aim to identify the target of HPr phosphorylation and if regulation of *atxA* is direct or through an indirect mechanism.

Chapter II.

Materials and Methods

2.1 Strains and growth conditions

Strains and plasmids are shown in Table 2-1. *B. anthracis* strains were derived from the Ames non-reverting, $pXO1^+$ $pXO2^-$ strain, ANR-1 (Welkos *et al.*, 2001). *Escherichia coli* strains TG1 and GM2163 were employed for cloning. Unless otherwise indicated, *E. coli* cultures were grown in Luria Burtani (LB) broth (Bertani, 1951) with shaking at 37 °C.

Inocula for all *B. anthracis* cultures were obtained from overnight cultures grown in brain-heart infusion (BHI) (Becton, Dickson and Company) medium with shaking at 30°C. The stationary phase cultures were transferred to fresh medium at a starting OD_{600} of 0.08 and incubated with shaking at 37°C. For preparation of cells for electroporation, subcultures were grown in BHI to an OD_{600} between 0.6-0.8. For preparation of cell lysates for β-galactosidase assays, RNA isolation, and western blotting, subcultures were grown in $CACO_3$ (Casamino Acids medium (Thorne & Belton, 1957, Hadjifrangiskou *et al.*, 2007) buffered with 100 mM HEPES [pH 8.0], and supplemented with 0.1% w/v glucose [or other sugars as specified], as well as 0.8 % w/v sodium bicarbonate) and incubated in 5% atmospheric CO_2. For strains harboring *atxA* under control of the *hyperspank* promoter (P*hyperspank*) (Britton *et al.*, 2002), expression was induced with isopropyl β-d-thiogalactoside (IPTG) during early exponential phase (2 h) and harvested at early stationary phase (4 h). Strains harboring *ptsH* and *ptsI* under a xylose inducible promoter were induced with 0.1 - 2% xylose 1 h post-inoculation and harvested at early stationary phase (4 h). Cell pellets were used immediately or stored at -80 °C.

Antibiotics were added to media when appropriate, at the following concentrations; carbenicillin (100 μg ml^{-1}), spectinomycin (100 μg ml^{-1}), erythromycin (300 μg ml^{-1}) for *E. coli* and (5 μg ml^{-1}) for *B. anthracis*.

2.2 DNA isolation and manipulation

Standard procedures were used for cloning in *E. coli* TG1. Primers used for PCR are shown in Table 2-2. Plasmid isolation from *E. coli* was performed using the Wizard® Plus SV Minipreps DNA Purification System (Promega, Madison, WI). *E. coli* GM2163 was used to isolate non-methylated plasmid DNA for electroporation into *B. anthracis* (Marrero & Welkos, 1995). *B. anthracis* DNA was obtained using UltraClean Microbial DNA Isolation Kit (Mo Bio Laboratories, Inc.). Restriction enzymes, T4 DNA ligase, and Phusion DNA polymerase were purchased from NEB. Bullseye Taq DNA Polymerase was purchased from MidSci (St. Louis, MO).

2.3 Generation of marker-less deletions

Markerless deletions in *B. anthracis* were constructed using the temperature-sensitive integration vector pHY304 as described previously (Pflughoeft *et al.*, 2011). The *ptsHI* operon was removed from the ANR-1 chromosome via homologous recombination as described above. Primers TH235 and TH245 were used to amplify the left flanking region surrounding the operon and primers TH246 and TH244 were used to amplify the right flanking region. The two amplicons were fused together by SOE-PCR, subcloned into pHY304, and used to transform *B. anthracis.*

The *ptsHI*, *atxA* double mutant UT448 was constructed by removing the *atxA* gene from the *ptsHI* mutant UT439 as described.

The *ccpA*-null mutant was generated following the same protocol described above using the primers NB063 and NB064 to generate the LFR and NB065 and NB066 to generate the RFR.

2.4 Generation of plcR::GBAA2500promoter-*atxA*-His6

The promoter of GBAA_2500 was chosen to control *atxA* transcription based on the observation that GBAA_2500 transcript levels were approximately the same as *atxA* transcript levels in the RNA sequencing experiment performed by Malik Raynor (Raynor *et al.*, 2018). The *atxA*-His_6 construct was fused to the promoter region and cloned into the *plcR* locus, a nonfunctional gene in *B. anthracis*. To confirm the promoter was not controlled by the PTS, the promoter-*atxA* fusion was cloned into a *ptsHI*-null mutant and AtxA-His_6 production was monitored, and compared to expression of the fusion cloned into a parent strain containing the *ptsHI* operon.

The *plcR*::GBAA2500promoter-*atxA*-His6 construct was generated by fusing two fragments together via SOE-PCR. The fragments were generated contained *atxA* with a C-terminal His6 tag and *Bam*HI RE, and the region upstream of GBAA_2500 predicted to contain the transcriptional start site and a *Bam*HI RE site.

The *plcR* flanking regions were amplified with a *Bam*HI cut site in the middle of the two regions in order to promote incorporation of the *plcR*::GBAA2500promoter-*atxA*-His6 construct

into the *plcR* locus via homologous recombination. Primers ES40 and ES41 were used to amplify the right flanking region upstream of the *plcR* locus. Primers ES42 and ES43 were used to amplify the left flanking region downstream of the *plcR* locus. The two flanking regions were fused via splicing by overlapping extension PCR (SOE-PCR) (Horton *et al.*, 1989).

2.5 Generation of the HPr and EI expression vectors

The His_6-EI (pUTE1141) and His_6-HPr (pUTE1142) constructs were generated in the following manner. The *ptsHI* operon was amplified from the *B. anthracis* genome using primers NB074 and NB075. The *atxA* RBS was added to the 5' end of the product by primer walking using NB074 and NB076. The NB7476 product was used a template for all the HPr and EI-expressing plasmids. pUTE1141, the pUTE657-based plasmid expressing His_6-EI, was constructed using primers NB074 and NB145 and sub-cloned into pUTE657 using *Sal*I and *Sph*I. pUTE1142, the pUTE657-based His_6-HPr expressing vector, was constructed using primers NB144 and NB076.

Site-directed mutagenesis was employed to create the HPr phosphovariants, primers listed in the primer Table 2-2.

To use the plasmid-based P*atxA-lacZ* reporter and the HPrEI expression vectors simultaneously, we employed the pAW285 vector (Wilson *et al.*, 2009) with a different origin of replication from the pHT304-*lacZ* based P*atxA-lacZ* reporter. To move His_6-HPr and His_6-EI from pUTE657 based plasmids the following primers were used. Primers NB146 and NB148 were used to amplify the *ptsHI* operon with His_6-tagged EI and His_6-tagged HPr from pUTE1140, a construct

I made containing the *ptsHI* operon, and the phosphovariants created by site-directed mutagenesis. Primers NB148 and NB149 were used to amplify His_6-HPr, and NB146 and NB147 were used to amplify His_6-EI. The constructs were subcloned into pAW285 using the restriction enzymes *Bam*HI and *Hind*III.

2.6 Overproduction of *Bacillus anthracis* proteins

For the *in vitro* phosphorylation assay, proteins were purified from *B. anthracis* cultures grown in 1 L of BHI at 37 °C. After two hours of growth 0.5 mM IPTG was added to the medium and cultures continued to incubate for four more hours. Cells were collected using a 0.22 µm pore-size filter unit and resuspended in Buffer A-PIC (20 mM Tris-Cl pH 8.0, 100 mM NaCl, 5% glycerol, 30 mM imidazole pH 7.9, 1X EDTA-free complete proteinase inhibitor cocktail) supplemented with 1 mM $MgCl_2$ and 10 units DNAse I, followed by centrifugation at 5000 x g and freezing of the cell pellets at -80°C.

Native levels of HPr were determined by western blot using an antibody raised against specific peptides within the HPr sequence (a gift from Bethyl Laboratories Inc., Montgomery, TX). A gradient of xylose was used to determine the proper induction levels of HPr and EI from the pAW285 constructs. EI is expressed from its native RBS within the *ptsH* coding sequence. We therefore determined the level of EI-His_6 expressed from the *ptsHI* locus with both *ptsH* and *ptsI* His-tagged, to determine the native levels of EI.

2.7 Purification of proteins from *Bacillus anthracis*

Frozen pellets were thawed on ice and resuspended in 10 mL Buffer A (10 mM Tris-HCl pH 7.5, 200 mM NaCl, 1mM imidazole) with complete EDTA-free proteinase inhibitor cocktail (Buf A+PIC), supplemented with 1 mM $MgCl_2$ and 10 µl DNase 1. Cells were lysed via French press (3 passages through a small cell set on 1000 psi or 5 passages through a large cell). Cell debris were collected by centrifugation at 16,000 x g for 20 min at 4°C. Soluble cell lysate was transferred to washed NTA-Ni resin. One ml NTA-Ni resin slurry (Qiagen, 50% resin solution) was washed twice with 4 volumes Buf A-PIC. The lysate was incubated with the resin in batch for 2 hr at 4°C. Beads were washed in batch, two times using 4 bead volumes of BufA-PIC. Beads were then resuspended in 1.25 ml BufA, transferred to a gravity column, and washed with 15 ml BufA. Proteins were eluted using 1 ml of Buffer E (Buffer A with imidazole) with a gradient of imidazole concentrations. The Bradford reagent was used to detect the protein in fractions. The fractions with protein were combined and dialized to maintain proteins in 50 mM HEPES pH 7.5, 5 mM $MgCl_2$, 5% glycerol and stored at 4°C.

2.8 Purification of PEP Carboxykinase

Troy Hammerstrom performed the following protocol. “PEP carboxykinase (His-PEPCK) was expressed and purified from the *E. coli* C41(DE3) harboring plasmid pKSM879 (gift from K. McIver, University of Maryland). A colony obtained from LB agar was used to inoculate three 2-L baffled flasks each containing 500 ml ZYP-5052 autoinduction medium (56). The cells were cultured at 37°C for 24 hours. After harvesting cells via centrifugation

(10 min, 6200 x g, 4 °C), the cell pellet was washed twice with 50 ml 100 mM NaH_2PO_4 pH 8.0 and stored at -80 °C. The cell pellet was resuspended in 35 ml Buffer 1 (20 mM imidazole, 20 mM NaH_2PO_4, 500 mM NaCl, pH 7.4) containing Complete EDTA-free proteinase inhibitor and cell membranes were ruptured during five passages through a French Pressure Cell. The sample was centrifuged at 6200 x g at 4° C for 10 min. The soluble material was transferred to a new tube and centrifuged for 20 min at 20,000 x g and 4° C before applying to 2 ml NTA-Ni resin prewashed with Buffer 1. After binding for 1 h at 4° C, the resin was washed in batch using 8 ml Buffer 1. The resin was transferred to a gravity-flow column and subsequently washed with 25 ml Buffer 1. PEPCK was eluted from the resin with 10 ml Buffer 2 (500 mM imidazole, 20 mM NaH_2PO_4, 500 mM NaCl, pH 7.4). 20 µl Ni chelation buffer (250 mM EDTA, 50 mM NaH_2PO_4) was added per ml fraction and fractions containing His-PEPCK were dialyzed four times against 1 L Buffer 3 (20 mM Tris-Cl pH 7.4, 1 mM EDTA, 100 mM KCl). The induction and purification yielded 100 mg His-PEPCK" (Hammerstrom, 2012).

2.9 Synthesis of ^{32}P-PEP

(Protocol was established in the lab and published by Troy Hammerstrom (Hammerstrom, 2012))

"^{32}P-PEP was synthesized and isolated according to methods established previously (58) using γ-^{32}P-ATP (PerkinElmer, Waltham, Massachusetts) and PEPCK. 0.5 ml reactions containing 50 mM HEPES pH 7.5, 12.5 mM KF, 5 mM $MgCl_2$, 1 mM

oxaloacetate, 500 µg PEPCK, 50 µM γ-^{32}P-ATP (2 mCi ml-1, 10 Ci mmol-1) were incubated for 5 min at room temperature (21° C). The reaction was diluted 10-fold with ddH_2O, and the newly synthesized ^{32}P-PEP was isolated via anion exchange chromatography using AG-1-X8 Bicarbonate resin. The hydroxide form of the AG-1-X8 resin (BioRad) was converted to the bicarbonate form according to the product manual. The PEP reaction was added to 2 ml of resin and ^{32}P-PEP was eluted using a step-wise gradient consisting of 5 ml 0.3 M, 0.4 M, 0.6 M, and 0.7 M triethylammonium bicarbonate. ^{32}P-PEP was present in fractions containing 0.6 M and 0.7 M triethylammonium. The fractions were concentrated 5 fold via vacuum centrifugation in a vacufuge (Eppendorf, Hamburg, Germany)" (Hammerstrom, 2012).

2.10 *In vitro* Phosphotransfer Assay

Phosphotransfer assays were conducted using purified His_6-EI, His_6-HPr, GlcT-His_6 and AtxA-His_6. Reactions contained 3 µg His_6-EI, 1.6 µg His_6-HPr, 2 µg AtxA-His_6,and 2 µg GlcT-His_6 in a total volume of 30 µl buffer (50 mM Tris-Cl pH 7.4, 5 mM $MgCl_2$). ^{32}P-PEP (0.5 µCi, 10 Ci mmol-1) was added to a final concentration of 10 µM and the solutions were incubated for 30 min at 37°C. Reactions were quenched by adding SDS-loading buffer (final concentration of loading buffer was 5% glycerol, 100 mM DTT, 2% SDS, 40 mM Tris-Cl pH 7.4). Samples were subjected to SDS-PAGE (12% poly-acrylamide SDS gel). The gels were dried and exposed to a phosphorimaging screen to detect ^{32}P-labeled protein. The screens were scanned using a STORM 840 scanner and analyzed with ImageJ software.

2.11 *In vivo* phosphorylation assay

B. anthracis strain UT376 (pUTE991) was subcultured from overnight cultures in 25 ml of specified cultures at a starting OD_{600} of 0.08. For LB air experiments, LB was inoculated with the overnight culture and incubated shaking at 37°C. For $CACO_3$ experiments, CA was prepared without phosphates and supplemented with ^{32}P-labeled phosphoric acid. At T2 AtxA-His_6 over-expression was induced with 40 μM IPTG and 1 mCi of $^{32}PO_4$ was added to the media. Samples were collected at T4 and AtxA-His_6 was purified following the AtxA-His_6 purification protocol published in Troy Hammerstrom's thesis (Hammerstrom, 2012). Following purification proteins were run on SDS-PAGE, the gels were semi-dried, exposed to screens, and imaged on STORM 840 scanner.

2.12 Western blot analysis

Four-ml culture samples were collected via centrifugation at 21,130 x g. Culture supernates and cell pellets were separated and processed immediately or stored at -80 °C. Cell pellets were resuspended in 550 µL KTE-PIC (10 mM Tris-HCl pH 8.0, 100 mM KCl, 10% eth5ylene glycol, and EDTA-free complete proteinase inhibitor) and transferred to tubes containing 400 µL 0.1 mm zirconia/silica beads (BioSpec Products, Barletsville, OK) and beaten for two min using a Mini BeadBeater (BioSpec Products) to lyse the cells. Lysates were centrifuged at 10,000 x g and the soluble fraction collected. SDS-loading buffer (final concentration of loading buffer was 0.05% bromophenol blue, 0.1M DTT, 10% glycerol, 2% SDS, and 5 mM Tris-Cl pH 6.8) was added to the soluble fractions.

Suspensions were boiled and subjected to SDS-PAGE. Proteins were transferred to polyvinylidene difluoride (PVDF) membranes, blocked with 5% milk in TBS-T (20mM Tris base, 137 mM NaCl, 0.1% Tween 20; pH 7.6), and probed with the appropriate primary antibodies. 1:1,000 for anti-EF serum and anti-PA antibody (List Labs, Campbell, California). His_6-tagged proteins were detected using THE^{TM}His antibody (Genscript, Piscataway, NJ, USA) diluted 1:5,000 in TBST. RNA polymerase β subunit was used as a load control and was probed with an antibody generated by ThermoFisher (Rockford, IL). Membranes were washed three times for five min each with TBST and probed with an HRP-conjugated secondary antibody. Membranes were washed again and developed using the SuperSignal West Dura chemiluminescent substrate (Thermo Scientific).

2.13 Use of Phostag^{TM} to detect phosphorylated proteins

Cell lysates and purified proteins were dissolved in SDS-loading buffer and loaded onto regular 6% acrylamide gels and the Phostag^{TM}-containing 6% acrylamide gel. 100 μM Phostag^{TM} and 200 μM $MnCl_2$ were used in making the Phostag^{TM}-containing gel. Gels were run at low voltage until the bromophenol blue dye on the regular acrylamide gel reached the bottom of the gel. Proteins were transferred to PVDF via standard protocol and western blots were performed as described above.

2.14 Use of pHis antibody to detect phosphorylated histidine residues

Cell lysates and purified proteins were subjected to SDS-PAGE on 15% acrylamide gels followed by transfer to PVDF membranes and probing with the pHis antibody. Samples were dissolved in 4X loading buffer ((160 mM Tris, pH 8.5, 40% (v/v) glycerol, 4% (w/v) SDS, 0.08%

(w/v) bromophenol blue, and 8% (v/v) BME) and electroblotted onto a PVDF membrane in Towbin buffer (25 mM Tris base, 192 mM glycine, pH 8.3, 10 % (v/v) methanol) at 100 V for 60 minutes. The membrane was blocked with 3% BSA in wash buffer (25 mM Tris, 137 mM NaCl, 2.7 mM KCl, 0.1% (v/v) Tween-20, pH 8.5) for 1 hour at room temperature followed by incubation with anti-pHis antibody (supplied by Thomas Miur, Ph.D., Princeton University) diluted 1:100 in wash buffer with 3% BSA for 1 hour at room temperature. The membranes were washed with wash buffer and incubated with goat anti-rabbit IgG-HRP conjugate (diluted 1:5000 in wash buffer with 3% BSA) for 1 hour, washed, and developed using the SuperSignal West Dura chemiluminescent substrate (Thermo Scientific).

2.15 Detecting phosphorylated tyrosine residue

Three μg of each protein was incubated with 3U of CIP at 37°C for 1 hr. Approximately 20μg of the positive control cell lysate (provided with the pTyr antibody) was loaded. Each protein (0.5 μg) and each CIP treated protein was loaded onto two 10% polyacrylamide gels (one for pTyr western and one for THEHisAb). The positive control came in buffer already, and was boiled at 100°C for 5 min per the protocol. For the rest of the proteins 5X SDS-loading buffer was added to the samples. The rest of the samples were not boiled prior to loading onto gel in order to preserve the phosphorylated histidine on EI to see if cross-reactivity would be detected with phosphorylated EI and not CIP treated EI. The proteins were transferred to PVDF membranes, and probed with 0.5 mg/ml α-pTyr antibody (Millipore Anti-phosphotyrosine, clone 4G10 Monoclonal Antibody Cat.# 05-321 Lot# 2310354) followed by 1:10,000 anti-mouse antibody conjugated to HRP.

2.16 BMH crosslinking

Cells of the *B. anthracis* strain UT376- derived strains harboring plasmids encoding WT AtxA-FLAG (pUTE991), EIIB-like FLAG (pUTE1022) and AtxA H379D (pUTE992H379D) were cultured in $CACO_3$ and induced with IPTG at early exponential phase. After two hours 20 ml of each culture was collected by centrifugation at 5,000 x g for 10 min at 4˚C and washed with PBS-EDTA. Cells were resuspended in PBS-EDTA and lysed by bead beating. Cell lysates were centrifuged at 10,000 x g for 5 min at 4˚C to pellet insoluble debris. For each experiment, 250 µl of the soluble lysate was mixed with 5 µl of 20 mM bis(maleimido)hexane (BMH, Thermo Scientific, prepared freshly in DMSO) and incubated at 4˚C with end-over-end mixing for 2 h. Control reactions lacking BMH contained DMSO only. Reactions were quenched by adding cysteine to a final concentration of 40 mM and vortexing for 15 min at room temperature. SDS-loading buffer (final concentration of loading buffer was 0.05% bromophenol blue, 0.1M DTT, 10% glycerol, 2% SDS, and 5 mM Tris-Cl pH 6.8) was added to the samples and samples were run on SDS-PAGE followed by western blotting using α-FLAG antibody (Genscript).

2.17 Determining solubility of AtxA

Cell lysates were collected at transition to stationary phase. Cells were resuspended in KTE-PIC, disrupted by mechanical perturbation, and separated into soluble and insoluble cell fractions. The insoluble fractions were rinsed with KTE-PIC and then treated with 8M urea and rocked at room temperature for 3 hours. 5X SDS-loading buffer was added to the soluble

fractions. Fractions were subjected to SDS-PAGE and probed with THEHis^{TM}mAB to detect AtxA. Relative levels of AtxA were determined using densitometry. The soluble fraction was arbitrarily set to 1 to determine the relative solubility of AtxA in each strain.

2.18 β-galactosidase assays

One-ml samples were collected from cultures grown to late exponential/transition phase. Liquid β-galactosidase assays were performed as previously described by Miller et al. (Miller, 1972). Cell pellets were resuspended in 1 ml Z-buffer (60 mM Na2HPO4 · 7H2O, 40 mM NaH_2PO_4 · H_2O, 10 mM KCl, 1 mM $MgSO_4$ · $7H_2O$, 50 mM β-mercaptoethanol [added just prior to use]), transferred to tubes containing 400 µL 0.1 mm zirconia/silica beads (BioSpec Products, Bartlesville, OK), and beaten for 1 min using a Mini BeadBeater (BioSpec Products) to lyse the cells. Lysates were centrifuged at 10,000 x g to pellet debris, and supernatant fractions were used to assay β-galactosidase activity. Figures show data averaged from at least three independent cultures.

2.19 RNA purification

RNA was isolated using a NucleoSpin®RNA RNA isolation kit (Macherey-Nagel, Düren, Germany) with the following modifications. Cells were resuspended in 100 µL TE and transferred to tubes containing 400 µL of 0.1 mm zirconia/silica beads (BioSpec Products, Barletsville, OK). Samples were subjected to bead beating for 2 min using a MiniBeadBeater (BioSpec Products) to

lyse the cells. Following centrifugation at 10,000 x g to remove cell debris, supernates was transferred to the column provided in the kit. The remaining steps were performed as recommended by the manufacturer with the exclusion of the on-column DNAse treatment. RNA was eluted from the columns with water, quantified using a NanoDrop Spectrophotometer ND-1000 (Thermo Scientific), and checked for quality by subjecting samples to agarose gel electrophoresis.

2.20 Real-time quantitative PCR (RT-qPCR)

A two-step reaction for RT-qPCR was employed. Step one was performed following the SuperScirpt III (Invitogen) insert: 1 µg RNA, 250 ng of Random Primers (Invitrogen), and 0.5 mM dNTPs were incubated at 65°C for 5 minutes, followed by at least one minute on ice. Next DTT, 5X buffer, and the SuperScriptIII enzyme were added to the reaction. The reaction was incubated at 25°C for five minutes, followed by 50°C for 60 minutes, and finally 70°C for 15 minutes. The resulting cDNA was cleaned using a DNA Clean and ConcentratorTM-5 kit (Zymo Research), and quantified using the ND-1000 NanoDrop. For the second step of qPCR 50ng of cDNA, IQ mix (BIORAD, Hercules, CA), and a primer probe mix from Thermo Fisher, assay numbers AIHSQBA (*gyrB*) and AII1OHI (*atxA*) were used to detect transcript of *atxA* and *gyrB* (internal standard). The second step was run on a BioRad real-time instrument using the following cycling conditions: 98˚C, 2 min; followed by 40 cycles of 98˚C, 12 sec and 60˚C, 30 sec. Data was transferred to Microsoft Excel, the relative values of *atxA* transcript in each strain was determined (*atxA*/*gyrB*)

and compared to the parent strain. Student T tests were performed to compare all samples to the parent strain to determine the significance of the results (p values <0.05).

2.21 Preparation of vegetative cells for I.V. injection

B. anthracis spores (~10^7) were incubated in 1 ml BHI at 37 °C shaking for 15 min. The entire spore outgrowth culture was transferred to 30 ml $CACO_3$ for 4 hours to an OD_{600} of 0.4-0.6. Vegetative cells were collected onto a filter membrane and rinsed twice with 25 ml Dubelco's phosphate buffered saline (DPBS) without calcium or magnesium (insert company name). Cells were resuspended in DPBS to an OD_{600} of ~0.4. Prior to infection, an aliquot of the resuspension was diluted and plated on LB agar to determine the final inoculation dose (in CFU ml^{-1}). 1 ml syringes with needles on (to account for dead space) were loaded with 100 μL vegetative cell suspension.

2.22 Mouse infections

All mouse protocols were approved by The University of Texas Health Science Center Institutional Animal Care and Use Committee and performed using accepted veterinary standards. Seven to eight week-old female A/J mice were purchased from The Jackson Laboratory (Bar Harbor, ME) and maintained in a pathogen-free vivarium at The University of Texas Health

Science Center. Food and water were supplied to the mice *ad libitum*. The animals were housed 3-5 per cage and were allowed to acclimate to their surroundings for 72 hours prior to being used in experiments. Mice were sedated with 3-6 mg kg^{-1} acepromazine 5-10 minutes prior to injection. Mice were infected intravenously via tail vein using 27 gauge needles (Becton, Dickinson and Company, Franklin Lakes, NJ) with 100 μL suspensions containing approximately 1,000 heat sensitive CFUs. Mice were monitored for two to six times per day for seven days according to the approved protocol. When mice presented with multiple signs of disease and were determined moribund, they were sacrificed and the liver, lungs, and spleen were collected to determine CFU per organ.

2.23 CFU determination and Statistics

Organs from deceased mice were collected, weighed, and resuspended in 1 mL sterile PBS and 400 μL 2.3 mm diameter zirconia/silica beads (BioSpec Products, Barletsville, OK). Tissues were homogenized by bead beating for 1 min, followed by 1 min on ice, and again bead beating for 1 min. Homogenates were diluted and plated on LB agar and incubated at 30 °C overnight. Plates containing 30-300 colonies were counted and used to calculate the CFU g- tissue. A two-sample permutation test (60) was performed to determine the significance of the differences in CFU per g and survival curves.

2.24 Phenotype Microarrays™ Biolog

B. anthracis strain UT428 harboring the vectors pUTE991 and pUTE991H379A were grown on LB agar containing spectinomycin overnight. Colonies were resuspended in 20 mL 1 X IF-0a, the reagent specific for PM plates (Biolog catalog #77268) to an OD_{600} of 0.012, or 81% transmittance. For PM 1,2 panels 1.76 mL of the cell suspension was added to 2.24 mL of PM 1,2 inoculating fluid (2 mM $MgCl_2 \bullet 6H_2O$, 1 mM $CaCl_2 \bullet 2H_2O$, 25 μM L-arginine HCl, 50 μM L-glutamate Na, 12.5 μM L-cystine, pH8.5, 25 μM 5'-UMP, 2Na, 0.005% yeast extract) with added bicarbonate to a final concentration of ~0.08%. Plates were inoculated with the cell suspension. Initial readings were taken; OD_{600} and OD_{509} -excitation at 395 nm, emission at 509, gain of 100. A Synergy™ Mx Microplate Reader (BioTek, Winooski, VT) was used to make the measurements. Cultures were incubated at 37°C shaking on an OrbiShaker™ MP (Benchmark Scientific, Sayreville, NJ) at 290 rpm for 7 hours. After 7 hours the cultures were pipetted up and down to break up any clumps that may have formed during the incubation period and measurements were repeated. The fluorescence readings were normalized to the cell densities for both time points ((485,528))/((600)), and then the T_0 value was subtracted from the T_8 value for each strain. Any numbers that were nagative were changed to zero and not used. In addition if a well contained a zero value from either strain, the well was not used in the analysis either. Wild-type value was subtracted from the H379A value so that any well with a positive value had more activity in the H379A strain, than the wild-type strain.

Table 2-1 *B. anthracis* strains and plasmids used in this study

Name	Description	Source
Strains		
ANR-1	*B. anthracis*, parent strain, pXO1^{+}, pXO2^{-}	(Welkos *et al.*, 2001)
UT374	ANR-1-derivative *atxA*-null	(Dale *et al.*, 2012)
UT376	ANR-1-derivative, *lef* promoter - *lacZ* fusion (P*lef-lacZ*) at native *lef* locus, *atxA*-null	(Hammerstrom *et al.*, 2011)
UT417	UT376- derivative, *lef* promoter - *lacZ* fusion (P*lef-lacZ*) at native *lef* locus, *atxA*-null, *ptsHI*-null	This work
UT425	ANR-1 derivative, AtxA-H379D in native *atxA* locus on pXO1	This work
UT428	7702-derivative, *lef* promoter- *gfp* fusion at native *lef* locus, *atxA*-null	This work
UT433	ANR-1-derivative *ccpA*-null	This work
UT439	ANR-1 derivative, *ptsHI*-null	This work
UT447	UT374-derived, GBAA_2500 promoter region fused to *atxA-His$_6$* and incorporated in to the *plcR* locus	This work
UT448	UT439-derived, *ptsHI*-null, *atxA*-null	This work
UT449	UT448-derived, *ptsHI*-null, *atxA*-null, GBAA_2500 promoter region fused to *atxA-His$_6$* and incorporated in to the *plcR* locus	This work
Plasmids		
pUTE657	Expression vector derived from pDR111 and pBC16 with IPTG-inducible P*hyper-spank*; Spec^{r} Amp^{r}	(Hammerstrom *et al.*, 2011)
pUTE839	pHT304-18z-derived atxA promoter-lacZ fusion vector; contains sequence from −770 to +99	(Dale *et al.*, 2012)
pUTE843	pHT304-18z-derived atxA promoter-lacZ fusion vector; contains sequence from −72 to +99	(Dale *et al.*, 2012)

pUTE991	pUTE657-derived expression vector for AtxA-His (6xHis-epitope on the C-terminus of AtxA) the *atxA* ribosome binding site and coding region controlled by P*hyper-spank*	(Hammerstrom *et al.*, 2011)
pUTE992	pUTE657-derived expression vector for AtxA-FLAG (FLAG-epitope on the C-terminus of AtxA) the *atxA* ribosome binding site and coding region controlled by P*hyper-spank*	(Hammerstrom *et al.*, 2011)
pUTE1022	pUTE657 - derived expression vector for AtxA385-475-FLAG (FLAG tag on the C-terminus)	(Hammerstrom *et al.*, 2011)
pUTE1034	pUTE657 - derived expression vector for HPr and EI; the *ptsH* ribosome binding site, *ptsH* coding region, *ptsI* ribosome binding site, and *ptsI* coding region controlled by P*hyper-spank*	This work
pUTE1098	pUTE657-derivative expression vector for GlcT-His_6 (C-terminally tagged GlcT); the AtxA ribosome binding site, *glcT* coding region controlled by P*hyper-spank*	This work
pUTE1141	pUTE657-derivative expression vector for His_6-EI (N-terminally tagged EI); the AtxA ribosome binding site, *ptsI* coding region controlled by P*hyper-spank*	This work
pUTE1142	pUTE657-derivative expression vector for His_6-HPr (N-terminally tagged HPr); the AtxA ribosome binding site, *ptsH* coding region controlled by P*hyper-spank*	This work
pUTE1143	pAW285-derived, His_6-HPr (N-terminally tagged HPr)	This work
pUTE1144	pAW285-derived, His_6-EI (N-terminally tagged EI)	This work
pUTE1145	pAW285-derived, His6-HPr His6-EI (N-terminally tagged HPr and EI)	This work
pUTE1151	pAW285-derived, His6-HPr His6-EI (N-terminally tagged HPr and EI) HPr H14A	This work
pUTE1152	pAW285-derived, His6-HPr His6-EI (N-terminally tagged HPr and EI) HPr H14D	This work
pUTE1153	pAW285-derived, His6-HPr His6-EI (N-terminally tagged HPr and EI) HPr S46A	This work
pUTE1154	pAW285-derived, His6-HPr His6-EI (N-terminally tagged HPr and EI) HPr H14A S46A	This work
pUTE1155	pAW285-derived, His6-HPr His6-EI (N-terminally tagged HPr and EI) HPr H14D S46A	This work
pAW285	Xylose-inducible expression vector; Cmr	(Wilson *et al.*, 2009)

Ap^r, ampicillin resistant; Cm^r, chloramphenicol; Sp^r, spectinomycin.

Table 2-2 Primers used in this study

Name	SEQUENCE (5' TO 3')	Short Description
NB063	AAACTGCAGGATACGAACATTGGAAATTGGAATGCG	*ccpA* KO, *Pst*I cut site (upstream of start site)
NB064	TTTTTATACTTACATCTCATCGCACACTCCTTC	*ccpA* KO, middle primer
NB065	CGATGAGATGTAAGTATAAAAAAGCTCACAGCGATTGC	*ccpA* KO, middle primer
NB066	AAAGTCGACGCTGGCAATGTGAAACAATATGATCC	*ccpA* KO, *Sal*I site (downstream of gene termination)
NB067	AAAGACTCGAGGAATATGCAGTGAGGCTCTTATGATT	LFR *lef* promoter for GFP construct, *Xho*I
NB070	AAAGAGAATTCAAGATGAAGATCGACAAAATGGCTC	RFR, downstream of *lef* gene for GFP construct, *EcoR*I
NB071	GCGCGTCGACCTCTAGATTTAAGAAGGAGATATAC	Amplify GFP, *Sal*I
NB072	GTAACTAGCGACTCAGGAATTGATGCTCGTCCAGCAACTCTACTT	HPr His14 → Asp
NB073	AAGTAGAGTTGCTGGACGAGCATCAATTCCTGAGTCGCTAGTTAC	HPr His14 → Asp
NB074	GCATGCATTATATGCTTTTAACTAGTTCAACAACTTCTTCAGC	Primer 1 (end of *ptsI* gene) to amplify *ptsHI* with His_6-HPr and *atxA* RBS *Sph*I site
NB075	ATGCACCACCACCACCACCACGAAAAAATCTTTAAAGTAACTAGCGAC TCAGG	Primer 2 (add His_6 to HPr) to amplify *ptsHI* with His_6 on HPr and *atxA* RBS
NB076	GTCGA**C**AGGAAAGGAGAATCAATTATAGACATGCACCACCACCACCA	Primer 3 (add *atxA* RBS and *Sal*I cut site) to amplify *ptsHI* with His_6 on HPr and *atxA* RBS
NB077	GCATGCCAGTGTCGACATAAAGACGGGACCACTCAAAG	LFR *lef* promoter for GFP construct, *SphI, SalI*
NB078	GTCGACACTGGCATGCGGGACCAGCCATTATGAAGCAAC	RFR, downstream of *lef* gene for GFP construct, *SphI,SalI*
NB079	AAAGCATGCTAGTGGTGATGGTGATGATGTTTGTATAGTTCATCCATG CCATG	Amplify GFP-His_6, *Sph*I, paired with NB071
NB144	ATGTTAAGAGTGTGGTGGTGGTGGTGGTGCATTATTCTCCTAATCCTTC GTTTTTCATAG	Add His_6 tag sequence to 5' end of *ptsI*, overlap with NB145
NB145	CTATGAAAAACGAAGGATTAGGAGAATAATGCACCACCACCACCACCA CACTCTTAACAT	Add His_6 tag sequence to 5' end of *ptsI*, overlap with NB144
NB150	AAGGATCCTTAGTGGTGGTGGTGGTGGTGTATTATCTTTTTGATTTCAT GAAAATCTCTTTCTG	*Bam*HI site, stop codon, C-terminal His_6 *atxA*
NB151	TTTCACAGCTAAGGAAAGGAGAATCAATTATAGACATGCTAAC	*atxA* RBS and overlap with GBAA_2500 promoter
NB152	TTCTCCTTTCCTTAGCTGTGAAATCTAAAGGATGATAATATCT	GBAA_2500 promoter with overlap to *atxA* RBS

NB153	TTGGATCCTCTACTATACAATAGCTCGCAACGTAATTG	GBAA_2500 promoter and *Bam*HI site
ES40	AACTGCAGTGTTGCGGAAACGTTAAAGA	PstI site, used to knockout plcR
ES41	CGGGATCCCGATTCAATTCGGCTCACTT	Used to knockout plcR
ES42	CGGGATCCTTGAAAACGCAATTGCAAAC	plcR knockout LFR
ES43	ACGCGTCGACTCGTATCTCCTGCCCAATTC	SalI cute site, plcR knockout LFR
LH17	GTTAACTTAAAAGCTATCATGGGCGTTATG	HPr Ser46 → Ala
LH18	CATAACGCCCATGATAGCTTTTAAGTTAAC	HPr Ser46 → Ala
LH44	GGTAGTCGACAGGAAAGGAGAATCAATTATAGACATGAGTAATTATCTAGAAATTAAAAAAG	*Sal*I, *atxA* RBS, GlcT F (48C)
LH47	TCAGCATGCTTAGTGGTGGTGGTGGTGGTGTCCTCCCACATGCTCTGCTTTCAC	*glcT,* His_6, STOP, *Sph*I R (48C)
MT10	GGTAGTCGACATTTAAAGGAGATAAATTATCATG	*ptsH* RBS (*Sal*I) (used to make pUTE1034)
MT13	GGGCATGCATCGACTCAGGTTTTTTTATTAATTA	*ptsI* stop codon (*Sph*I) (used to make pUTE1034)
TH235	GAGATCTAGACTAGTAGCACTTGGTGGTAAAG	LFR *ptsHI* KO, *Xba*I
TH245	CGACTCAGGTTTTTTTATTAATTACATGATAATTTATCTCC	LFR *ptsHI* KO
TH246	GGAGATAAATTATCATGTAATTAATAAAAAAACCTGAGTCG	RFR *ptsHI* KO
TH244	CAGCCTCGAGTTCATACGGAAGCTTTATCGCAC	RFR *ptsHI* KO, *Xho*I
TH310	GTAACTAGCGACTCAGGAATTGCTGCTCGTCCAGCAACTCTACTTG	HPr His14 → Ala (___ is the changed sequence)
TH311	CAAGTAGAGTTGCTGGACGAGCAGCAATTCCTGAGTCGCTAGTTAC	HPr His14 → Ala (___ is the changed sequence)

Chapter III.

The relationship of the PTS with AtxA and virulence in *Bacillus anthracis*

3.1 Introduction

The high resolution structure of the AtxA protein suggests carbohydrate import and metabolism may be important environmental signals for AtxA activity (Hammerstrom *et al.*, 2015). The structural organization of AtxA is conserved among a class of transcriptional regulators subject to phosphorylation by the PTS known as PRD-containing regulators (Stulke *et al.*, 1998, Hammerstrom *et al.*, 2015). At the N-terminus of the protein are two helix-turn-helix domains, indicative of DNA binding; in the center of the protein are two PTS regulatory domains, typically targets for PTS phosphorylation; and at the C-terminus, a domain resembling EIIB of the PTS, sometimes a target for phosphorylation and/or protein-protein interactions (Hammerstrom *et al.*, 2015). AtxA is phosphorylated at two histidine residues within the PRDs, and the EIIB domain is necessary for homomultimerization. Phosphorylation of the H199 within PRD1 allows for AtxA activity as a positive transcription regulator, and phosphorylation at H379 within PRDII inhibits AtxA multimerization and activity (Hammerstrom *et al.*, 2015, Hammerstrom *et al.*, 2011, Tsvetanova *et al.*, 2007).

PRD-containing regulators are subject to phosphorylation by up to three components of the PTS (Stulke *et al.*, 1998). Most transcriptional regulators with PRDs are activated through phosphorylation by His15-P at a conserved histidine. When a readily metabolizable substrate, such as glucose or fructose, is present, His-15 is in its dephosphorylated form, and therefore doesn't phosphorylate PRD-containing regulators, resulting in their inactivity (Deutscher *et al.*, 2014). The EIIA and EIIB components of cognate PTS systems can phosphorylate a cognate PRD-containing regulator to deactivate the protein activity. In the presence of the associated sugar the

phosphate is transferred from the EII components to the incoming sugar, and EII doesn't phosphorylate the PRD-containing regulator, thus relieving the repression and activating the regulator (Galinier & Deutscher, 2017).

AtxA, like other PRD-containing regulators is subject to phosphorylation; however, the conditions under which it is phosphorylated, and the system responsible for the phosphorylation in *B. anthracis* have not been elucidated. Evidence of the involvement of the PTS in AtxA activity exists in the non-native host *B. subtilis*. In a *B. subtilis* strain engineered to express AtxA, and a reporter for AtxA activity, a *pag-lacZ* reporter, the PTS appears to play an inhibitory role in AtxA activity (Tsvetanova *et al.*, 2007). AtxA activity at the pagA-*lacZ* reporter was increased in the *ptsHI* mutant of *B. subtilis*, suggesting HPr may responsible for phosphorylated AtxA and inhibiting its activity. PTS-mediated regulation of PRD-containing regulators may differ between organisms (Joyet *et al.*, 2015) and thus I sought to explore the relationship of the PTS and AtxA in the native host, *Bacillus anthracis*.

3.2 Results

3.2.1 Toxin synthesis and virulence in a PTS-deficient *B. anthracis* mutant is diminished.

I wanted to determine if the PTS affects AtxA-mediated toxin gene expression in *B. anthracis*. I generated a *ptsHI*-null mutant, UT439, from the parent *B. anthracis* strain, ANR1. Culture supernates from cultures grown in CA medium with 0.08% dissolved bicarbonate in 5% atmospheric CO_2 ($CACO_3$), conditions reported to allow high levels of toxin production (Haines *et al.*, 1965), were probed with anti-LF, anti-EF, and anti-PA sera using western blotting. As shown

in Figure 3.1, the toxins were readily detected in culture supernates of the parent strain, but were not detected in culture supernates of the *ptsHI*-null mutant harboring an empty vector. Ectopic expression of *ptsH* or *ptsI* in this mutant was not sufficient to restore toxin synthesis. However, when both *ptsH* and *ptsI* were present on the complementation vector, toxin production was restored to a level similar to that of the parent strain.

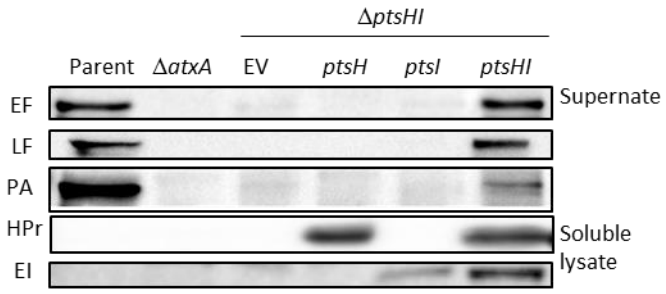

Figure 3-1 Toxin production by parent and mutant strains. Culture lysates and supernates were obtained during the transition phase (4h) of growth from cultures grown in $CACO_3$ medium. Samples of culture supernatants were concentrated 10X and subjected to SDS-PAGE followed by western blot with α-LF serum, and α-THE^{TM}His mAb to detect HPr and EI. Δ*ptsHI* (UT439) was complemented with EV (empty vector pAW285) or genes *ptsH* (pUTE1143), *ptsI* (pUTE1144), or *ptsHI* (pUTE1145) as indicated.

To determine if the PTS plays an important role in the toxin-dependent A/J model, I compared the virulence of the parent strain to that of the *ptsHI*-null mutant UT439. A/J mice are complement-deficient and are susceptible to toxin-mediated infection with the non-capsulated Sterne-type strain, ANR-1. Our previous studies have demonstrated that an *atxA*-null mutant is avirulent in this model when mice are injected via the tail vein with up to 10^9 spores (Dai *et al.*, 1995). As shown in Figure 3-2, all mice infected with the parent strain were moribund within 96 hours and *B. anthracis* was recovered from the liver, lung, and spleen. All mice infected with UT439 survived the seven-day experiment with no symptoms of disease, and *B anthracis* was not recovered from tissue of the collected organs.

The structure of AtxA, the phosphorylation events in the AtxA PRDs to control AtxA activity and dimerization, the decrease in toxin production *in vitro*, and the drastic effect on virulence *in vivo*, support the hypothesis that the PTS is required for AtxA activity.

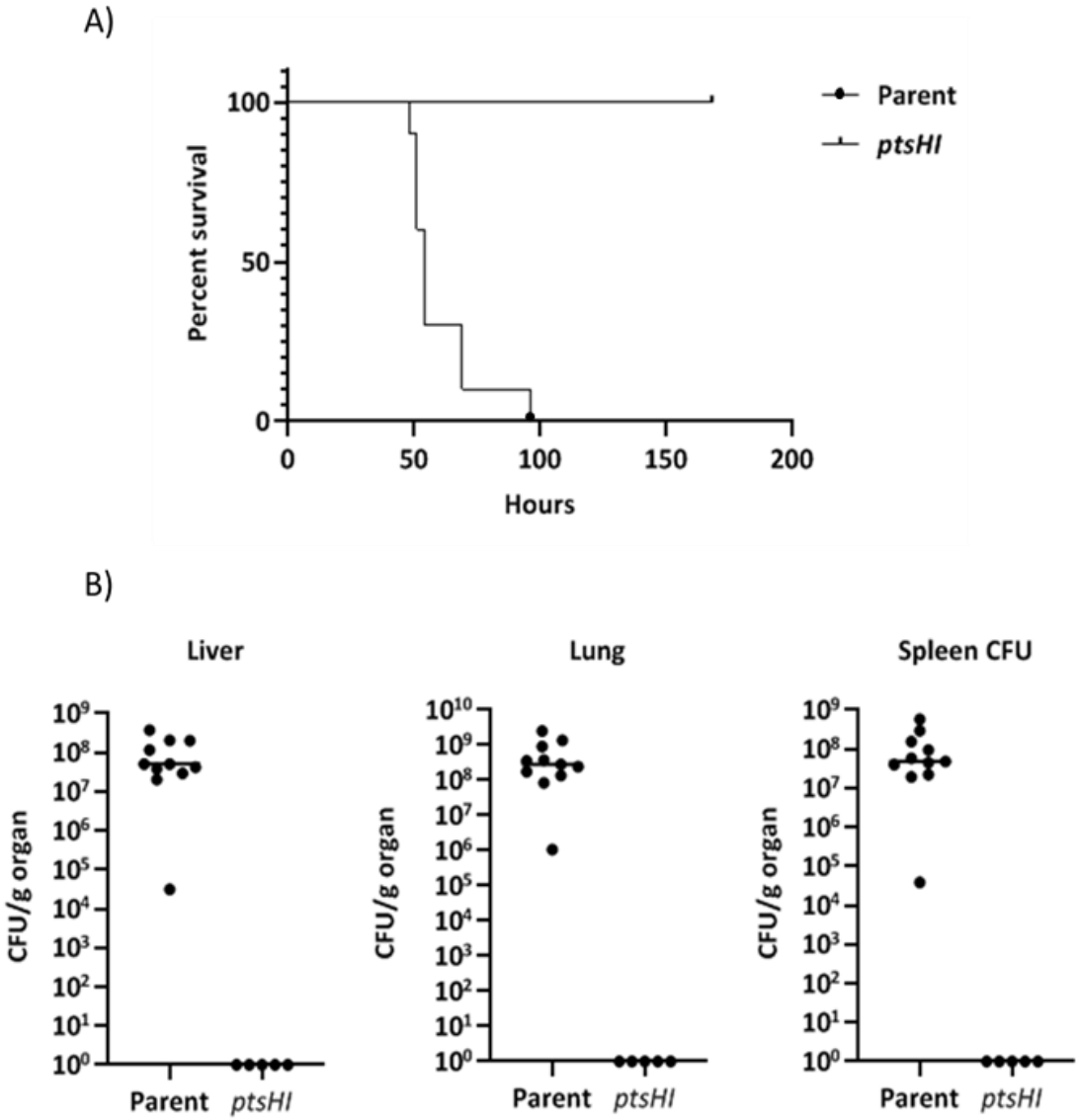

Figure 3-2. Virulence of parent and *ptsHI* mutants. A) Survival curves of mice infected intravenously with vegetative *B. anthracis* are shown. A/J mice were injected i.v. with 2.75 X 10^3 CFU of the parent (black solid line; *n* = 6), and 3 × 10^3 CFU of *ptsHI*-null (gray solid line; *n* = 6), vegetative cells. B) CFU/g of tissue collected.

3.2.2 Influence of PTS sugars and the PTS proteins HPr and EI on AtxA activity *in vivo*.

The influence of the PTS on PRD-containing regulators differs in response to specific sugars (Deutscher *et al.*, 2006). When a PTS substrate is present in the medium, the cognate EII PTS components are stimulated to relay phosphate to the incoming sugar, thus affecting the flux of phosphate through the system. To ascertain whether AtxA activity is affected by the presence of PTS substrates (PTS sugars) compared to sugars transported by alternative means (non-PTS sugars), I assessed AtxA activity in cultures grown in $CACO_3$ medium supplemented with 0.1% glycerol and 0.1% of the specified added sugar. Our *in vivo* assay for AtxA activity employs strain UT376 (pUTE991). In this strain *atxA* is deleted from its native locus and expressed from an IPTG inducible promoter, and the *lef* promoter at the native locus is fused to a promoter-less *lacZ* gene (Hammerstrom *et al.*, 2011). In this strain, transcriptional control of atxA is uncoupled from AtxA function, allowing quantitative assessment of AtxA activity upon IPTG-induction. β-galactosidase activity was measured in cell lysates from cultures grown in the presence of the PTS substrates (glucose, fructose, or mannitol) and in the presence of non-PTS sugars (glycerol or melibiose). As shown in Figure 3-3, there was no significant difference in AtxA activity in the cultures containing PTS and non-PTS sugars. These data indicate that engagement of the PTS components and flux of phosphate through the system does not influence AtxA activity.

To further investigate the potential role of the PTS in AtxA function, I used the P*lef-lacZ* reporter system to compare AtxA activity in the PTS-containing strain UT376 (pUTE991) and PTS-null mutant, UT408 (pUTE991). Cultures of the strains were grown in $CACO_3$ medium, AtxA expression was induced using IPTG, and activity at the P*lef-lacZ* reporter was determined. The

PTS mutant in this case had variable growth and made loading the proper protein amount difficult. Proteins levels were normalized to the internal loading control, the β-subunit of RNA polymerase. β-galactosidase activity was comparable between the PTS-containing strain and the PTS-lacking mutant in cultures containing similar levels of AtxA (Fig. 3-4), supporting the conclusion that the PTS does not function to activate AtxA activity.

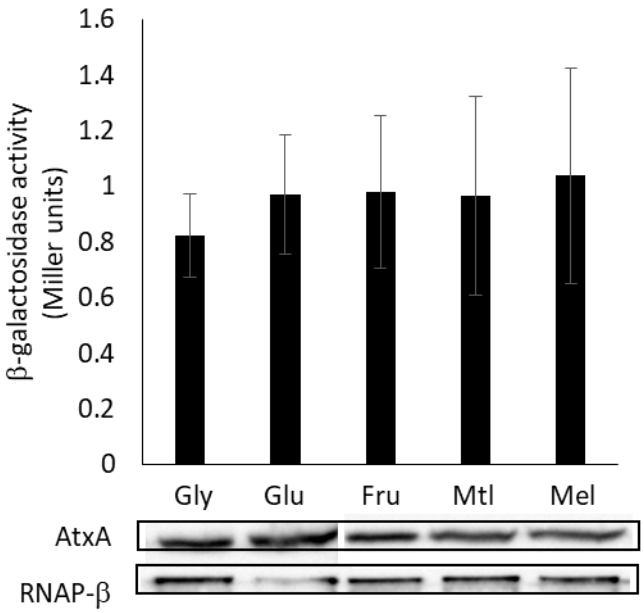

Figure 3-3. AtxA activity at the *lef* promoter in the presence of PTS sugars. Cultures of the *B. anthracis* reporter strain UT376(pUTE991) were grown in $CACO_3$ medium containing 0.1% glycerol and 0.1% added sugar as indicated. Gly is glycerol, glu is glucose, fru is fructose, mtl is mannitol, and mel is melibiose. Cells were collected from cultures at late exponential phase (4h growth) for AtxA activity assays and western blotting with α-THE^{TM}His antibody. AtxA activity was assessed as β-galactosidase activity from a P*lef-lacZ* transcriptional fusion. Data represent the average of three independent experiments. A student's T-test was performed to determine significant differences between AtxA activity in glycerol compared to the other sugars. All p- values in this assay were greater than 0.05 and were not noted on the graph.

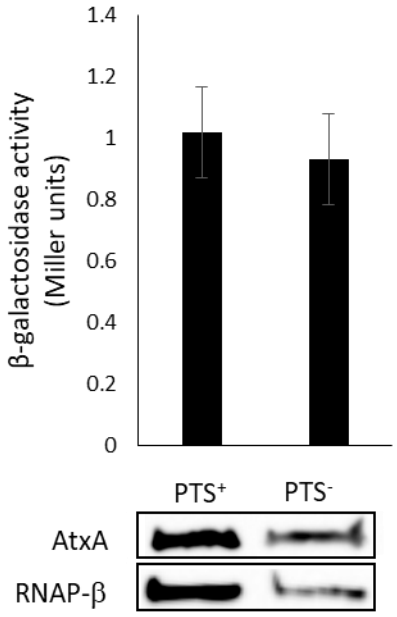

Figure 3-4. AtxA activity at the *lef* promoter in the absence of the PTS. Cultures of the *B. anthracis* reporter strains UT376(pUTE991) (PTS+) and the *ptsHI*-null mutant (PTS-) expressing *atxA* from a plasmid UT417(pUTE991) were grown in $CACO_3$ medium. Cells were collected from cultures at late exponential phase for AtxA activity assays and western blotting with α-THE^{TM}His antibody. AtxA activity was assessed as β-galactosidase activity from a P*lef-lacZ* transcriptional fusion. β-galactosidase activity presented is the average of at least three separate experiments. A representative western is shown. A student's T-test was performed, the p-value was greater than 0.05 and was therefore not noted on the graph.

3.2.3 *In vitro* phosphorylation of AtxA

The *B. subtilis* transcriptional antiterminators GlcT and SacY are two examples of PRD-containing regulators subject to phosphorylation by HPr, for which the protein activity is independent of HPr phosphorylation. GlcT and SacY are phosphorylated by HPr, but this phosphorylation does not control protein activity (Crutz *et al.*, 1990, Stulke *et al.*, 1997). The observation that AtxA activity is unaffected by different sugars in the medium, and that AtxA activity was the same in the parent and *ptsHI* mutant, led me to ask whether AtxA, like GlcT and SacY, may be phosphorylated by the PTS despite PTS-independent activity.

To detect EI- and HPr-mediated phosphorylation of AtxA in conditions similar to those reported for other PRD-containing proteins, His_6-tagged proteins were purified from *B. anthracis* and incubated in various combinations with ^{32}P-labeled-PEP using conditions previously reported (Joyet *et al.*, 2010, Tortosa *et al.*, 2001, Martin-Verstraete *et al.*, 1998). *In vitro* transfer of phosphate from PTS proteins to PRD-containing regulators has been demonstrated for many PRD-containing regulators (Joyet *et al.*, 2010, Schmalisch *et al.*, 2003, Tortosa *et al.*, 2001). Reactions were subjected to SDS-PAGE followed by phosphor-imaging to assess protein phosphorylation (Fig. 4). The *B. anthracis* homologue of GlcT, a well-studied PRD-containing regulator from *B. subtilis*, was used as a positive control. As seen in Figure 3-5, EI was successfully labeled with the ^{32}P-PO_4 when incubated alone or with other proteins (lanes 1 and 5-11). A radiolabeled band corresponding to phosphorylated HPr was detected when HPr and EI were incubated together (lanes 5 and 8-11), but not when HPr was incubated without EI (lanes 2 12,

A)

	1	2	3	4	5	6	7	8	9	10	11	12	13
EI	+				+	+	+	+	+	+	+		
HPr		+			+			+	+	+	+	+	+
GlcT			+			+		+				+	
AtxA				+			+		+	+[1]	+[2]		+

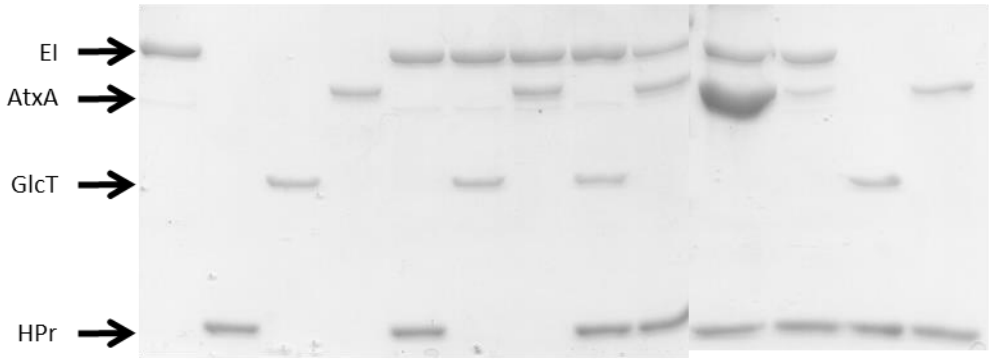

B)

	1	2	3	4	5	6	7	8	9	10	11	12	13
EI	+				+	+	+	+	+	+	+		
HPr		+			+			+	+	+	+	+	+
GlcT			+			+		+				+	
AtxA				+			+		+	+[1]	+[2]		+

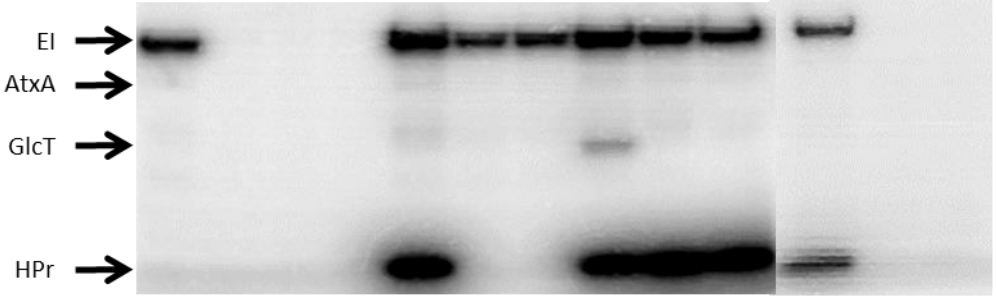

Figure 3-5. *In vitro* phosphorylation assay with the PTS proteins HPr and EI. Proteins present in each lane are indicated by "+". Hexa-His EI, HPr, GlcT, and AtxA were induced in *B. anthracis* and purified via nickel-affinity purification. ^{32}P-PEP was mixed with the proteins and incubated at 37° C for 30 min. A) Samples were separated on 10% poly-acrylamide-SDS gels and stained with Coumassie blue. B) The proteins were subjected to SDS-PAGE, dried, and exposed to a phosphor-imaging screen. Proteins present in each lane are indicated by the table. [1]Ten fold more AtxA was added to the reaction. [2]Purified AtxA was treated with calf-intestine alkaline phosphatase followed by removal of the phosphatase, prior to incubation.

and 13), indicating transfer from phosphorylated EI to HPr, as expected. Phosphorylated GlcT was detected when incubated with EI and HPr (lane 8), indicating that the purified PTS proteins were functional in transferring ^{32}P-PO_4 to a PRD-containing regulator in our system. We did not detect phosphorylated AtxA when the protein was incubated with ^{32}P-PEP and any combination of the PTS proteins, including a reaction containing excess AtxA (lane 10). To exclude the possibility that AtxA was purified in its fully phosphorylated form, and therefore unable to accept ^{32}P-PO_4, purified AtxA was treated with agarose-bound alkaline phosphatase prior to incubation with HPr and EI. Again, phosphorylated AtxA was not detected (lane 11).

Although HPr successfully phosphorylated *B.a.* GlcT under the conditions I used, there is a possibility that my *in vitro* phosphorylation assay for AtxA phosphorylation was not working. AtxA is a recalcitrant protein that requires high salt concentrations to remain soluble in solution, and may not be in its native conformation under these buffer conditions. To date our lab has not been successful in establishing an assay to assess AtxA activity *in vitro*, therefore I was unable to determine via AtxA activity if purified AtxA is in its functional form. To control for the possibility that AtxA is not in the native conformation *in vitro* and cannot be phosphorylated by HPr *in vitro* I wanted to take an *in vivo* approach to detect phosphorylated AtxA as had initially been done by Tsvetanova (2007). Several approaches may be taken to detect phosphorylation of proteins. Using radiolabeled ^{32}P phosphorylated proteins may be detected *in vitro* or *in vivo.* Mass spectrometry can measure the difference in mass of a protein in its unphosphorylated and phosphorylated forms. A technology called PhosTag™ may be added to SDS-PAGE gels to slow the mobility of phosphorylated through the gels such that unphosphorylated and phosphorylated

forms of the protein form distinct bands. The ability to generate antibodies toward specific amino acid residues in the phosphorylated form has improved the field and provided a relatively easy way to distinguish phosphorylated proteins from their unphosphorylated state.

3.2.4 *In vivo* phosphorylation of AtxA

Phosphorylated histidine residues have historically been difficult to study due to the unstable nature of the high energy phosphoramidate bond's susceptibility to acids and other nucleophiles. Due to the acid-labile nature of phosphorylated histidine residues mass spectrometry is not yet an option to detect proteins phosphorylated at histidine residues. Many scientists have tried to raise antibodies against phosphorylated histidine residues, but again, the bond appears to be too labile and could not successfully stimulate production of a pan-His-P antibody. In recent years the Miur lab at Princeton University successfully generated a pan-specific antibody for the detection of phosphorylated histidine (70). I took several approaches to detect phosphorylated AtxA *in vitro* and *in vivo* including using the pHis antibody to try to detect AtxA *in vivo.*

AtxA was first detected using an *in vivo* phosphorylation assay in which cultures of *B. anthracis* were grown in the presence of ^{32}P and AtxA was purified, subjected to SDS-PAGE, and imaged using a phosphorimager (Tsvetanova *et al.*, 2007). Troy Hammerstrom published in his thesis that he had tried to replicate the work to detect AtxA *in vivo* but had been unsuccessful. Having made slight improvements to the protocol I tried to replicate the work of Tsvetanova and performed *in vivo* phosphorylation assays to detect AtxA.

I purified AtxA-His6 from cultures grown in LB air supplemented with 1 mCi of ^{32}P (Fig 3-9, panel A), and cultures grown in phosphate-free $CACO_3$ supplemented with ^{32}P (Fig 3-9, panel B). As a positive control, cultures expressing EI-His6 were grown in parallel and I purified radiolabeled EI-His6. Phosphorylated EI was detected under both conditions, however a band corresponding to AtxA was not observed in either case. A faint band was observed in Figure 3-6, panel B, which may have corresponded to AtxA but was not readily reproducible and therefore I did not feel confident in my ability to observe AtxA phosphorylation *in vivo* with and without the PTS present.

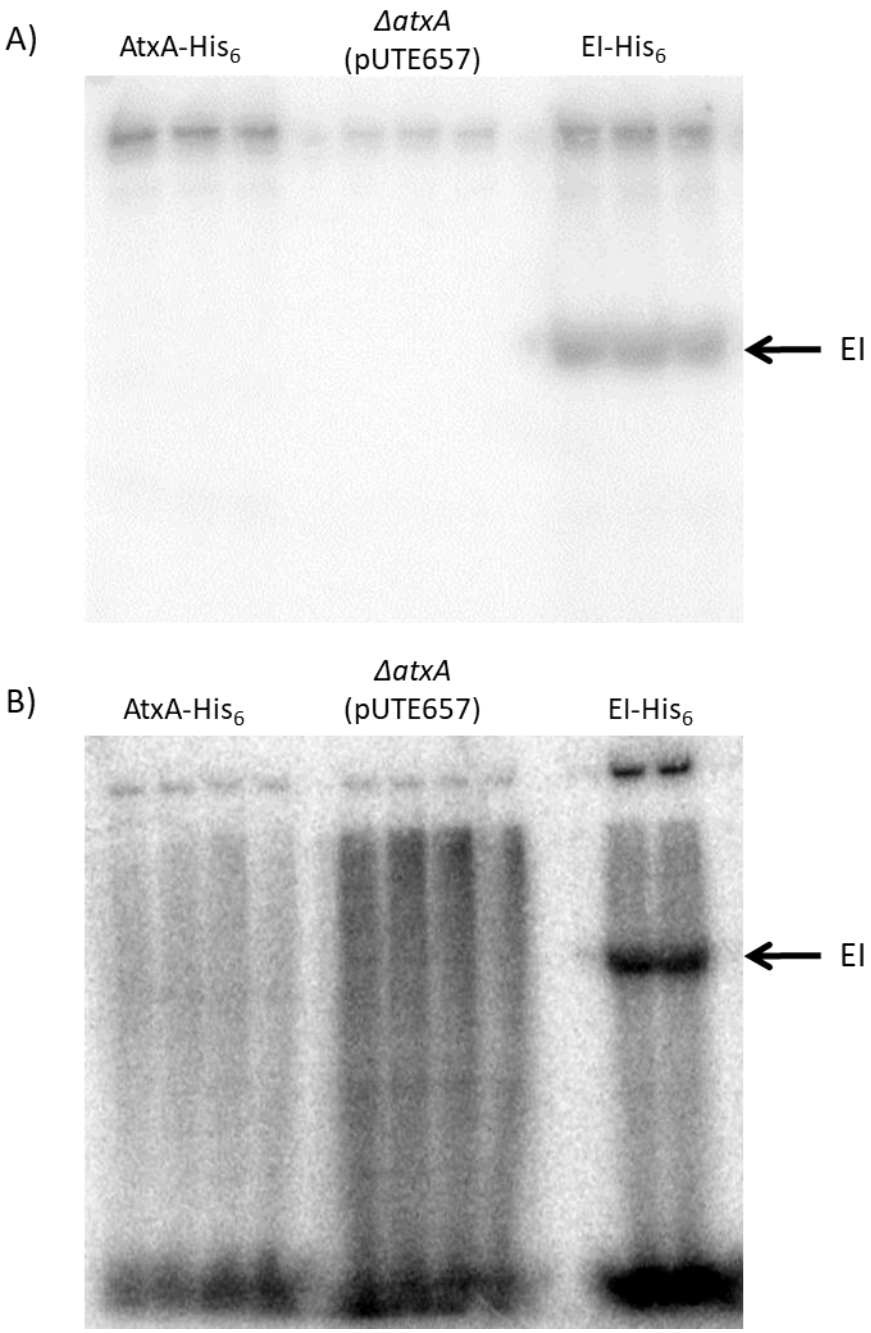

Figure 3-6. ***In vivo*** **phosphorylation to detect phosphorylated AtxA-His$_6$.** Cultures were grown in A) LB air supplemented, or B) phosphate-free $CACO_3$ medium supplemented with 1 mCi PO_4 . His_6-tagged protein production was induced after two hours of growth. Samples were collected after two hours of induction and incubation with ^{32}P-PO4. Cells were collected and the His_6 protein was purified following the AtxA purification protocol. Following purification the proteins were subjected to SDS-PAGE and exposed on a phosphorimager.

I next tried to use the Phos-Tag™ technology to detect phosphorylated AtxA-His6. The Phos-Tag™ reagent is a dinuclear metal complex capable of binding phosphomonoester dianions with a high affinity and anion selectivity toward the phenyl phosphate dianion. When phosphorylated proteins move through a polyacrylamide gel copolymerized with Phos-Tag™, the complex interacts in a reversible manner with the phosphorylated residue and slows the proteins' mobility through the gel (Kinoshita *et al.*, 2006). The mobility shift generates two separate bands on the gel of the same protein: correlating to the phosphorylated and non-phosphorylated forms of the protein. Phos-Tag™ acrylamide gels have been used to characterize phosphorylation patterns of proteins from Gram-positive and Gram-negative bacteria, both *in vivo* and *in vitro* (Barbieri & Stock, 2008, Tao *et al.*, 2012).

Using the Phos-Tag™ PAGE guidebook I tested conditions to optimize SDS-PAGE with Phos-tag™ acrylamide such that phosphorylated and non-phosphorylated forms of AtxA would run at different rates and produce distinct bands on a western blot. Each protein behaves differently and the conditions must be optimized for each protein individually, therefore the use of a positive control such as phosphorylated EI was not possible. In Figure 3-7 western blots of Phos-tag™ and regular acrylamide gels were compared to determine if two distinct bands of AtxA could be detected in the Phos-tag™ gel as opposed to one band in the regular acrylamide gel. Cell lysates (fig 3-7, panel A) of cultures induced with 10 μM IPTG to express native levels of AtxA, and of cultures induced with 40 μM IPTG to overexpress AtxA, were subjected to SDS-PAGE and membranes probed with THE™His-mAB. The phosphovariant of AtxA H199AH379A which is unable to be phosphorylated was used as a negative control. Protein levels of AtxA H199AH379A

appeared to be lower than the wild-type AtxA, but for the bands observed, a distinct second band corresponding to phosphorylated AtxA was not detected. Two bands were detected in both gels, corresponding to the AtxA monomer and AtxA dimer as previously seen by our lab (15). I did not detect a separate band corresponding to phosphorylated AtxA.

Purified AtxA, both the wild-type (WT) and H199AH379A (AA) phosphovariant, were also subjected to this analysis (fig 3-6, panel B). Additionally purified proteins were pre-treated with calf-intestine alkaline phosphatase as a negative control. Again, an additional band corresponding to phosphorylated AtxA was not detected when purified protein was subjected to PhosTag^{TM} gel electrophoresis.

Having tried *in vitro, in vivo,* and Phos-Tag^{TM} experiments, I next tried to use an antibody to detect phosphorylated histidine residues. Dr. Thomas Miur's lab at Princeton University was the first lab to generate a pan-specific pHis antibody. The Miur lab gifted me a portion of the antibody because it was not yet commercially available. To assess the phosphorylation state of AtxA *in vivo* I grew cultures in casamino acids medium in either air (CA-air) or in 5% atmospheric CO_2 ($CACO_3$). An *atxA*-null mutant, as well as a strain overexpressing the phosphoablative variant of AtxA (H199AH379A) were used as negative controls. Cells were collected and lysates subjected to SDS-PAGE followed by western blotting with pHis antibody. A band corresponding to AtxA (56kDa) was not observed on the α-pHis blot (Fig 3-7). AtxA is not very abundant in the cells, about 200 molecules of the protein are present (unpublished data from Malik Raynor). To test

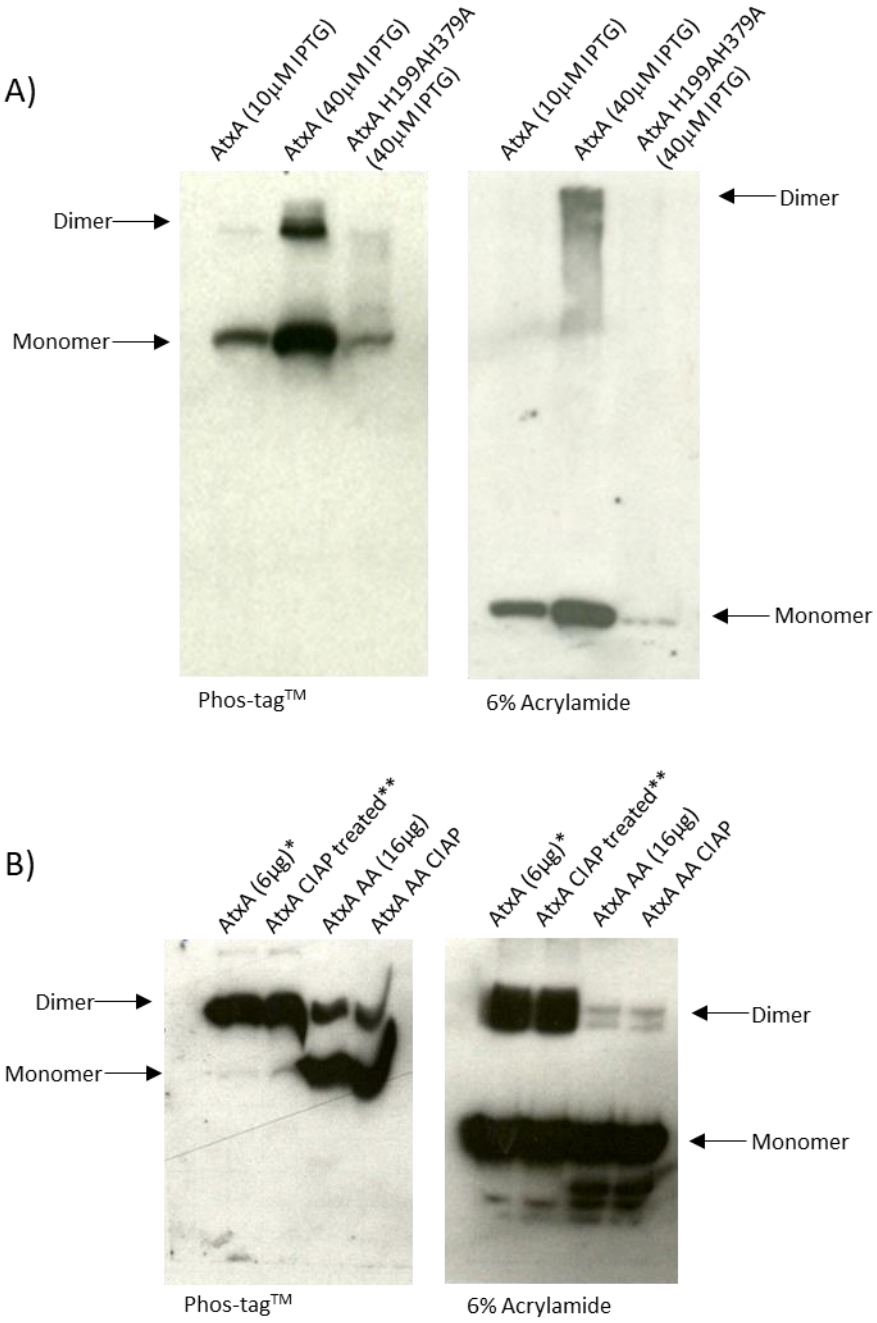

Figure 3-7. Use of Phos-tag™ technology to visualize phosphorylated AtxA . A) Cell lysates of cultures expressing AtxA-His_6 and B) purified proteins, were subjected to SDS-PAGE followed by western blotting with THE™His-mAb. Where specified 100 mM Phos-tag™ and 200 mM $MnCl_2$ were added to 6% acrylamide gels. CIAP was used to pretreat purified proteins as specified in the lanes.

the possibility that AtxA was not detected in cell lysates because the antibody was bound to other, more abundant, phosphorylated proteins, I purified AtxA.

I purified wild-type AtxA-His and AtxA(H199AH379A)-His from cell cultures and subjected the samples to western blotting with α-pHis (Fig 3-8). The phosphohistidine bond is both heat and acid labile, therefore proteins were treated with heat, and TCA precipitated as negative controls. Both forms of the protein were detected using the antibody despite treatment with heat and tricarboxylic acid. This was surprising because previous reports suggest AtxA is only phosphorylated at H199 and H379 and the double alanine mutant should not be phosphorylated (Tsvetanova *et al.*, 2007). In the Tsvetanova paper the authors grew *B. anthracis* cultures in LB medium supplemented with ^{32}P-H_3PO_4 and subsequently purified AtxA from cell lysates using a recombinant antibody specific for AtxA. Wild-type AtxA and AtxA carrying single alanine substitutions at H199 and H379 were detected using a phosphorimager. No radioactive band was observed when AtxA H199AH379A was purified, suggesting that H199 and H379 are the only two sites of phosphorylation under those experimental conditions.

Three possibilities exist for the observed binding of the pHis antibody to AtxA H199AH379A; 1) AtxA is phosphorylated at another histidine residue, 2) AtxA is phosphorylated at a tyrosine residue, such that the antibody interacts with the phosphorylated tyrosine as seen by Kee et al. (2013), or 3) the pHis antibody interacts with AtxA in a non-specific manner.

Culture conditions varied between the previously published work and the experiment done in this work. The Tsvetanova study was carried out in LB medium. Radiolabeled phosphoric

acid was added at the transition into stationary phase and AtxA was purified from samples collected from stationary phase cultures. My experiments were performed using CA medium, and collected just before the transition into stationary phase, the point at which AtxA levels are highest as determined by a previous student in our lab. It is possible that Tsvetanova didn't observe phosphorylation of the purified double alanine mutant of AtxA due to a low abundance of phosphorylated species. Phosphorylated histidine are acid and heat labile. To rule out phosphorylation at other histidine residues I subjected purified AtxA-6XHis, AtxAH199AH379A-6XHis and EI-6XHis to treatment with acid or heat. As demonstrated in Figure 3-8, panel A the treatments effectively abolished the phosphohistidine signal from purified EI, phosphorylated on a conserved H189, but did not prevent α-pHis interaction with AtxA wild-type or H199AH379A, suggesting the signal is not from phosphorylation of another histidine residue.

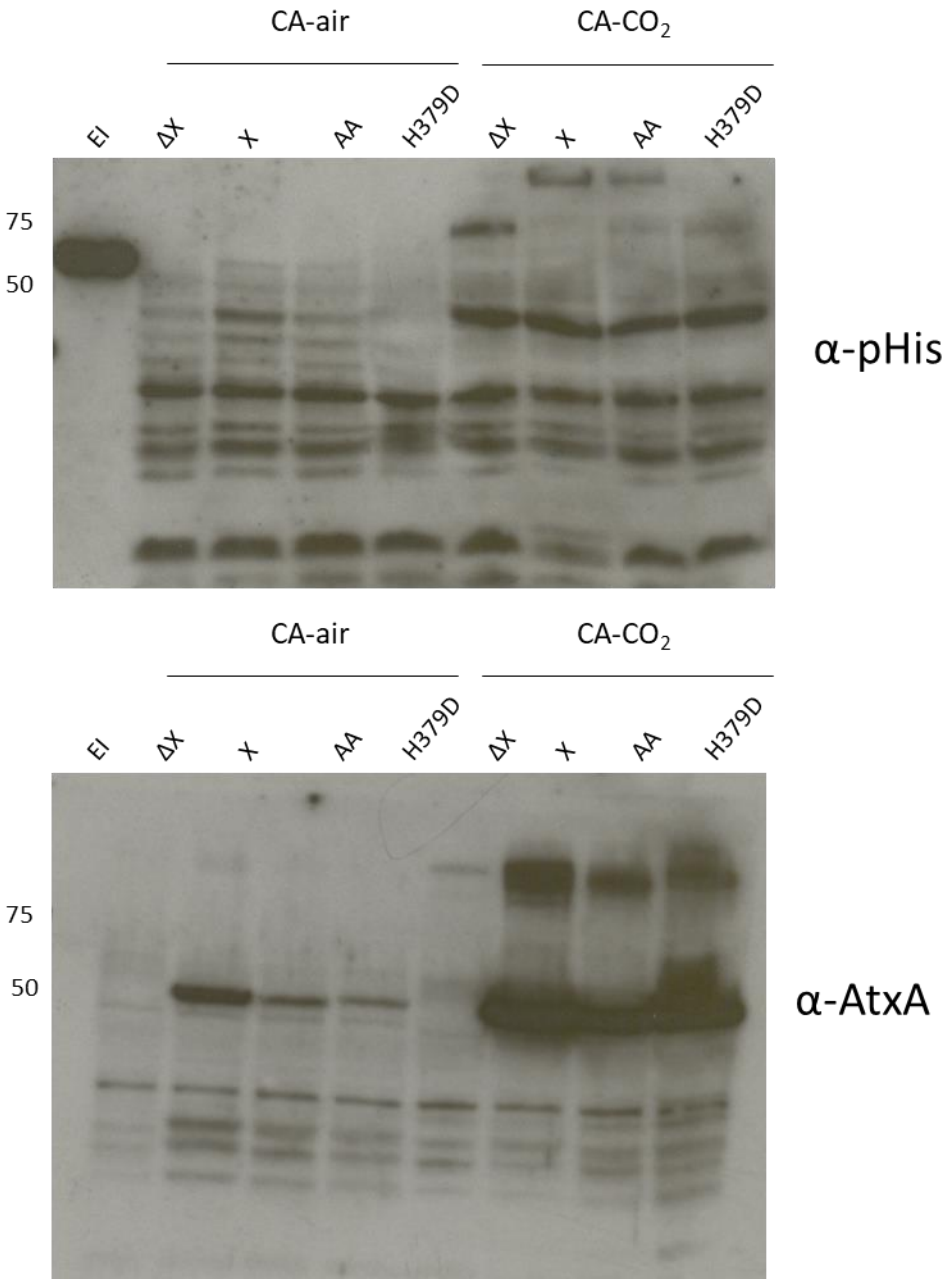

Figure 3-8. Probing cell lysates with α-pHis. Cell lysates of cultures grown in CA medium in air or in CO_2 were subjected to SDS-PAGE and probed with the phosphor-histidine-specific antibody (pHis) or AtxA specific sera. Purified EI was included as a positive control.

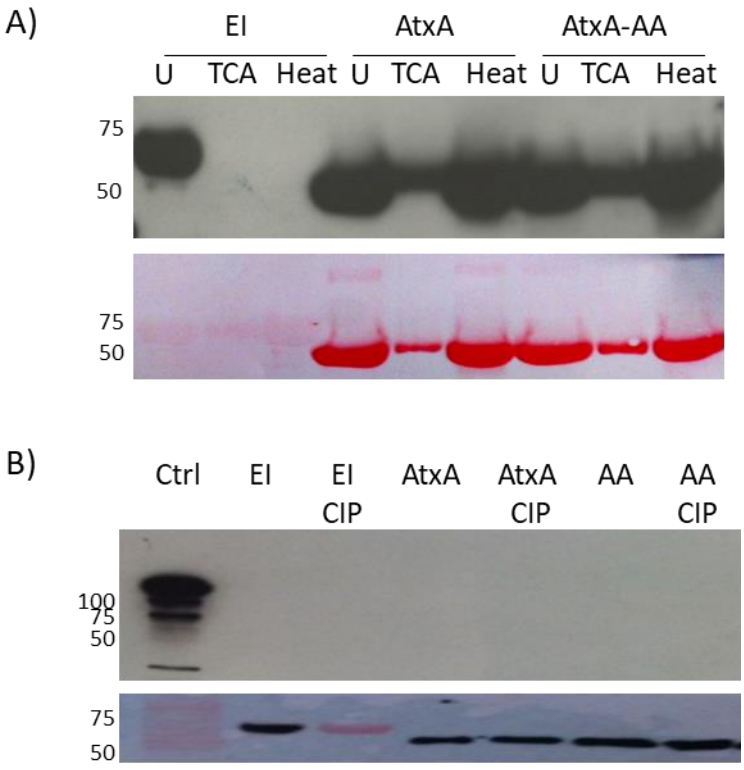

Figure 3-9. Use of the α-pHis and α-pTyr to detect proteins phosphorylated at histidine and/or tyrosine residues. A) Purified proteins were subjected to TCA precipitation (TCA), heated (heat), or untreated (U), and subjected to SDS-PAGE. The membrane was stained with PonceauS stain, and then probed with the α-pHis. B) Purified proteins were subjected to SDS-PAGE followed by PonceauS staining, and western blot to identify the proteins present and to detect any protein phosphorylated at a tyrosine residue. An antibody specific toward phosphorylated tyrosine residues was used, as well as THEHis™ mAB antibody. The PonceauS stain and THEHis™ mAB blot are overlaid to show the presence of each protein. A positive control provided with the antibody, A-431 lysate, was run in the first lane of the blot presented.

In the publication describing pan-specific pHis antibody, the authors noted some cross reactivity with pTyr residues (Kee *et al.*, 2013). Phosphorylated tyrosines are stable in both heat and acid. The detection of acid- and heat-treated AtxA with the pHis antibody may result from an interaction with a phosphorylated tyrosine. I purchased the pTyr antibody used in the pHis paper (Kee *et al.*, 2013) and performed a western blot analysis with purified proteins. The pTyr antibody was used to probe purified EI-6XHis, AtxA-6XHis and H199AH379A-6XHis, untreated, and treated with calf intestine phosphatase (CIP). As seen in Figure 3-8 panel B, only the positive control that came with the purchased antibody was observed on the western blot, suggesting AtxA is not phosphorylated at a tyrosine residue.

The results of Figure 3-8 showing interaction of AtxA with the pHis antibody regardless of treatment, as well as the negative results suggesting AtxA is not phosphorylated on a tyrosine residue, supports the conclusion that the pHis antibody interacts with AtxA in a non-specific manner.

3.3 Discussion

In this chapter data was presented demonstrating that the absence of the PTS proteins HPr and EI affects toxin production in culture and virulence in a toxin-dependent murine model for infection. I hypothesized that the PTS effect on toxin production was mediated by PTS control of AtxA phosphorylation and activity. Data obtained from physiological, genetic, and biochemical approaches do not support the hypothesis, but rather support the conclusion that the PTS does not affect AtxA activity *in vivo* and does not phosphorylate AtxA *in vitro*. Although AtxA

phosphorylation by the PTS *in vivo* could not be examined due to technical difficulties detecting phosphorylated AtxA, data obtained from the *in vivo* AtxA activity assays performed in the presence of various sugars and in the *ptsHI*-null mutant support the conclusion that the PTS is not involved in regulating AtxA activity. AtxA activity was the same at the P*lef-lacZ* reporter in both the parent and *pts-null* mutant, suggesting the presence of the PTS does not affect AtxA activity. AtxA activity is affected by phosphorylation of H199 and H379 as demonstrated previously (Tsvetanova *et al.*, 2007, Hammerstrom *et al.*, 2015, Hammerstrom *et al.*, 2011) and therefore would be expected to change in the presence or absence of the kinase responsible for the phosphorylation.

The initial observation of PTS involvement in AtxA activity was made in the non-pathogenic *B. subtilis*. Tsvetanova and coworkers ectopically expressed AtxA and *pagA-lacZ* in *B. subtilis* and assessed AtxA activity at the *pagA* promoter in the parent and *pts-null* mutant of *B. subtilis*. In their experiments they observed an increase in *pagA-lacZ* expression in the PTS-null mutant compared to the parent strain, suggesting the PTS plays an inhibitory role in AtxA activity. My data assessing toxin expression and virulence *in vivo* contradict the findings of Tsvetanova. I found a decrease in toxin production and virulence in the absence of the PTS, not an increase. This difference in data suggests the findings may be host-specific and that the PTS may function differently in the two organisms. AtxA is native to *B. anthracis* and thus it is important to explore the relationship of the PTS and AtxA in the native organism.

Although we could not test AtxA phosphorylation *in vivo* in the presence and absence of the PTS, the likelihood that the PTS is responsible for AtxA phosphorylation is very small. Phosphovariants of AtxA such that H199 and H379 are changed to mimic phosphorylated residues (H→D) or unphosphorylated residues (H→A) have altered AtxA activity and homomultimerization patterns (Tsvetanova *et al.*, 2007, Hammerstrom *et al.*, 2015, Hammerstrom *et al.*, 2011). These results suggest that phosphorylation of AtxA is effective in controlling AtxA activity, thus if the PTS was responsible for phosphorylation a difference in AtxA activity should have been observed in the PTS- strain relative to the parent, however it was not (Figure 3-4). It is more likely that AtxA is subject to phosphorylation by an unknown kinase of a yet to be identified system. Possible alternative systems and approaches to identifying the system and kinase is discussed in more detail in Chapter 6 of this work.

Chapter IV.

Transcription of *atxA* is influenced by the PTS in an HPr- and EI- dependent manner.

4.1 Introduction

Although many studies of PRD-containing proteins have focused on protein function and regulation of activity, relatively little is known regarding potential influence of carbohydrate metabolism and signaling on transcription of the genes encoding these regulators. The above evidence supporting a role for the PTS in toxin production through a mechanism other than control of AtxA protein activity led me to question the relationship of the PTS with *atxA* transcription.

Carbon catabolite repression (CCR) plays a role in regulating the transcription of genes related to carbohydrate import, metabolism, and utilization. In Gram-positive organisms CCR is carried out by CcpA binding to *cre* sites within promoters, mediated by HPrS46-P, and by control of PRD-containing regulators via phosphorylation by HPr and EII proteins (Deutscher *et al.*, 2014). In *B. anthracis* CcpA mediates a two-fold increase in *atxA* transcription in response to glucose in the medium. However, the promoter of *atxA* does not have a *cre* site, and direct binding of CcpA to the *atxA* promoter was not observed (Chiang *et al.*, 2011). In *B. subtilis* and other Gram-positive bacteria, CcpA is activated in the presence of rapidly metabolized carbon sources; ATP stimulates HPr kinase to phosphorylate HPr at a conserved serine residue, and HPr-SerP interacts with CcpA to positively allow for binding of CcpA to target *cre* sites (Deutscher *et al.*, 1995). To explore the possibility that the decrease in toxin production in the absence of the PTS was due to CcpA control on *atxA* transcription, I assessed the P*atxA-lacZ* reporter in parent, PTS-null, and *ccpA*-null mutants.

4.2 Results

4.2.1 Transcripts of *atxA* are reduced in the absence of HPr and EI.

Transcription of the P*atxA*-*lacZ* reporter was decreased in the *ptsHI*-null mutant compared to the parent, but was unaffected in the *ccpA*-null (Fig 4-1). Reporter activity in the *ptsHI*-null was restored when both HPr and EI were expressed, but not when either HPr or EI were expressed individually. In agreement with decreased levels of *atxA* transcript in the PTS-null mutant, lethal factor was undetectable in the supernates of this strain, as well (Fig. 4-1). According to the model developed in *B. subtilis*, and the observation made by Chiang, et al. (2011) in *B. anthracis*, HPr is expected to play a role in enhancing transcription of *atxA* in the presence of glucose by mediating CcpA activity. The requirement for the presence of both HPr and EI to restore *atxA* transcription to the parent level, suggested a mechanism independent of CcpA.

Generally, HPr affects transcription of genes through two pathways; by interacting with the catabolite control protein, CcpA in its HPrs-Ser46 phosphorylated form, and by phosphorylating PRD-containing transcriptional regulators. A third mechanism exists in *B. subtilis*, in which His15-phosphorylated HPr directly activates the transcription factor YesS similar to how HPrSer46P interacts with CcpA (Poncet *et al.*, 2009b). The need for both EI and HPr to restore *atxA* transcription in the PTS mutant suggests HPr affects *atxA* transcription in an EI dependent manner; either through phosphotransfer to a downstream, PRD-containing regulator, or by direct interaction with a downstream regulator in its His14 phosphorylated form. To discern between these possibilities we generated phosphovariants of HPr and assessed their ability to

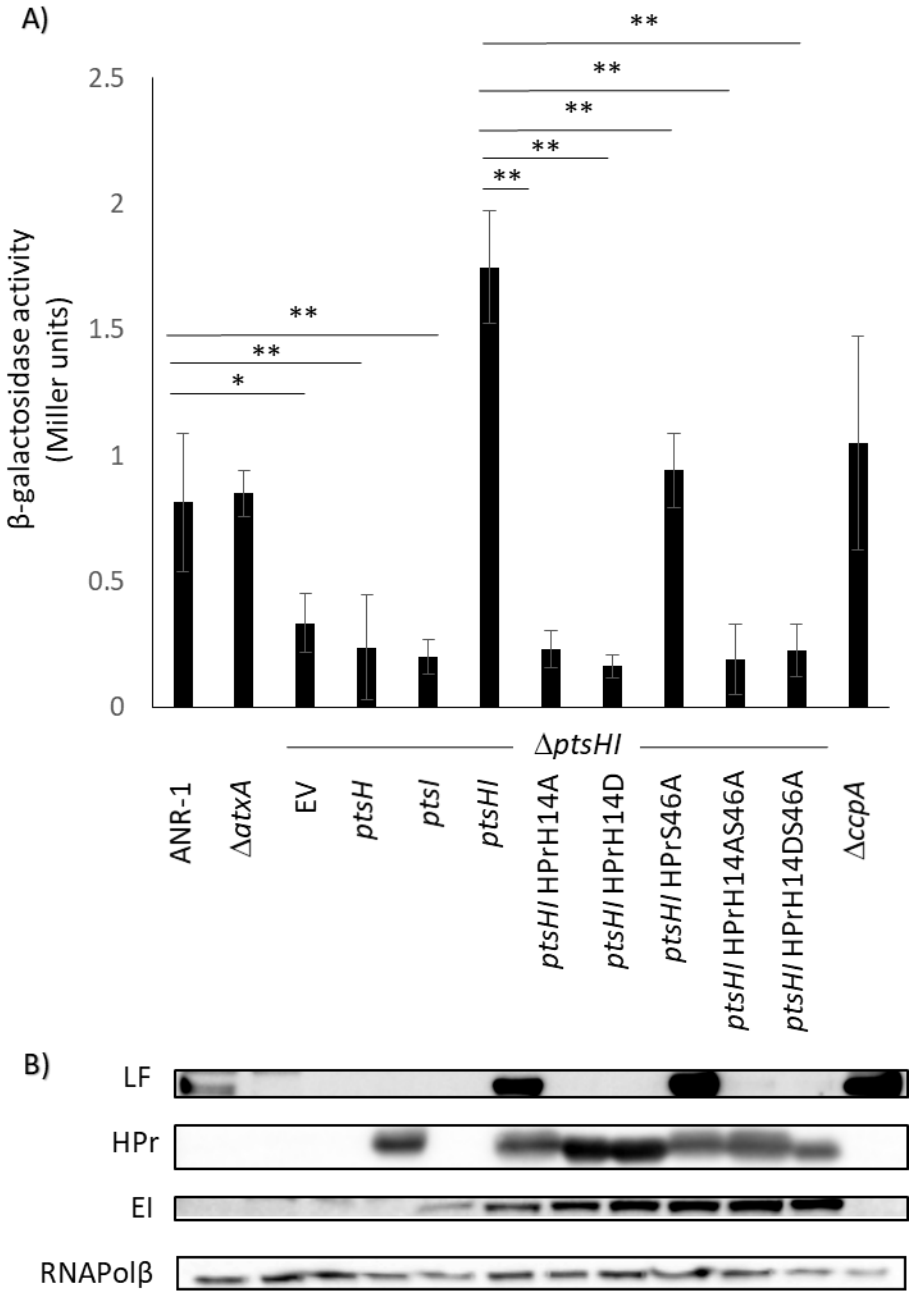

Figure 4-1. Transcription of P*atxA-lacZ*. Cultures of parent, PTS mutant, and PTS complementation strains carrying the P*atxA-lacZ* reporter pUTE843 were grown in $CACO_3$ to transition phase and collected for β-galactosidase assays and western blot analysis. A) β-gal activity from the P*atxA-lacZ* transcriptional fusion. B) Western blot of concentrated culture supernatants and cell lysates to detect lethal factor, HPr-His6, EI-His6, and RNAPolβ. * $p < 0.05$, ** $p < 0.01$

complement the *ptsHI*-null mutant when co-expressed with EI. If phosphotransfer activity is necessary, any substitutions to HPr-His14 would not functionally complement the *ptsHI* mutant, however, if HPr directly interacts with a downstream regulator in its His14-phosphorylated form, mimicking phosphorylation using a His to Asp substitution should allow for a functional complementation of the PTS mutant.

The phosphovariants with substitutions at H14 (H14A and H14D) were unable to complement the PTS-null phenotype (Fig 4-1), suggesting phosphotransferase activity associated with this residue is necessary for *atxA* transcription. A His to Ala substitution at HPr S46 did not affect *atxA* transcription, in agreement with no change in *atxA* observed in the *ccpA* mutant. The change measured by β-galactosidase assays was small, but significant, and enough to strongly affect toxin production. As shown in Figure 4-1, the decrease in *atxA* transcription observed in the PTS mutant and non-functional HPr complementation strains, correlated with undetectable toxin levels in the culture supernates. Overall these data support a model in which the PTS functions to phosphorylate a downstream regulator that directly or indirectly affects *atxA* transcription, and that this regulation is important for virulence factor production.

4.2.2. The PTS affects transcription from the primary promoter of *atxA* P1.

Transcription of *atxA* is initiated from two promoters; PI is the most predominant start site and is proximal to the translation start site, in contrast P2 is located approximately 600 bp upstream from P1 and is expressed weakly (Dai *et al.*, 1995, Bongiorni *et al.*, 2008). To further discern the PTS effect on *atxA* transcription, I determined at which promoter the PTS effect is

exerted. Using the transcriptional reporter assay with either the full length (P1 +P2) promoter region, or solely the proximal (P1) promoter region, I assessed activation of transcription at these loci in the parent and PTS-null mutant containing the reporter plasmid. As shown in Figure 4-2, transcription of *atxA* was decreased in the PTS-null mutant for both reporter constructs, regardless of the presence of P2, indicating that P1 is the promoter at which the PTS exerts its effect.

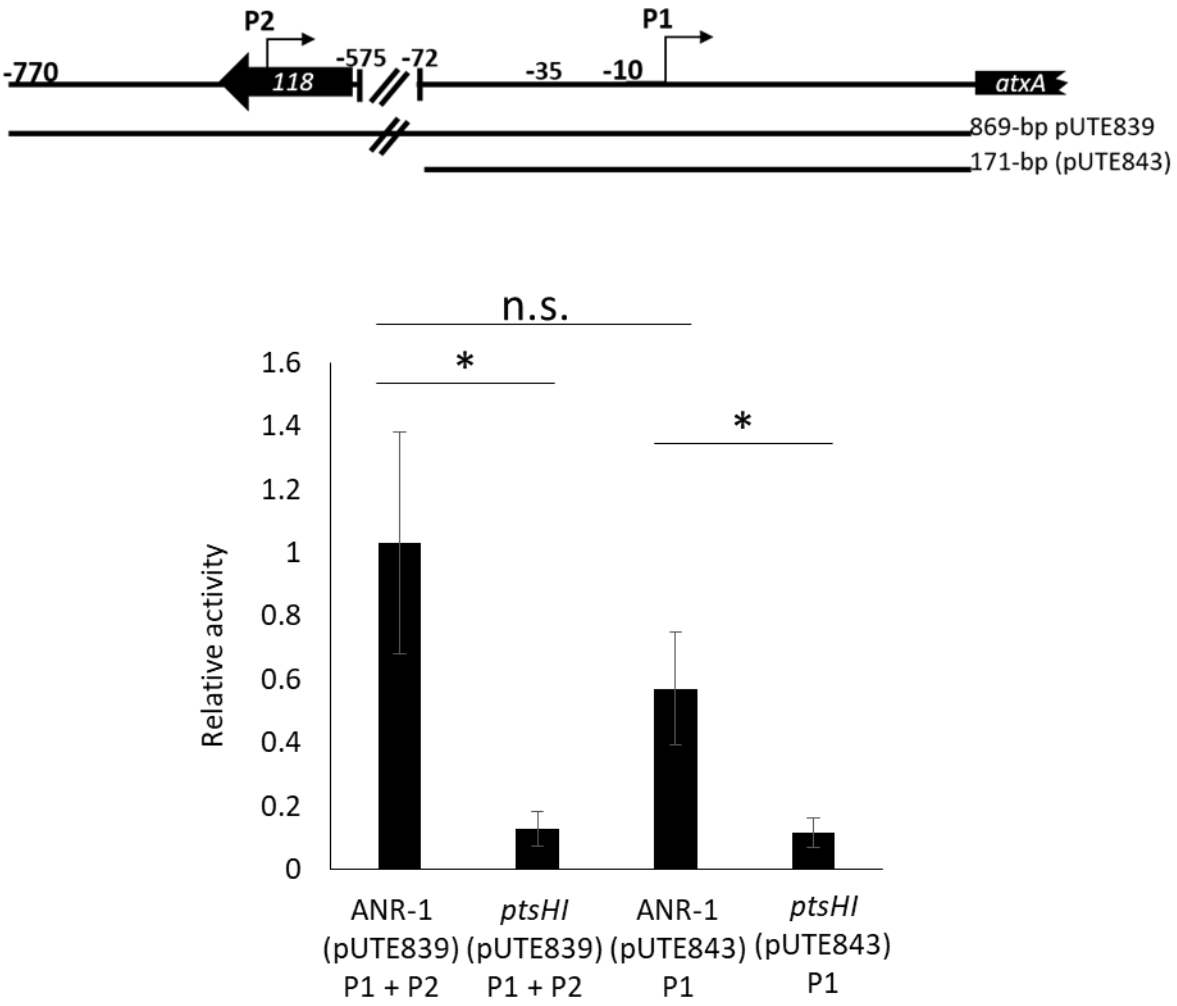

Figure 4-2. Relative expression of *lacZ* driven by *atxA* promoter regions P1+P2 (-770 bp to translational start) and P1 alone (-72 bp to translational start). Cultures of the B. anthracis harboring P*atxA*-*lacZ* constructs were grown in casamino acids medium containing 0.2% glucose and 0.9 % bicarbonate in 5% atmospheric CO_2. Cells were collected from cultures at late exponential phase (4h growth) for analysis of β-galactosidase activity representative of activity from the *atxA* promoter regions. Graph is representative of three biological replicates. Student's t-tests were performed to determine statistical significance between samples. * $p < 0.05$.

4.2.3. Using qRT-PCR to detect transcript levels of *atxA*

Transcription reporter systems are indirect methods for quantifying transcript levels. I attempted to assess *atxA* transcripts directly using quantitative reverse transcription PCR (qRT-PCR). I developed a TaqMan-based qRT-PCR assay to detect transcripts of *atxA* and, as an internal control, *gyrB*. Cultures of the parent, *ptsHI*-nulll mutant and the complemented strain *ptsHI(pptsHI)* were grown in $CACO_3$ medium to early transition to stationary phase and cells were collected for RNA isolation and qRT-PCR analysis. All transcripts were normalized to *gyrB*. The results presented in Figure 4-3 indicated that *atxA* transcript levels were about five times lower in the *ptsHI*-null mutant as compared to the parent consistent with the results from the transcriptional *lacZ*-fusion (Fig 4-1). *atxA* transcript levels were restored when wild-type HPr and EI were expressed in the cell from a complementation vector. Consistent with the β-galactosidase assays, expression of wild-type EI with the phosphovariants of HPr H14A and H14D could not complement the *ptsHI*-null phenotype.

Problems arose in the qRT-PCR assay after some time had lapsed between experiments. The same strains (parent, *ptsHI*-nulll, *ptsHI(pptsHI)*) and conditions were used, however the results were no longer reproducible. The assay had become qualitative; simply, if *atxA* transcript was present, regardless of abundance, the signal would be amplified without any quantitative pattern. To troubleshoot and determine what had changed I took the following steps; 1) I streaked the cells on plates to see if there were multiple colony morphologies and if

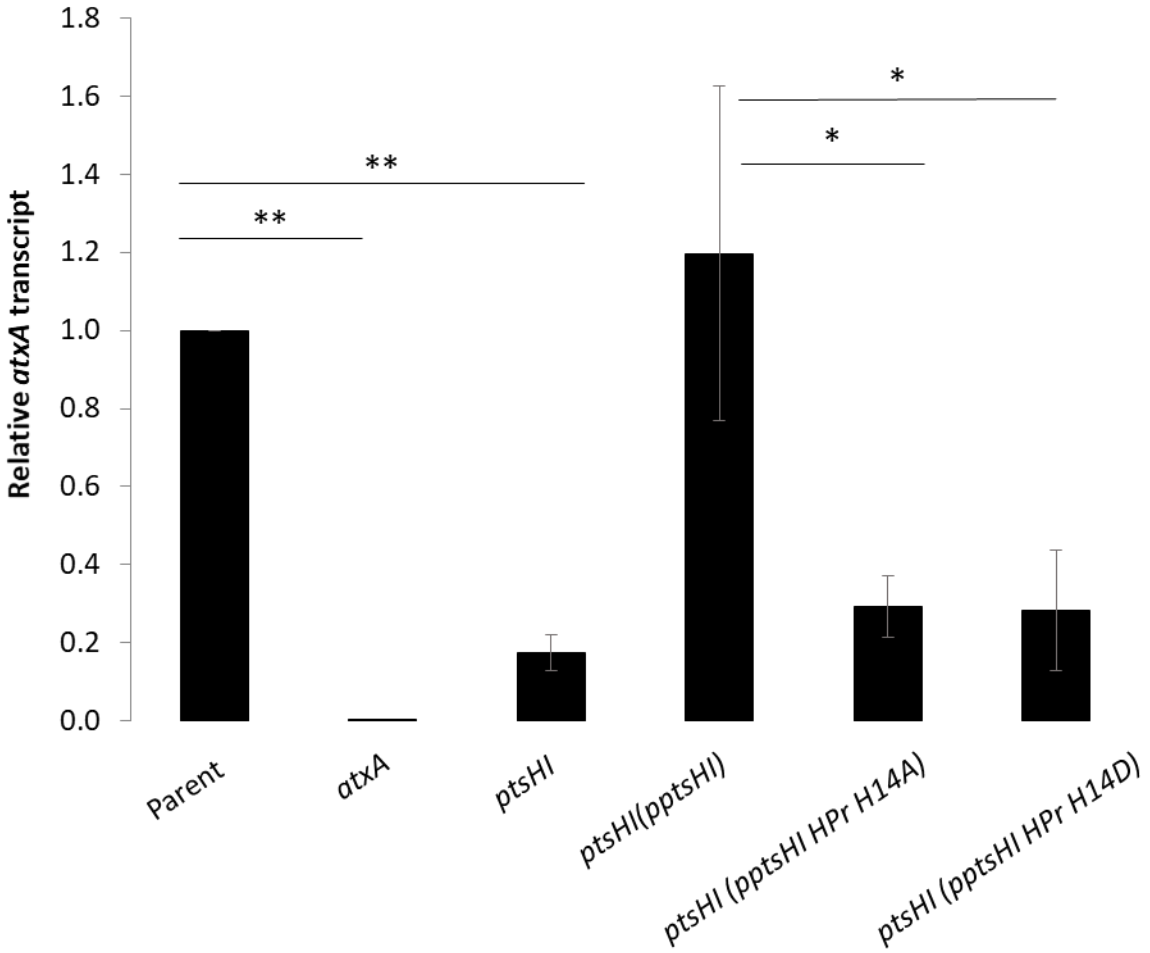

Figure 4-3. Relative levels of *atxA* in the PTS mutants. qRT-PCR results of a Taqman assay. *atxA* transcripts were normalized to *gyrB*. Data presented are on average of at least three biological replicates. Two technical replicates were performed per experiment. A student's T-test was used to determine the significance between *atxA* in the PTS mutant complemented with WT HPr and EI and the mutant complemented with phosphovariants of HPr and WT EI. Student's T test * $p < 0.05$, ** $p < 0.001$

contamination had occurred, 2) I performed colony PCR using primers flanking the *ptsHI* operon to confirm the *ptsHI* deletion, 3) I performed qRT-PCR using another *ptsHI* mutant in the lab, 4) I performed qRT-PCR using strains that had been previously published to have two fold-increased and decreased *atxA* expression patterns, 5) I performed qRT-PCR using genomic DNA as the template to be sure the Ct value for *atxA* changed with varying amount of template, 6) I performed the analysis on two instruments simultaneously, and 7) I designed two new sets of primers and probes. None of my efforts were successful in identifying or fixing the problem.

4.2.4. The PTS effect on *atxA* transcription affects virulence in a murine model for anthrax.

I sought to determine if the PTS and native regulated expression of *atxA* influenced *B. anthracis* virulence in a murine model for late stage anthrax infection in which toxin synthesis is critical. Our previous studies have demonstrated that an *atxA*-null mutant is avirulent in the A/J mouse model when mice are injected via the tail vein with up to 10^9 spores (Dai *et al.*, 1995).

To determine if the attenuation of virulence of the *ptsHI*-null strain (Fig 3-2) was due to transcriptional control of *atxA* I created UT447, a mutant in which *atxA* is expressed from a non-PTS-controlled promoter (*atxA**). Mice infected with UT447 succumbed to disease (Fig 4-3, panel A) and the bacterium disseminated to all tissues tested (Fig 4, panel B), but the infected mice exhibited significantly prolonged survival, indicating that native transcriptional control of *atxA* affects virulence. Mutant UT449 which contains *atxA** but is deleted for *ptsHI*, was not further attenuated for virulence, suggesting that the avirulent phenotype of the *ptsHI*-null mutant UT439 is due to the effect of the PTS on *atxA* expression.

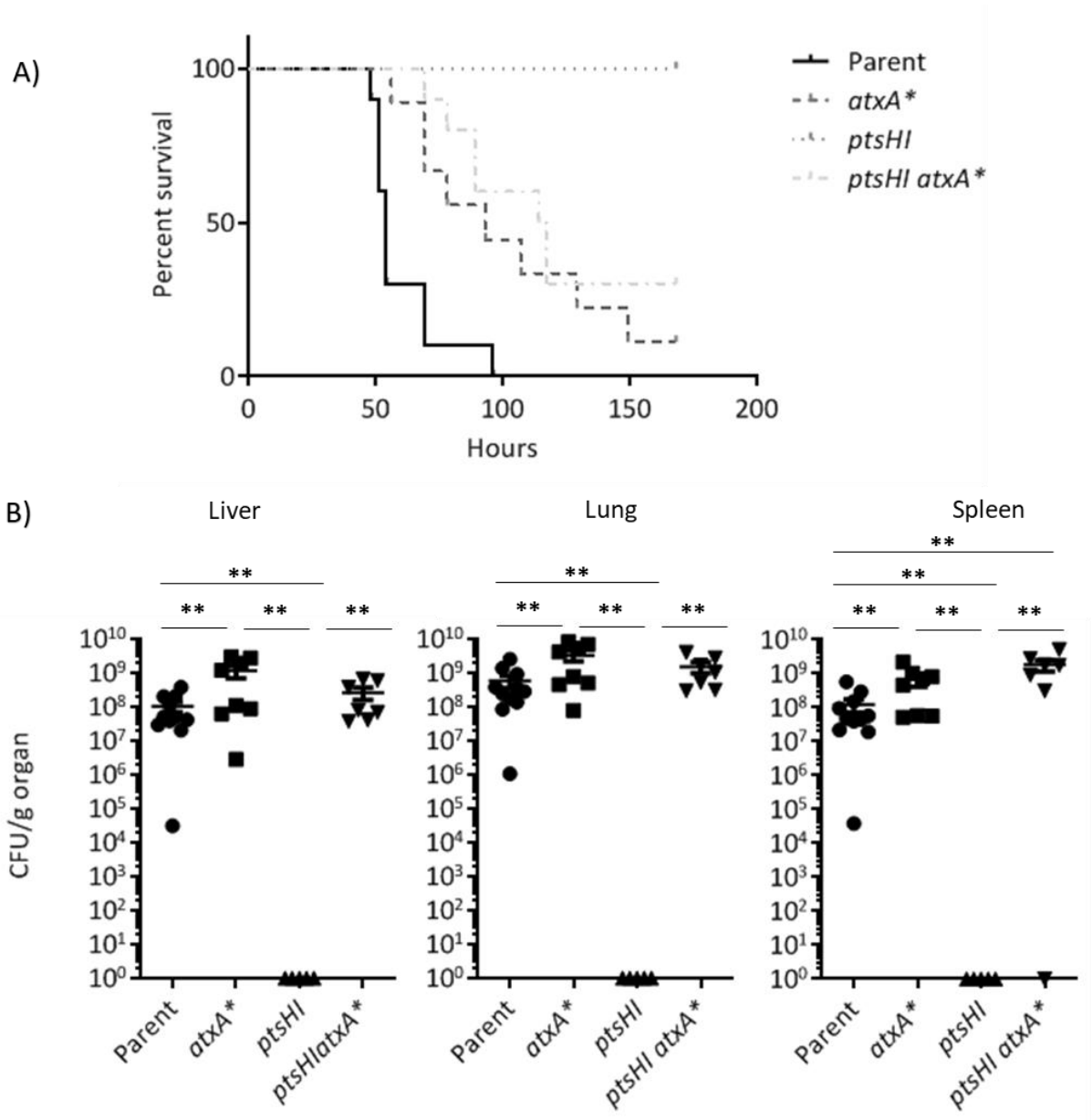

Figure 4-4. Virulence of parent and *ptsHI* mutants. A) Survival curves of mice infected intravenously with vegetative *B. anthracis* are shown. A/J mice were injected i.v. with 2.75 X 10^3 CFU of the parent (black solid line; *n* = 6), 4.5 × 10^3 CFU of parent constitutively expressing *atxA* (ANR-1 atxA*) (black dashed line; *n* = 6), 3 × 10^3 CFU of *ptsHI*-null (gray solid line; *n* = 6), or 3 × 10^3 CFU of *ptsHI* atxA* (gray dashed line, n=6) vegetative cells. B) CFU/g of tissue collected. Two sample permutation analysis was performed to compare each strain to the other. ** $p < 0.05$

4.3 Discussion

The observation that toxin production was reduced in the *ptsHI* mutant strain, but was unaffected in the same PTS mutant strain when *atxA* expression was controlled by IPTG, led to the hypothesis that the PTS effects *atxA* transcription. Interestingly, the data obtained suggest PTS control of *atxA* is dependent on both EI and HPr, as opposed to the previously proposed model of control in which HPr influences *atxA* transcription through CcpA. The inability of HPr-His14 phosphovariants to complement the *ptsHI*-null phenotype suggests phosphotransfer activity of HPr is necessary for *atxA* transcription. HPr-His14-P (His15 in *B. subtilis*) has been implicated in three main regulatory functions studied in *B. subtilis* and other Gram-positive organisms; 1) His15-P transfers phosphate to PRD-containing regulators to affect transcription of the PRD-regulator target genes, 2) His15-P interacts with the transcriptional regulator YesS in *B. subtilis* to influence expression of the pectin/rhamnogalacturonan genes, and 3) His-15-P phosphorylates and activates glycerol kinase (GlpK) to prevent inducer exclusion, because without the HPr-mediated phosphorylation GlpK interacts with transporters to enable inducer exclusion. Based on the necessity of HPr-His-P phospohotransfer activity, the most likely mechanism of HPr-mediated control of *atxA* transcription is HPr-mediated phosphorylation of a yet to be identified PRD-containing regulator. Interestingly, this would be the first example to my knowledge of a PRD-containing regulator controlling the transcription of another PRD-containing regulator.

The PTS effect on *atxA* transcription seems to be a 2- to 5- fold effect based on β-galactosidase assays. The β-galactosidase assays are less direct in determining actual transcript

levels, as the assay is a read out of activation at the *atxA* promoter, as opposed to actual *atxA* transcript reads from qRT-PCR. The relevance of the PTS activity on *atxA* transcription is readily discernable in the effect on toxin protein levels (Fig 3-1 and Fig 4-1, panel B) and even more so in the attenuation of virulence of the PTS mutant in the murine model for late stage, toxin-dependent, anthrax.

Further experiments are necessary to identify the intermediate factor involved in HPr-mediated transcription activation of the *atxA* promoter P1. Transcript levels of *atxA* start to appear at early exponential phase and peak at transition to stationary phase (Saile & Koehler, 2002). Crosslinking HPr to proteins during late exponential and transition to stationary phase, followed by purification and mass spectrometry of the HPr-protein complexes may aid in the identification of the intermediate factor. I made several attempts at purifying HPr-His_6 after formaldehyde-crosslinking growing cells, but was unable to optimize the technique and did not detect positive controls such as CcpA and EI. Further optimization of the copurification technique is necessary.

Searching through the genome of *B. anthracis*, I found two potential PRD-containing regulators based on predicted domain annotations, GBAA_0790 and GBAA_5437, both of which are predicted to be involved in cellobiose metabolism, a sugar I have not yet tested. Another experiment that may lead to potential targets for identification of the unknown regulator would be to determine which, if any specific, PTS-sugars influence *atxA* transcription above baseline non-PTS glycerol. In a preliminary experiment (data not shown) using LB +/- glucose, fructose, or

mannitol I observed an increase in P*atxA-lacZ* production in the presence of glucose and fructose relative to LB only, but not mannitol, suggesting there is some specificity in sugar influence on *atxA* transcription. Overall this work has uncovered a new level of regulation of *atxA* transcription and further work will help elucidate the molecular mechanism of control to further the field's understanding of *atxA* and overall virulence factor regulation in *B. anthracis*.

Chapter V.

The effects of phosphorylation of AtxA at H379 on virulence, solubility, and protein-protein interactions

5.1 Introduction

The phosphorylation states of AtxA are known to dictate the protein activity. Using phosphoablative and phosphomimetic substitutions at the histidine residues subject to phosphorylation, it was determined that phosphorylation at residue 199 allows for AtxA activity, whereas phosphorylation at position 379 inhibits AtxA activity (Tsvetanova *et al.*, 2007, Hammerstrom *et al.*, 2011). Phosphorylation at position H379 has a dominant negative effect relative to phosphorylation at H199 on AtxA activity and prevents multimerization of the protein, and multimerization of AtxA appears to be important for activity (Hammerstrom *et al.*, 2015).

Protein-protein interactions also regulated the activity for some PRD-containing regulators. The *B. subtilis* transcriptional activator MtlR, is activated via sequestration of the protein to the cell membrane. The interaction between $EIIB^{MtlR}$ and the C-terminus of MtlR is required for full activation of MtlR activity (Joyet *et al.*, 2015). ManR of *L. monocytogenes* interacts with the soluble protein EIIB domain of the MpoABCD mannose-type transporter system (Deutscher *et al.*, 2014). In his initial studies of AtxA mutlimerization, Troy Hammerstrom used a crosslinking agent, bis (maleimido)hexane (BMH), to determine protein-protein interactions at cysteine residues within AtxA. He used full length AtxA as well as truncated versions of AtxA to study the crosslinking patterns. The truncation of AtxA that expressed only the C-terminal domain, $AtxA^{385-475}$, had a different crosslinking pattern than the full length AtxA (Hammerstrom *et al.*, 2011).

In this chapter I aimed to determine if the H379D variant of AtxA was altered for virulence, solubility, and/or protein interactions.

5.2 Results

5.2.1 *B. anthracis* producing AtxA-H379D is attenuated in a murine model for anthrax.

Previous studies showed that AtxA H379D does not multimerize and is inactive *in vitro (Hammerstrom et al., 2015, Hammerstrom et al., 2011)*. To determine if mimicking phosphorylation affects AtxA activity *in vivo* I created an ANR-1 derived strain with an allelic variation at the native *atxA* locus to express AtxA-H379D, UT425, and compared the virulence of this strain and the parent ANR-1. Using our model for late-stage anthrax infection I injected three groups of mice in the tail vein; one group with 10^3 CFU of ANR-1, one with 10^3 CFU of UT425, and the last group with 10^4 CFU of UT425. Mice were monitored until they were found moribund or deceased. As shown in Figure 5-1, all mice infected with ANR-1 were moribund within 72 hours post infection. Mice infected with UT425 survived the 7 day with no signs of disease. These results suggest mimicking phosphorylation at H379 inhibits AtxA activity *in vivo* and is important during infection.

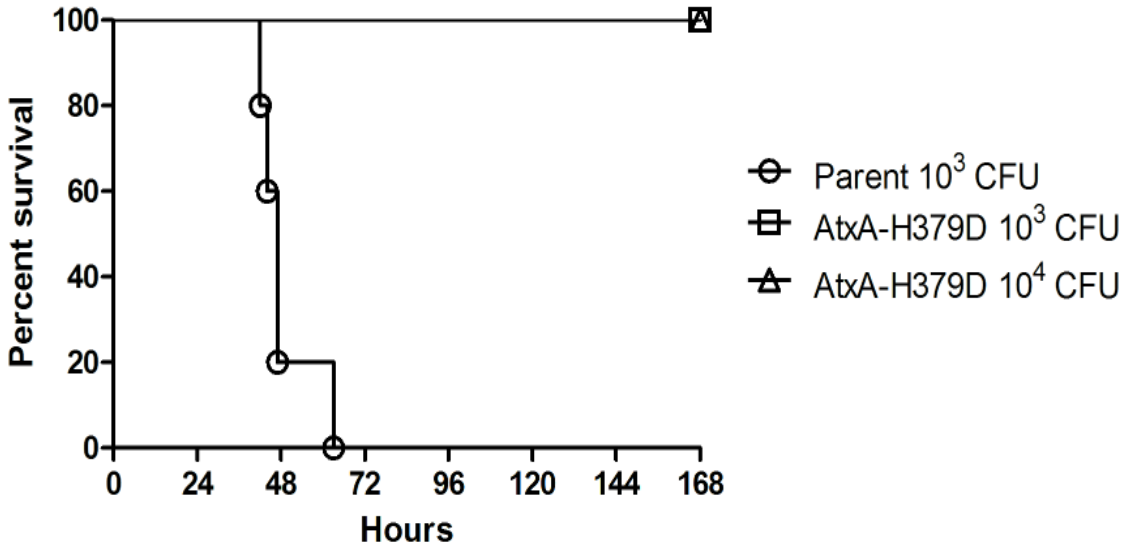

Figure 5-1. Virulence of parent and AtxA-H379D-expressing mutant. A) Survival curves of mice infected intravenously with vegetative *B. anthracis* are shown. A/J mice were injected i.v. with 2.75 X 10^3 CFU of the parent (open circle; *n* = 6), 4.50 × 10^3 CFU of ANR-1 engineered to express *atxA* H379D (open square; *n* = 6), 3.0 × 10^4 CFU of ANR-1 engineered to express *atxA* H379D (open triangle; *n* = 6)) vegetative cells.

5.2.2 Solubility of AtxA H379D

During my studies, and previous studies in the Koehler Lab, we observed that the AtxA phosphovariant H379D required more IPTG induction to obtain similar steady state levels of AtxA H379D compared to the wild-type AtxA. AtxA H379D may have decreased solubility and/or stability and would therefore require move overall production of the protein to detect levels similar to wild-type AtxA in the soluble fractions. It is possible that AtxA H379D interacts with membrane-bound proteins and is therefore found at lower levels in the soluble fractions of cell lysates compared to wild-type AtxA. Alternatively, if AtxA H379D is less stable that the wild-type AtxA it may be degraded faster, or coagulate and come insoluble.

To assess solubility of AtxA H379D I collected both soluble and insoluble cellular fractions of lysates generated from cultures expressing wild-type AtxA and AtxA H379D, and assessed if relative amounts of the proteins in the fractions. As observed previously, and assessed if there was increased H379D AtxA in the insoluble fraction relative to the wild-type levels. As observed previously, when AtxA H379D expression was induced with the same concentration of IPTG as WT AtxA, 10 μM, there was less overall protein detected (Fig 5-2). Additionally, when comparing soluble and insoluble fractions, there was an increase in AtxA H379D in the insoluble fraction relative to the soluble fraction. However, the difference in proportion of soluble and insoluble of AtxA H379D relative to WT AtxA was not observed when more IPTG (40 μM) was used to express AtxA H379D. The β subunit of RNA polymerase was used as a control for a generally soluble protein and the ratio of this protein stayed consistent in the various samples. It is possible that

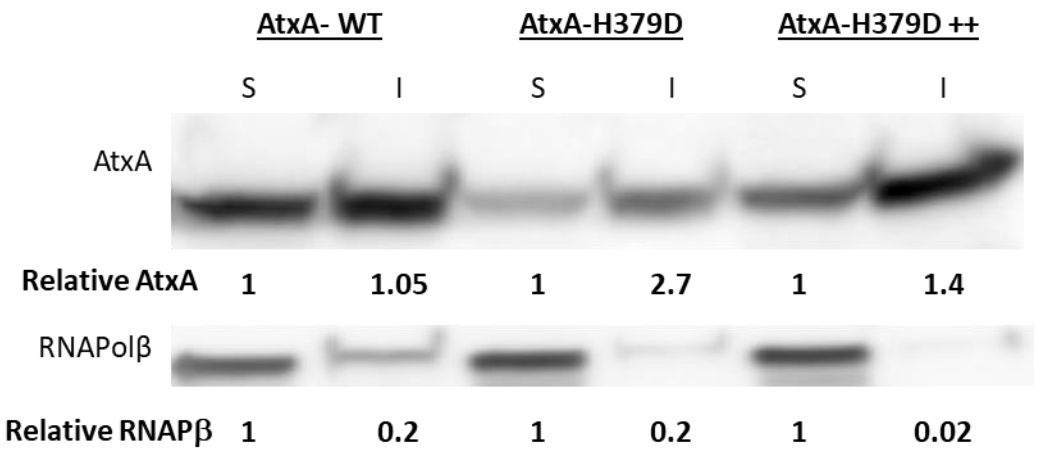

Figure 5-2. Solubility of AtxA. Solubility of AtxA. Cell lysates were collected at transition to stationary phase. Cells were rinsed with PBS. Cells were resuspended in KTE-PIC, disrupted by mechanical perturbation, and separated into soluble (S) and insoluble (I) cell fractions. 5X protein loading buffer was added to the soluble fractions. The insoluble fractions were treated with 8M urea and incubated for 3 hours. Fractions were subjected to SDS-PAGE and probed with THEHis^{TM}mAB to detect AtxA. Relative levels of AtxA were determined using densitometry. The soluble fraction was arbitrarily set to 1 to determine the relative solubility of AtxA in each strain.

AtxA solubility decreases when H379 is phosphorylated and that insoluble AtxA is likely not able to interact with DNA to promote transcription of target genes, adding a layer of regulation.

5.2.3 Protein-protein interaction of AtxA H379D

PRD-containing regulators MtlR of *B. subtilis* and ManR of *L. monocytogenes* interact with the EIIB domains of specific PTS systems in their respective organisms (Deutscher *et al.*, 2014). In his work, Troy Hammerstrom found that when he expressed the EIIB-like domain of AtxA ($AtxA^{385-475}$) and used the cross-linker BMH, the EIIB-like domain crosslinked with a distinct pattern relative to the full-length AtxA. Based on his observations that mimicking phosphorylation at H379 leads to abrogation of AtxA dimers, I questioned if phosphorylated AtxA interacts with other proteins at the AtxA EIIB-like domain as occurs for MtlR in *B. subtilis*. I used BMH crosslinking *in vivo* as described by Hammerstrom, et al. (Hammerstrom *et al.*, 2011) to crosslink wild-type AtxA-Flag, the EIIB-like domain of AtxA alone, $AtxA^{385-475}$-Flag, and AtxA H379D-Flag. The results presented in Figure 5-3 did not reveal any interactions of AtxA H379D when crosslinked with BMH. As was previously observed (Hammerstrom *et al.*, 2011), wild-type AtxA-Flag formed dimers and higher order multimers, and $AtxA^{385-475}$-Flag had multiple higher molecular weight bands. BMH crosslinks free cysteine residues within 13 Å of each other. AtxA has cysteine residues at positions 96, 161, 202, 356, 370 and 402. Troy determined that C402 is the residue crosslinked by BMH when two monomers of AtxA interact (Hammerstrom *et al.*, 2011). The EIIB-like domain alone forms protein-protein interactions with cysteine residues in close enough proximity to crosslink using BMH. It is possible that phosphorylation at H379

changes the conformation of the neighboring domain and therefore interferes with the crosslinking of the EIIB-like domain to the unknown proteins, or that full length AtxA H379D doesn't interact with the same interaction partners as the EIIB-like domain alone.

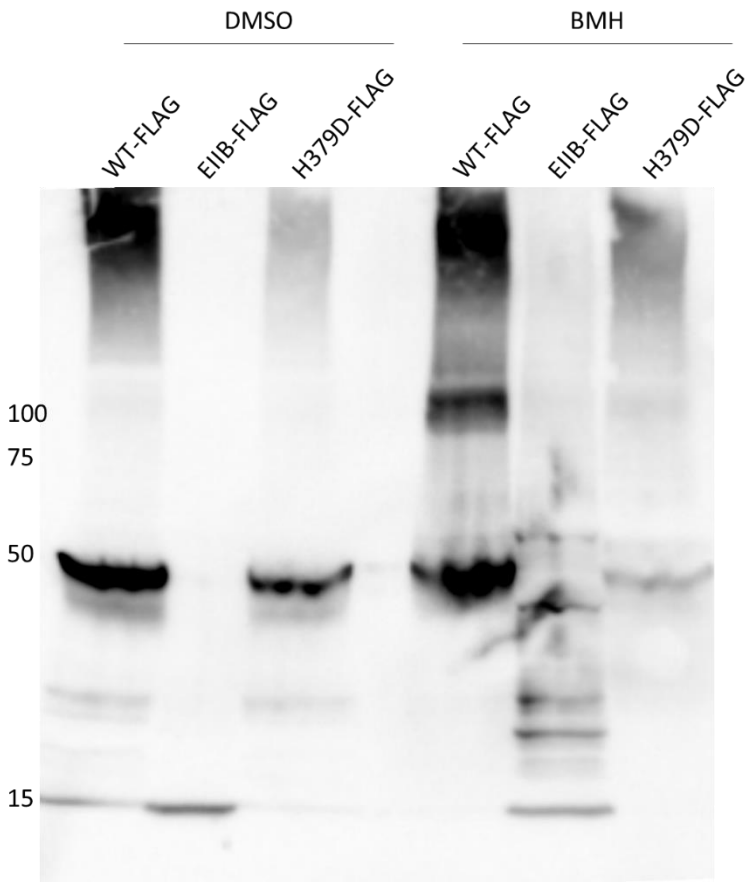

Figure 5-3. BMH crosslinking of AtxA and AtxA variants.
Multimerization of AtxA385-475. Cell lysates of *atxA*-null strains (UT376) containing wild-type AtxA-FLAG (pUTE992), AtxA385-475-FLAG (pUTE1022-FLAG), and AtxA H379D (pUTE992H379D) induced using 30–50 μM IPTG were treated with the cross-linking agent BMH. Cell lysates were subjected to SDS-PAGE (4–20%) and western blots with FLAG-specific antibody to detect various forms of AtxA.

5.3 Discussion

In agreement with assessments of AtxA activity in lab cultures I found that expressing AtxA H379D, mimicking the phosphorylated state, rendered *B. anthracis* attenuated for virulence in the mouse model used.

To further our understanding of AtxA in the H379-phosphorylated state I studied the solubility and protein-protein interaction of the phosphovariant AtxA H379D. AtxA H379D requires induction with more IPTG than the wild-type AtxA. When the same concentration of IPTG was used to induce the wild-type AtxA and AtxA H379D lower levels of overall protein were observed for AtxA H379D, and the ratios of AtxA H379D in the soluble and insoluble fractions were different than those of wild-type AtxA. However, when AtxA H379D expression was induced with higher concentrations of IPTG leading to similar levels of overall protein abundance as wild-type AtxA, a difference in solubility was not observed. These observations suggest an equilibrium may be reached when AtxA is relatively abundant in the cells compared to when AtxA is somewhat limited. It is possible that AtxA is not as stable when in the monomeric form and is therefore present in lower levels when expressed as AtxA H379D. A follow up experiment would be to perform a modified pulse-chase experiments in which AtxA H379D would be induced with IPTG, sometime later cultures would be collected and resuspended in IPTG-free medium supplemented with sub-inhibitory concentrations of chloramphenicol to prevent further protein synthesis, and samples collected at multiple time points to probed for AtxA.

AtxA has been previously shown to form homomultimers *in vivo*. Troy Hammerstrom had observed that the EIIB-like domain of AtxA, AtxA$^{385-475}$, crosslinked with BMH resulting in a

number of protein bands. Some of these bands may be homomultimers of AtxA$^{385-475}$, but not all the bands had molecular weights equal to multiples of 16 kDa, the molecular weight of the EIIB-like domain alone. The observed difference in banding patterns of the EIIB-like domain relative to full length AtxA suggested the EIIB-like domain is able to interact with other proteins. One possibility is that AtxA when phosphorylated at H379 is in a monomeric form and the EIIB-like domain may be free to mediate the interaction of AtxA with other proteins. My results using BMH crosslinking with the H379D variant suggest this isn't the case, or that cysteine residues of AtxA H379D interacting partners are not within 13 Å as is the case when the EIIB-like domain interacts on its own. A more general experiment to do in the future will be to perform a general crosslinking experiment to determine if AtxA interacts with other proteins besides itself, and to determine if the interactions change depending on the phosphorylation state of H199 and H379.

Chapter VI.

Alternative systems that potentially influence AtxA phosphorylation and/or activity.

6.1 Introduction

The model for PTS function in Gram-positive bacteria was largely determined in *B. subtilis*. A comparison of the predicted open reading frames of *B. subtilis* to the *B. cereus sensu lato* group suggests the pathogenic bacilli have evolved to have a greater capacity to use peptides and amino acids compared to carbohydrates and sugars (Table 6-1). The annotated *B. anthracis* and *B. subtilis* genomes show a large difference in the number of genes potentially involved in carbohydrate and peptide metabolism. *B. subtilis* contains 41 genes predicted to be involved in carbohydrate polymer degradation, whereas *B. anthracis* only has 15 (Ivanova *et al.*, 2003, Read *et al.*, 2003). *B. anthracis* appears to have an expanded capacity for amino acid and peptide utilization; there are 48 predicted proteases in *B. anthracis* compared to 30 in *B. subtilis*, there are 17 ABC-type peptide binding proteins in *B. anthracis*, and only four in *B. subtilis* (Ivanova *et al.*, 2003, Read *et al.*, 2003, Han *et al.*, 2006). *B. anthracis* contains nine homologues of the BrnQ BCAA transporter whereas *B. subtilis* has only two. Similar trends exist for *B. cereus* and *B. thuringensis* as noted in Table 6-1.

The metabolic state of cells influences gene regulation. CodY is a conserved transcriptional regulator in Gram-positive bacteria that responds to the metabolic state of the cell to mediate adaptation to changing nutrient availability. In most organisms studied CodY is activated by binding BCAAs and GTP. When bound by BCAAs CodY binds target promoter regions to repress transcription of target genes. Thus, when nutrients are abundant CodY represses targets. When nutrients become limited CodY is no longer bound to the activating metabolites and releases from its target promoters allowing transcription to occur (Kaiser & Heinrichs, 2018).

Utilization and functions	No. of genes[a]			
	B. subtilis	*B. anthracis*	*B. cereus*	*B. thuringiensis*
Sugar utilization				
PTS- sugar transporter	25	19	18	20
Carbohydrate polymer degradation	41	12	12	12
Mannose, arabinose, rhamnose catabolic pathway	Yes	No	No	No
Amino acid and peptide utilization				
Peptide ABC transporter-ATP binding protein	7	18	23	18
Branched chain amino acid transporter	4	11	11	14
LysE/RhtB/CadD amino acid efflux system	2	6	8	8
Peptidase	30	64	91	90
Protease	24	50	49	52
Amino acid and amine catabolism	34	52	55	55

Table 6-1. Comparison of predicted ORFs among *Bacillus* species. Adapted from Han CS. et al, 2006. The number of predicted ORFs related to sugar utilization and peptide/amino acid utilization in *Bacillus* species are listed. [a]No and yes indicate the absence and presence, respectively, of genes in the pathway.

CodY has been implicated in regulation of virulence for a number of Gram-positive pathogens. In *B. anthracis* CodY, through an unknown mechanism, affects the stability of AtxA and a *codY*-null mutant has decreased toxin production and decreased virulence in a murine model of toxinogenic anthrax (van Schaik *et al.*, 2009). In *L. monocytogenes* a *codY*-null mutant is attenuated in a murine model of systemic infection (Kaiser & Heinrichs, 2018). Under BCAA replete conditions, CodY represses a number of metabolic genes, but also activates flagellar genes involved in pathogenesis. A unique feature of CodY in *L. monocytogenes* is that CodY can bind DNA under BCAA depleted conditions as well. When BCAA levels are low CodY acts to directly activate a number of genes including the virulence regulator of *L. monocytogenes* PrfA. In *S. aureus* CodY is active under BCAA replete conditions and primarily acts as a repressor of virulence genes (Kaiser & Heinrichs, 2018).

Branched chain amino acid transporters and biosynthesis genes have been implicated in virulence regulation beyond their role in activating CodY (Kaiser & Heinrichs, 2018). During systemic infection and nasal colonization, *S. aureus* requires two BCAA transporters, BrnQ1 and BcaP for optimal survival (Kaiser *et al.*, 2015, Kaiser *et al.*, 2016). BCAA biosynthesis plays a role in invasion of host tissues for *S. pneumonia* following intranasal colonization, and BCAA transporters are important for growth in models of systemic infection, pneumonia, and meningitis (Kaiser & Heinrichs, 2018). BCAA biosynthesis and transporter genes have not yet been studied for their role in *B. anthracis* virulence, however, recent data revealing AtxA strongly represses many of these genes imply the genes may be important for virulence. In cultures grown in the toxin-inducing medium $CACO_3$, AtxA strongly represses the predicted BCAA biosynthesis

genes *ilvA, ilvB2, ilvC2, ilvD, ilvE2, ilvE1, ilvB, ilvC1, leuA, and leuB* 30-60 fold, and the predicted BCAA transporters *brnQ3* and *brnQ6* 34- and 21- fold, respectively (Raynor *et al.*, 2018). Interestingly, when *B. anthracis* is grown in bovine blood the genes encoding predicted amino acid transporters, *brnQ2* and *brnQ6* are induced 100- and 20- fold respectively, relative to growth in LB (Carlson *et al.*, 2015). The strong repression of BCAA-involved genes by AtxA led me to ask whether BCAAs affect AtxA activity directly.

6.2 Results

6.2.1 AtxA activity increases with increasing concentrations of BCAA in the medium.

The evidence suggesting AtxA phosphorylation and activity are unaffected by the PTS lead me to question what other system may be responsible for regulating AtxA activity and toxin production. Based on the over representation of peptide associated genes in the *B. anthracis* genome compared to *B. subtilis*, I hypothesized that peptides or amino acids are responsible for controlling AtxA activity. The finding that AtxA strongly influences transcription of genes related to BCAA biosynthesis and transport led me to assess the relationship of AtxA activity and BCAAs in the medium.

I grew cultures of UT376(pUTE991) in R medium, a defined medium containing the components of casamino acids medium and easily manipulated (Ristroph & Ivins, 1983). I induced AtxA expression with IPTG and compared AtxA activity at P*lef-lacZ* in cultures containing varying concentrations of the three BCAAs. As seen in Figure 6-2 AtxA activity increased in a dose-dependent manner. As BCAA concentration was increased AtxA activity was as well. Importantly

the growth rate of the cultures grown in 0.1 mM and 1 mM BCAA was the same, however the β-galactosidase activity was increased about 2-fold in the presence of 1 mM BCAA.

To determine if the increase in AtxA activity could be elicited by a single BCAA I grew cultures in R medium, this time adding only a single BCAA to the medium and comparing AtxA activity. There was no significant increase in AtxA activity when 3 mM of any individual BCAA was added to the medium, relative to the culture that did not contain any BCAAs (Fig 6-3). To follow up the observation that BCAAs increase AtxA activity I would like to determine if CodY mediates this effect. I generated a *codY*-null mutation in *B. anthracis*. At this point I handed over the project to an incoming post-doctoral trainee to continue the investigations of the relationship of BCAAs and virulence in *B. anthracis.*

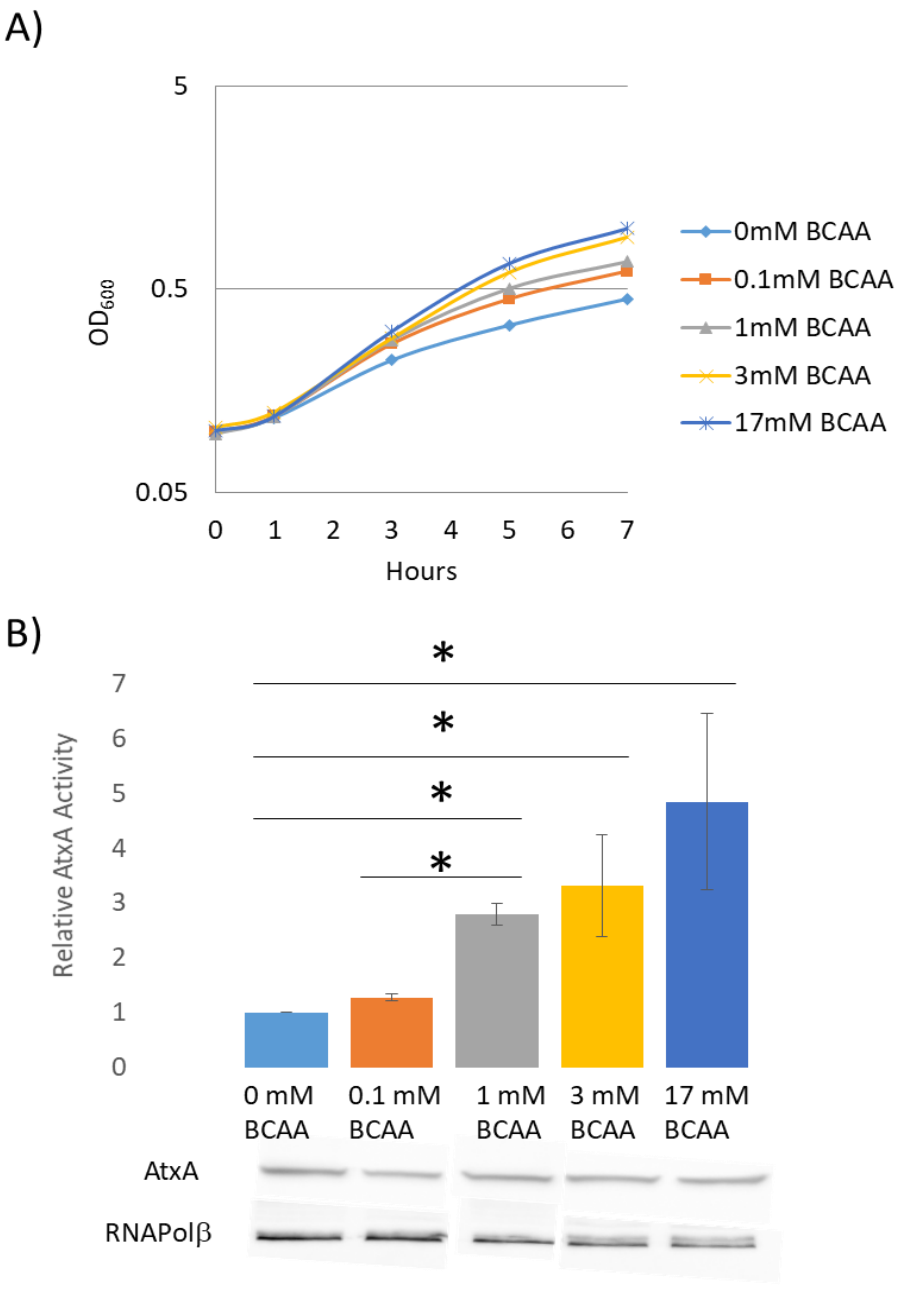

Figure 6-1. AtxA activity in the presence of BCAAs.
Cultures of the *B. anthracis* reporter strain UT376(pUTE991) were grown in R-medium supplemented with BCAAs as indicated. A) Growth curve B) β-galactosidase activity and western blots. Cells were collected from cultures at late exponential phase (4h growth) for AtxA activity assays and western blotting with α-THE^{TM}His antibody. AtxA activity was assessed as β-galactosidase activity from a P*lef-lacZ* transcriptional fusion. Data represent the average of at least three independent biological replicates. Student's T-test was performed to determine statistical significant between samples. *p value <0.05

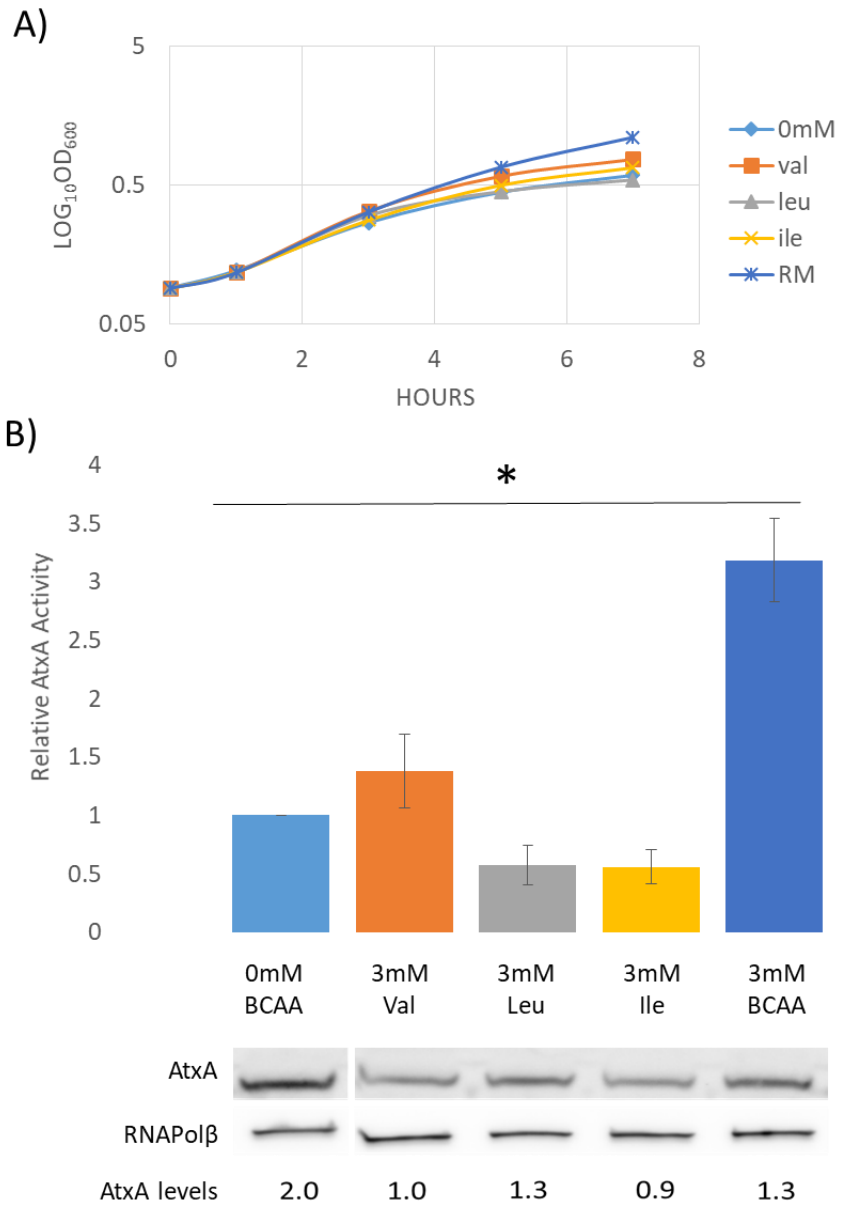

Figure 6-2. AtxA activity in the presence of individual BCAAs.
Cultures of the *B. anthracis* reporter strain UT376(pUTE991) were grown in R-medium supplemented with individual BCAAs as indicated. A) Growth curve B) β-galactosidase activity and western blots. Cells were collected from cultures at late exponential phase (4h growth) for AtxA activity assays and western blotting with α-THE™His antibody. AtxA activity was assessed as β-galactosidase activity from a P*lef-lacZ* transcriptional fusion. Data represent the average of at least three independent biological replicates. Student's T-test was performed to determine statistical significant between samples. *p value <0.05

6.2.2 Development of an assay to identify metabolites that affect AtxA activity.

In addition to testing BCAAs and their role in AtxA activity, I wanted to take a more global approach and develop a screen that will help identify systems potentially responsible for AtxA phosphorylation. To do I used the Phenotype Microarray™ (PM) plates from Biolog (Hayward, CA). The PM plates are 96-well plates containing different compounds in each well that are designed to test for specific cellular phenotypes. My goal was to use the PM plates 1-3, which contain carbohydrates and nitrogen sources, to determine what, if any, compound has an effect on AtxA activity. I compared wild-type AtxA to AtxA H379A, the form of AtxA that cannot be inactivated by phosphorylation at H379 due to the alanine substitution. *B. anthracis* strain ANR-1 tends to grow in clumps under a number of conditions, the specifics of which are unknown, and clumps make reading optical densities in a 96-well plate difficult. Therefore, for this assay I used *B. anthracis* strain 7702, a strain that usually grows uniformly in liquid culture. I generated strain UT428, a 7702-derivative engineered to express GFP from the *lef* promoter and removed *atxA* from its native locus. I expressed AtxA from an IPTG inducible promoter on plasmid pUTE991. Strain UT428 is depicted in Figure 6-4 panel A. The design of exogenous expression of AtxA allowed me to bypass any effects the test compounds may have on *atxA* transcription and control the level of AtxA in the cells. The *lef-gfp* fusion allows for detection of AtxA activity in intact cells over time without having to perform β-galactosidase assays as had been done with *lef-lacZ* reporter strains.

Comparing wild-type AtxA activity to AtxA H379A should allow me to identify potential metabolites that affect AtxA phosphorylation at H379. In theory if a substrate stimulates the

phosphorylation of H379, then wild-type AtxA activity should decrease in the well containing the substrate, decreasing the GFP signal, while AtxA H379A activity should remain the same, producing GFP (simulated in panel B of Figure 6-3).

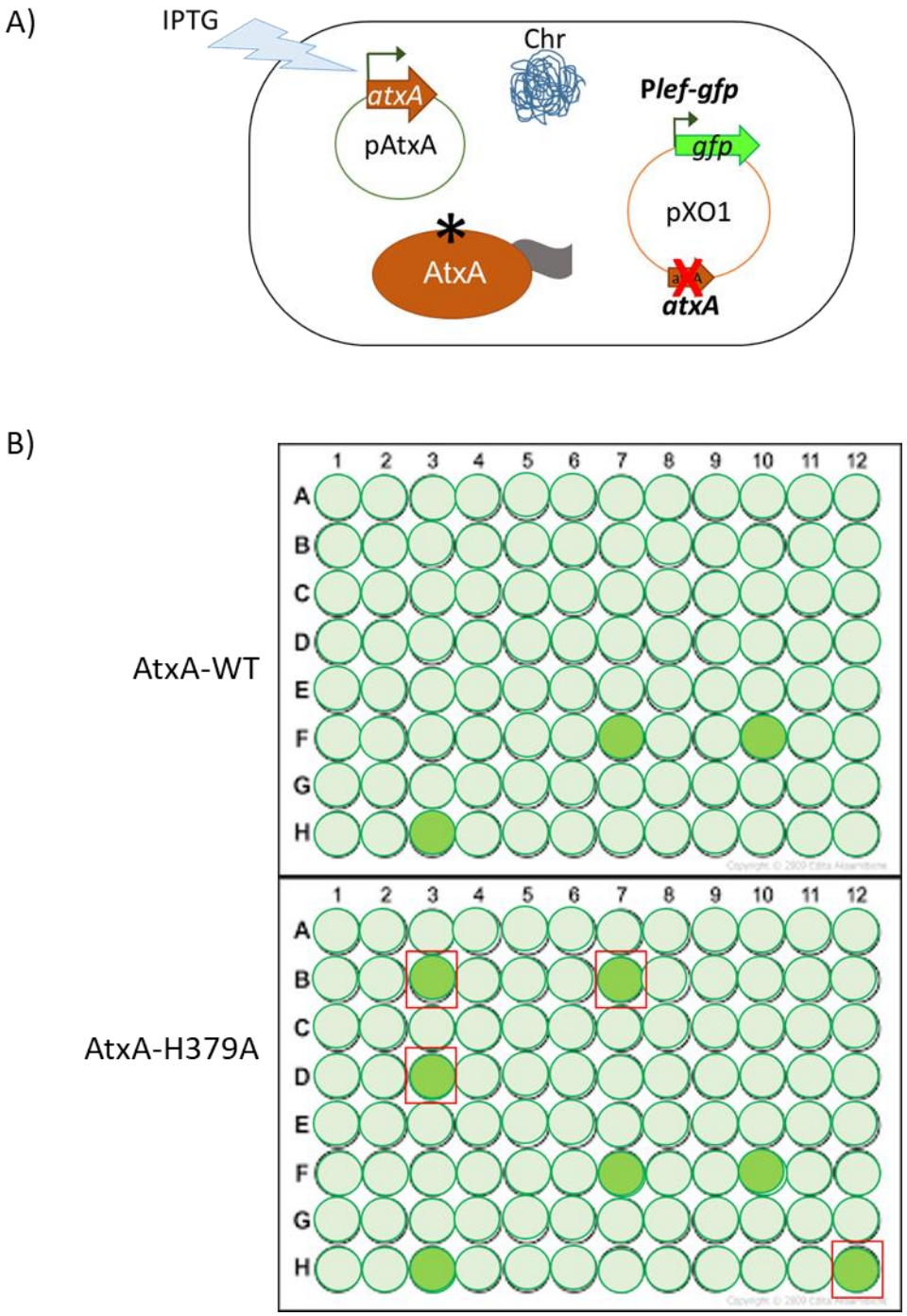

Figure 6-3. Design of Biolog PM Assay to determine conditions under which AtxA is phosphorylated at H379. A) Graphic representation of the *B. anthracis* strain used in this assay. Native *atxA* has been deleted, and expression of an epitope tagged *atxA* occurs from an IPTG inducible promoter on a plasmid, a promoterless GFP is fused to the promoter of *lef*. B) Graphic representation of anticipated results showing GFP expression of the WT AtxA and AtxA H379A.

After many experiments to determine the proper growth conditions and shaking speeds I was able to obtain somewhat reproducible data. The assay is very crude and does not take into account all quantitative controls. Instead, the assay is meant to generate ideas of which substrates to test in our well-established flask based growth curves and activity assays. To control for differences in growth rate in the various conditions the OD_{600} of each well was measured and used to calculate the relative activities of the AtxA phosphovariants. To generate the numbers presented in Figure 6-4, I did the following. I took two readings at two time points: at the start of the experiment (T0) and eight hours later (T8). Read 1 was to read GFP fluorescence, the excitation wavelength was 485 nm and read at 528 nm. Read 2 was the OD of the cells, 600 nm. I normalized the fluorescence readings to the cell densities for both time points ((485,528))/((600)), and then subtracted T0 from T8 for each strain. Any numbers that were negative were adjusted to zero and not used. If a well contained a zero value for either strain, the well was not used in the analysis either. I then subtracted the wild-type signal from the H379A signal so that any well with a positive number had more activity in the H379A strain than the strain expressing wild-type AtxA. I did this experiment in duplicate to be sure the reads were reproducible. There were some wells that were positive in one assay and negative in the other, I did not include these in my analysis. The data I obtained from my experiment is presented in Figure 6-4. There were only six wells that elicited a reproducible and substantial difference in activity between WT AtxA and H379A. Dihydroxyacetone elicited the greatest difference, 2500 units of activity. There are many improvements that can be made to this assay to increase

reproducibility. In the future improvements should be made and this experiment repeated with the PM3 plates containing nitrogen sources.

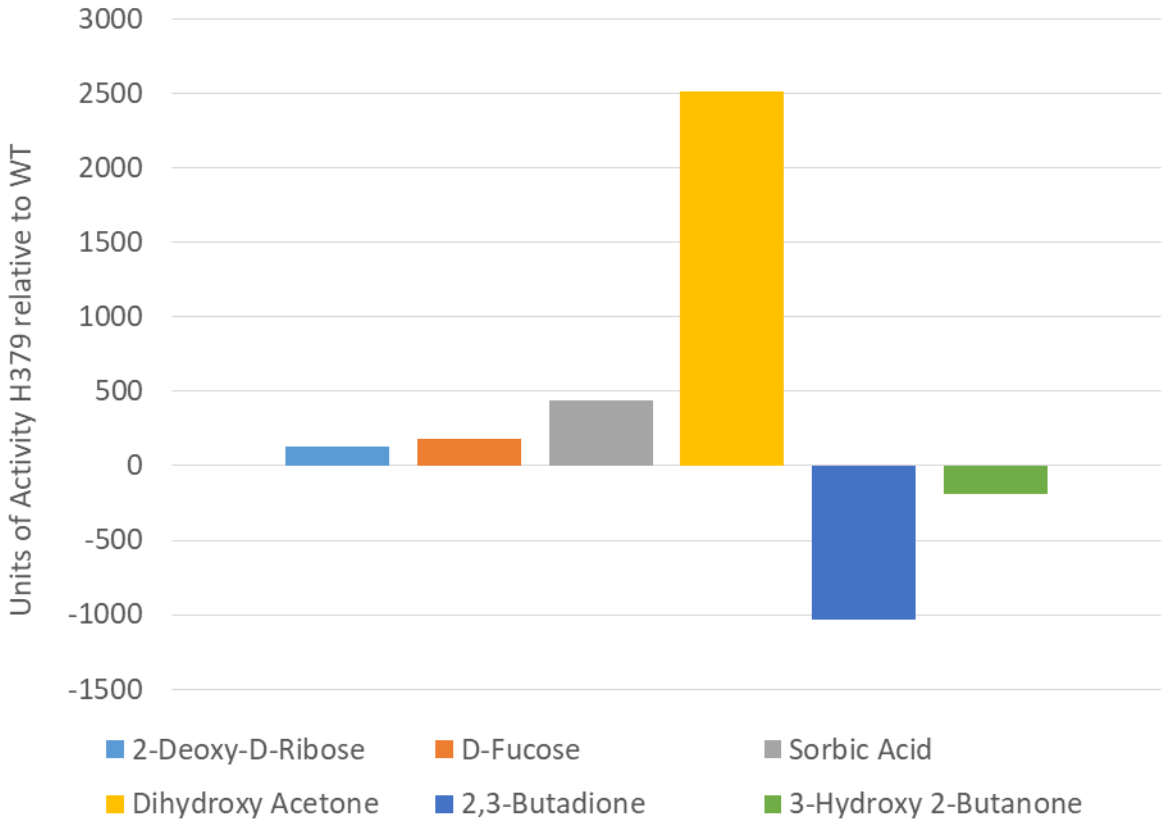

Figure 6-4. Activity of AtxA H379A relative to wild-type in the presence of specified substrates. Activity of AtxA was calculated using OD600 and OD485,528 and a comparison of activity of AtxA wild-type and AtxA H379A was performed. Presented is the relative difference of activity of H379A as compared to wild-type AtxA. These data were calculated from two independent PM assays and averaged.

6.3 Discussion

The observation that AtxA activity is affected by BCAAs is intriguing. The protein structure of AtxA does not have predicted BCAA binding sites, in fact, as discussed at length in this work, the structure of AtxA suggests a relationship with sugar import and metabolism as opposed to amino acids. CodY has been shown to affect AtxA protein stability via an unknown mechanism (van Schaik *et al.*, 2009). The CodY protein contains a BCAA binding region and CodY activity is affected by BCAA concentrations in the cell (Shivers & Sonenshein, 2004). Although I did not observe a change in AtxA stability in cultures grown in various BCAA concentrations, it is possible that the increase in AtxA activity in the presence of higher levels of BCAA is due to increased CodY activity. The same experiments assessing AtxA activity with various BCAA levels will need to be performed in a *codY*-null background to determine if CodY is mediating this effect.

The compound eliciting the greatest difference in AtxA activity between H379A and wild type AtxA was dihydroxyacetone, a compound that is produced during glycolysis in its phosphorylated form (DHAP). For DHAP to elicit a difference in AtxA activity is interesting considering my data suggesting sugar metabolism, at least metabolism that involves the PTS, is not involved in AtxA activity. In agreement with my findings that the PTS does not affect AtxA activity, the sugars, 2-Deoxy-D-Ribose and D-fucose, identified in this screen are predicted to be transported by dedicated ABC transporters, and not by the PTS. Interestingly, growth and AtxA activity was observed in the well containing sorbic acid, a common preservative of foods shown to inhibit growth of *B. cereus* and *B. subtilis* (Raevuori, 1976). Also of interest are two compounds in which the wild-type activity was much greater than the H379A activity (the negative numbers

in the graph). The methyl ketones acetoin (3-hydroxy-2-butanone) and its oxidized form 2,3-butanedione result from decarboxylation of fatty acids are derived from pyruvate fermentation under anaerobic conditions (84). It is possible that changing H379 affects a residue nearby and that these compounds specifically affect stability, and/or activity of only the wild-type AtxA. Further experiments adding these compounds to cultures grown in flasks, using the UT376(pUTE991) *lef-lacZ* reporter should be performed to validate these findings.

Chapter VII.

Discussion

7.1 General findings of this work

In this work I explored the relationship of the sugar phosphotransferase system and AtxA activity and transcription in the pathogenic bacterium *Bacillus anthracis*. I have shown that HPr was unable to phosphorylate AtxA *in vitro*, that deletion of the genes encoding HPr and EI did not affect AtxA activity in its native host *B. anthracis*, and that AtxA activity stayed constant regardless of the sugar carbohydrate source added to the medium. AtxA phosphorylation does not appear to affect AtxA solubility drastically, nor does it change the pattern of AtxA protein interactions involving the cysteine residues in the C-terminus of the protein. In this work I present preliminary investigations probing the relationship of AtxA and branched chain amino acids. My data suggest further studies exploring BCAA transport and biosynthesis in the context of AtxA activity will be worthwhile in uncovering another mechanism of control and possibly a feedback loop of AtxA activity and regulation. Most importantly, the data I present support a model in which HPr and EI regulate *atxA* gene transcription. I propose that the regulation of the *atxA* gene transcription is achieved through the phosphorylation of a downstream transcriptional regulator that either directly or indirectly controls transcription initiation at the primary promoter of *atxA*. Transcriptional control of *atxA* by the PTS is important in a mouse model of late-stage anthrax infection, and bacterial load and time to death may not be directly related for *B. anthracis* pathogenesis.

7.2 The unexpected relationship of the PTS and the master virulence regulator of *B. anthracis*

PRD containing regulators have been well studied since the early 1990's. Classically, these regulators control the transcription of genes involved in sugar import and metabolism. Many

studies have explored the relationship between regulator activity and carbohydrate availability (Deutscher *et al.*, 2014, Galinier & Deutscher, 2017). I hypothesized that growing *B. anthracis* in various sugars would engage the PTS and modulate AtxA activity. However my results suggest that AtxA activity is not affected by the presence of the PTS sugars glucose, fructose and mannitol, nor is it affected when the PTS is not engaged by the use of melibiose or glycerol, suggesting that under the conditions tested the PTS does not play a role in modulating AtxA activity.

In order to determine if EI and HPr play a role in AtxA activity, through activation or inhibition, I assessed AtxA in the parent and *ptsHI*-null strain and compared AtxA activity in the presence and absence of EI and HPr. In *B. subtilis* AtxA activity was increased in the absence of HPr (Tsvetanova *et al.*, 2007), thus I expected to see a similar phenotype. In *B anthracis* AtxA activity was unaffected by the absence of HPr and EI suggesting the previous observation may be specific to *B. subtilis*. For the PRD-containing regulator MtlR host-specific regulation of the protein has been observed. Despite the high degree of MtlR amino acid sequence conservation between *L. casei*, *B. subtilis* and *Geobacillus stearothermophilus*, the mechanisms for MtlR control in these organisms differ. In *B. subtilis* and *G. stearothermophilus*, MtlR is phosphorylated by HPr and EI at a conserved histidine in PRD2 to activate protein activity, whereas in *L. casei* it is not. In *B. subtilis* MtlR must be sequestered to the membrane via interaction with unphosphorylated $EIIB^{Mtl}$ in order to be active (Joyet *et al.*, 2015). The observation that AtxA is controlled differently in *B. anthracis* and *B. subtilis* raises the possibility that the systems may function differently in the two organisms. *B. cereus* a close relative of *B. anthracis* can cause food-

borne illnesses, and in a few documented cases has caused anthrax-like disease (Hoffmaster *et al.*, 2004, Brezillon *et al.*, 2015, Klee *et al.*, 2006). *B. cereus* G9241 expresses AtxA and AtxA2. Similar to AtxA in *B. anthracis*, in *B. cereus* G9241 AtxA forms homomultimers and AtxA2 does as well, but to a lesser extent (Scarff *et al.*, 2016). It will be interesting to study the relationship of the PTS and AtxA phosphorylation and activity in *B. cereus* G9241 as well as other Gram-positive organisms to determine if there is host-specific PTS involvement in regulating the PRD-containing regulator AtxA.

Better characterization of the PTS in *B. anthracis* compared to *B. subtilis* is important for understanding basic physiological processes in this important pathogen. There is potential to exploit the PTS for potential interventions by understanding how virulence factor production is influenced by the PTS and somehow blocking activation, or stimulating inactivation. An understanding of the system in the pathogen is essential before a potential inhibitor could be identified or synthesized. Purified HPr from *B. anthracis* was functional in phosphorylating the *B. anthracis* homologue of the well-studied PRD regulator, GlcT, of *B. subtilis* (Fig 3-5), suggesting there is some functional overlap between the PTS in *B. anthracis* and *B. subtilis*. However, as noted in Table 6-1 the predicted open reading frames involved in PTS transport and carbohydrate catabolism differs between *B. subilits* and the three members of the Cereus group presented.

7.3 Comparison of AtxA and other PRD-containing regulators

The observations that AtxA is not post-translationally controlled by the PTS is not entirely surprising. The hypothesis that AtxA is subject to post-translational modification by the PTS is

based on the structure of AtxA, the phosphorylation of AtxA at two histidine residues within conserved PTS regulation domains, and the regulation on AtxA dimerization and activity that phosphorylation events exert (Hammerstrom *et al.*, 2015, Hammerstrom *et al.*, 2011, Tsvetanova *et al.*, 2007). However, the initial observation of regulation by HPr in *B. subtilis* suggests AtxA is different than typical PRD-containing regulators. Phosphorylation of PRD-containing regulators by HPr almost always activates the regulator activity (Deutscher *et al.*, 2014). In *B. subtilis* AtxA activity at the *pagA*, promoter is increased in the absence of HPr, suggesting that phosphorylation of AtxA by HPr serves a negative regulatory function, which is unique among PRD-containing regulators subject to phosphorylation by HPr (Tsvetanova *et al.*, 2007).

There are key characteristic differences that set AtxA apart from other PRD-containing regulators. Unlike other PRD-containing regulators, the regulon of AtxA does not appear to include PTS or PTS-related genes, nor any other notable genes related to carbohydrate metabolism (Bourgogne *et al.*, 2003, Raynor *et al.*, 2018). Additionally, PRD-containing regulators are defined by three qualifiers: evidence of predicted structure of duplicated domains in tandem; the regulator activity is affected by phosphorylation of specific histidine residues within those domains; and phosphorylation occurs via the PTS. AtxA has two of these qualifiers, but phosphorylation by the PTS was not detected and does not seem likely based on my work. Unlike classical PRD-containing regulators, the histidine residues subject to phosphorylation in AtxA are not highly conserved. In fact in an analysis of PRDs from classic, PTS-controlled PRD-containing regulators and PCVRs it appears PCVRs have diverged from PRD-containing regulators in the placement and conservation of histidine residues. In an amino acid sequence alignment

performed by Stulke (Stulke *et al.*, 1998), PRDs are described to have a histidine residue at position seven of the PRD alignment presented and a conserved arginine at position 14 in the alignment (Fig 7-1 modified from Stulke, 1998). Interestingly, this histidine at position seven is phosphorylated for most of the proteins aligned (Fig 7-1 highlighted in red). When the alignment is modified to include the emerging class of PCVRs, the PCVRs appear to differ in histidine placement, as well as phosphorylation sites (for those regulators for which phosphorylation sites has have been identified) (Fig 7-1).

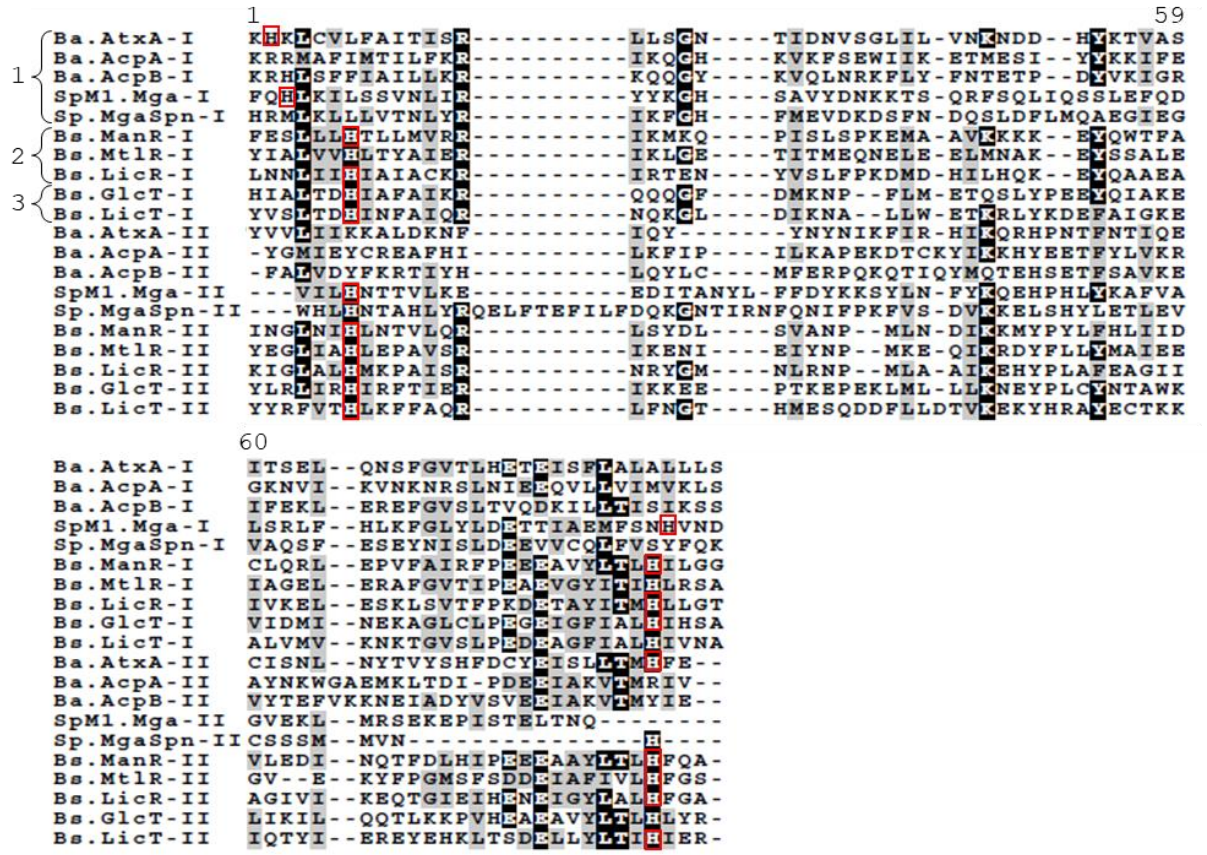

Figure 7-1. Alignment of PTS Regulation Domains. Modified from Stulke et al, 1998. "I" denotes PRD1, the PRD proximal to the N-terminus and "II" denotes PRD2, proximal to the C-terminus. Group "1" are PCVRs in Gram-positive organisms; group "2" are PRD-containing transcriptional activators; group "3" are PRD-containing transcriptional antiterminators. Highly conserved sequences are highlighted in black. Residues with similarity are highlighted in gray. Red box indicates evidence of phosphorylation at the indicated histidine residue.

7.4 Transcriptional control of *atxA* by the PTS and its importance during infection.

The overall model by which the PTS affects transcription in bacteria includes many aspects of HPr function. These activities include (1) HPr-mediated phosphotransfer to PRD-containing transcriptional regulators, (2) interaction of HPrSer46P with CcpA, and, in the case of *B. subtilis*, (3) interaction of HPrHis15P with YesS, a transcriptional activator of pectin/rhamnogalacturonan utilization genes (Poncet *et al.*, 2009b). My results suggest that regulation of *atxA* transcription is achieved through control of an unidentified upstream regulator that is controlled by HPr and EI to affect transcription from the primary promoter of *atxA*. The *B. anthracis* genome does not indicate the presence of a YesS homologue and we have not been successful in identifying another PRD-containing regulator that affects *atxA* transcription. Two putative PRD-containing regulators have been identified in the genome, GBAA_0790 and GBAA_5437. In the future genetic deletions will be tested using the P*atxA-lacZ* reporter strain to determine if either of these putative PRD-containing regulators affects *atxA* transcription and could be the unidentified upstream regulator.

Interestingly a report by Chiang and coworkers (2011) showed CcpA elevated *atxA* transcript levels two-fold in response to the presence of glucose. My data did not reveal a significant difference in expression of the AtxA reporter P*atxA-lacZ* between the parent and *ccpA*-null strain. It is possible that the conflicting data are due to strain differences or assay sensitivity. We note that CcpA control of the close *atxA* homologue *mga* in Group A *Streptococcus* has been reported, but there are many differences in regulation of *mga* and *atxA* transcription. For

example, *mga* is autogenously regulated (Almengor *et al.*, 2007b), while *atxA* is not subject to such control, as indicted by evidence of transcriptional activity from the P*atxA*-*lacZ* reporter in the *atxA*-null mutant (Fig 4-1).

Control of PCVRs by the PTS extends the influence of this sugar import system, such that in addition to regulating bacterial physiology, the PTS can also affect virulence gene expression in infected hosts. In this study, I found that the PTS-null mutant is attenuated for virulence and virulence was restored when *atxA* transcription was under control of a non-PTS responsive promoter.

Interestingly, the data showed that placement of *atxA* under control of a different promoter results in attenuation for virulence relative to the parent ANR-1. These results are not entirely unexpected. In *Listeria monocytogenes* and *Yersinia pestis* altering virulence determinants such that they are constitutively active, attenuates virulence to different degrees (Mitchell *et al.*, 2017, Krypotou *et al.*, 2019). For *B. anthracis*, the attenuation of virulence does correlate with bacterial load in various tissues. In fact, strains expressing *atxA* from the non-native promoter showed an increase in CFU per gram of infected organs relative to ANR-1-infected mice. The attenuation of the strains expressing *atxA* constitutively intimates a more complex process leading to death of the host rather than simply a change in dissemination and/or proliferation.

7.5 Branched chain amino acids as a source of regulation for AtxA activity.

The observation that AtxA is not affected by carbohydrate availability and that the *B. cereus* group is predicted to have a decreased capacity in carbohydrate utilization and an increased capacity for protein/peptide utilization led me to question whether amino acids affect AtxA phosphorylation and activity. AtxA strongly represses the transcription of predicted BCAA transporters and biosynthesis operons and thus I started my exploration of the relationship of AtxA and amino acids with BCAAs. My preliminary experiments assessing AtxA activity at the P*lef-lacZ* reporter demonstrate an increase in AtxA activity with increasing concentrations of BCAAs in the medium. Supplementation with single BCAAs did not elicit an increase in AtxA activity, suggesting the overall intracellular pool of BCAAs influences AtxA. CodY affects virulence factor production in a number of pathogenic bacteria, however, in most cases CodY directly impacts gene transcription. In the case of CodY and virulence factor production in *B. anthracis*, CodY appears to affect AtxA stability (van Schaik *et al.*, 2009). An important follow up experiment will be to monitor AtxA activity in a *codY*-null mutant grown in varying concentrations of BCAAs.

Further studies of BCAA and AtxA activity should be performed, including *in vitro* studies using bovine blood. When AtxA is active toxin is produced to suppress the host-immune response, allowing cells to freely metabolize and replicate in the host. *B. anthracis* produces proteases to free host-derived BCAAs for import into cells, rather than expending the energy to synthesize BCAAs in the cell. In congruence with this idea ABC transporters and two BCAA transporters were expressed during growth in blood (Carlson *et al.*, 2015). It's interesting to note that two of the six predicted BCAA BrnQ transporters are also highly repressed by AtxA during

grown in R medium (Raynor *et al.*, 2018). BcaP is a non-homologous BCAA transporter for many Gram-positive bacteria, also repressed by AtxA. The functionality of the six predicted BrnQ and single BcaP proteins have not yet been established. The possibility remains that while AtxA suppresses two *brnQ* genes and *bcaP*, four other predicted transporters are transcribed. An important follow up study will be to test the predicted transporters for functionality as transporters *in vivo*. The possibility exists that the predicted transporters have roles as signal receptors and transmitters and don't actually transport BCAAs into the cell, which would be interesting, as well.

7.6 Improvements to the design and optimization of P*lef-GFP* and Biolog PM assay

The observation that AtxA activity is affected by BCAAs does not preclude the involvement of other peptide- or amino acid- responsive systems as potential regulators of AtxA activity. It is therefore important to assess AtxA activity in the presence of multiple nitrogen sources. The phenotype microarray plates from Biolog present a good option for screening multiple media efficiently. In this work I tried to optimize the conditions under which a P*lef-GFP* tag would provide an easy *in vivo* read out for AtxA activity that wouldn't involve manipulation of the 96-well plates after growth. Using the knowledge that BCAAs combined affect AtxA activity I would add all three BCAAs to one of the 96-well plates and use as a positive control in the comparison of plates grown with wild-type AtxA and H199A- the phosphovariant that cannot be activated via phosphorylation at H199.

To improve the Biolog assay, a fluorescent protein with a distinct emission spectrum from GFP could be used to normalize cell density and growth rate. This would be advantageous over the current method of normalization using the OD_{600} because of the clumping phenotype observed for *B. anthracis* cultures.

7.7 Further studies

A number of follow up studies should be performed to better elucidate the mechanism by which the PTS affects *atxA* transcription and to identify the system responsible for AtxA phosphorylation. Further characterization of the relationship between AtxA and BCAAs would be beneficial, as well. Studies to better understand the mechanism by which the PTS exerts its control on *atxA* transcription would be useful in potentially developing therapies for anthrax toxemia. Knowing what sugars affect *atxA* transcription, we could use sugar analogs to occupy the receptors and prevent flux of phosphate through the system and potentially prevent activation of gene transcription. Homologues of PTS proteins have not been identified in the human genome and therefore present as potential target for antimicrobial agents.

To identify HPr-interacting proteins as potential mediators of *atxA* transcription, and to further the field's understanding of the PTS in *B. anthracis*, I propose using genome-wide yeast two-hybrid of *B. anthracis* genome to identify HPr-interacting partners. The yeast two-hybrid screen can be performed with two different set ups, HPr expressed alone, or with HPr and EI coexpressed to ensure EI phosphorylation of HPr, as was described in the experiments that led to the identification of YesS in *B. subtilis* (Poncet et al., 2009b). The yeast two-hybrid system can

also be used with AtxA to identify interacting partners and potentially the kinase responsible for phosphorylating AtxA.

Improvements can be made to the phostag experiments to try and detect phosphorylated AtxA. The protein loading buffer should have a higher pH and resemble the loading buffer used for pHis antibody analyses which has been optimized for detection of proteins phosphorylated at histidine residues. A single gel should be run in an electrophoresis box, as opposed to running two gels in the same box, to reduce resistance and heating, and the gel should be run at a very low voltage in the cold-room overnight. These improvements may help maintain the integrity of the very labile phosphohistidine bond to enable the interaction with the Phos-tag and allow for retardation of the phosphorylated form of the protein.

Following up on the observation that BCAAs affect AtxA activity, a *codY*-null mutant should be tested to determine if the BCAA effect is mediated by CodY. If it is not CodY-dependent it would be interesting to do *in vitro* DNA binding assays with AtxA in the presence of BCAAs to see if BCAAs increase AtxA binding to DNA. AtxA is not predicted to have a BCAA binding domain as seen in CodY however, the possibility for a new mechanism of BCAA-mediated increase in transcription factor activity exists. AtxA binds DNA in i*n vitro* DNA-binding assays non-specifically, it will be interesting to see if adding BCAAs to the AtxA DNA mixtures to see if a change in DNA binding is observed.

7.8 Concluding remarks

In Figure 7-2 I present the updated model for AtxA regulation in *B. anthracis* based on the work I have presented in this dissertation. Through an unknown mechanism, HPr in its His14 - phosphorylated form, phosphorylates an unknown transcriptional regulator, presumably a PRD-containing regulator, to affect *atxA* transcription from the primary promoter, P1. My work has demonstrated that the PTS in *B. anthracis* does not affect AtxA activity, and is not likely the system responsible for phosphorylation *in vivo*. The kinase responsible for AtxA phosphorylation has not yet been identified, but the PM Biolog-based P*lef-GFP* assay developed aims to identify substrates that affect AtxA phosphorylation, and will lead to future investigation into potential kinases.

I have shown that branched chain amino acids elicit an increase in AtxA activity *in vivo*. Recent data has demonstrated AtxA represses BCAA transporters and biosynthesis operons. Future work determining the relationship of the BCAA-related genes, intracellular levels of BCAAs and AtxA activity will be of importance to understand the mechanism of control. AtxA activity is increased in the presence of BCAAs, AtxA suppresses the transcription of genes responsible for synthesizing more BCAAs and for transporting them, thereby modulating BCAA levels in the cell to modulate AtxA activity.

Overall the work in this dissertation has led to important findings in the field and has highlighted the need for further investigation into metabolism and virulence in *B. anthracis*. The

knowledge gained serves to improve the general knowledge of basic biology of this bacterium, as well as specific knowledge to potentially aid in the development of anti-virulence factor drugs.

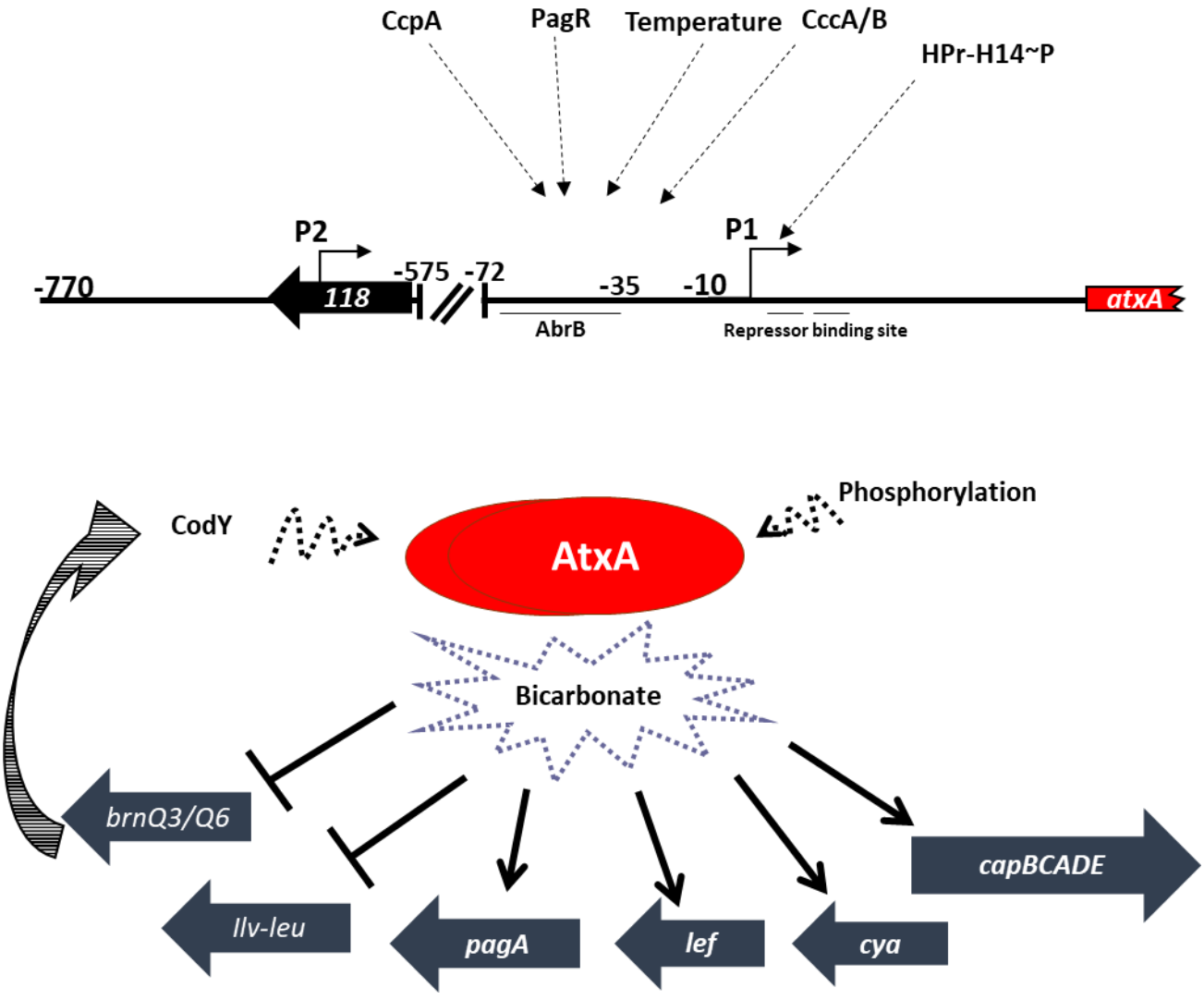

Figure 7-2. Updated model for regulation of AtxA in *B. anthracis.*
An updated model of the multiple levels of regulation of AtxA. Many factors have been shown to affect *atxA* transcription and post-translational stability and activity, but the mechanisms have not yet been defined (demonstrated by dotted arrows).

References

1. Almengor, A.C., Kinkel, T.L., Day, S.J., and McIver, K.S. (2007) The catabolite control protein CcpA binds to Pmga and influences expression of the virulence regulator Mga in the Group A *Streptococcus*. *Journal of bacteriology* **189**: 8405-8416.
2. Barbieri, C.M., and Stock, A.M. (2008) Universally applicable methods for monitoring response regulator aspartate phosphorylation both *in vitro* and *in vivo* using Phos-tag-based reagents. *Anal Biochem* **376**: 73-82.
3. Baum, M., Watad, M., Smith, S.N., Alteri, C.J., Gordon, N., Rosenshine, I., Mobley, H.L., and Amster-Choder, O. (2014) PafR, a novel transcription regulator, is important for pathogenesis in uropathogenic *Escherichia coli*. *Infection and immunity* **82**: 4241-4252.
4. Bertani, G. (1951) Studies on lysogenesis. I. The mode of phage liberation by lysogenic *Escherichia coli*. *Journal of bacteriology* **62**: 293-300.
5. Bongiorni, C., Fukushima, T., Wilson, A.C., Chiang, C., Mansilla, M.C., Hoch, J.A., and Perego, M. (2008) Dual promoters control expression of the *Bacillus anthracis* virulence factor AtxA. *Journal of bacteriology* **190**: 6483-6492.
6. Bourgogne, A., Drysdale, M., Hilsenbeck, S.G., Peterson, S.N., and Koehler, T.M. (2003) Global effects of virulence gene regulators in a *Bacillus anthracis* strain with both virulence plasmids. *Infection and immunity* **71**: 2736-2743.
7. Brezillon, C., Haustant, M., Dupke, S., Corre, J.P., Lander, A., Franz, T., Monot, M., Couture-Tosi, E., Jouvion, G., Leendertz, F.H., Grunow, R., Mock, M.E., Klee, S.R., and Goossens, P.L. (2015)

Capsules, toxins and AtxA as virulence factors of emerging *Bacillus cereus* biovar anthracis. *PLoS Negl Trop Dis* **9**: e0003455.

8. Britton, R.A., Eichenberger, P., Gonzalez-Pastor, J.E., Fawcett, P., Monson, R., Losick, R., and Grossman, A.D. (2002) Genome-Wide Analysis of the Stationary-Phase Sigma Factor (Sigma-H) Regulon of *Bacillus subtilis*. *J. Bacteriol.* **184**: 4881-4890.
9. Carlson, P.E., Jr., Bourgis, A.E., Hagan, A.K., and Hanna, P.C. (2015) Global gene expression by *Bacillus anthracis* during growth in mammalian blood. *Pathog Dis* **73**: ftv061.
10. Chiang, C., Bongiorni, C., and Perego, M. (2011) Glucose-dependent activation of *Bacillus anthracis* toxin gene expression and virulence requires the carbon catabolite protein CcpA. *Journal of bacteriology* **193**: 52-62.
11. Crutz, A.M., Steinmetz, M., Aymerich, S., Richter, R., and Le Coq, D. (1990) Induction of levansucrase in *Bacillus subtilis*: an antitermination mechanism negatively controlled by the phosphotransferase system. *Journal of bacteriology* **172**: 1043-1050.
12. Dai, Z., and Koehler, T.M. (1997) Regulation of anthrax toxin activator gene (*atxA*) expression in *Bacillus anthracis*: temperature, not CO2/bicarbonate, affects AtxA synthesis. *Infection and immunity* **65**: 2576-2582.
13. Dai, Z., Sirard, J.C., Mock, M., and Koehler, T.M. (1995) The *atxA* gene product activates transcription of the anthrax toxin genes and is essential for virulence. *Molecular microbiology* **16**: 1171-1181.
14. Dale, J.L., Raynor, M.J., Dwivedi, P., and Koehler, T.M. (2012) *cis*-Acting elements that control expression of the master virulence regulatory gene *atxA* in *Bacillus anthracis*. *Journal of bacteriology* **194**: 4069-4079.

15. Dale, J.L., Raynor, M.J., Ty, M.C., Hadjifrangiskou, M., and Koehler, T.M. (2018) A Dual Role for the *Bacillus anthracis* Master Virulence Regulator AtxA: Control of Sporulation and Anthrax Toxin Production. *Front Microbiol* **9**: 482.
16. Deutscher, J., Ake, F.M., Derkaoui, M., Zebre, A.C., Cao, T.N., Bouraoui, H., Kentache, T., Mokhtari, A., Milohanic, E., and Joyet, P. (2014) The bacterial phosphoenolpyruvate:carbohydrate phosphotransferase system: regulation by protein phosphorylation and phosphorylation-dependent protein-protein interactions. *Microbiology and molecular biology reviews : MMBR* **78**: 231-256.
17. Deutscher, J., Francke, C., and Postma, P.W. (2006) How phosphotransferase system-related protein phosphorylation regulates carbohydrate metabolism in bacteria. *Microbiology and Molecular Biology Reviews: MMBR* **70**: 939-1031.
18. Deutscher, J., Kuster, E., Bergstedt, U., Charrier, V., and Hillen, W. (1995) Protein kinase-dependent HPr/CcpA interaction links glycolytic activity to carbon catabolite repression in Gram-positive bacteria. *Molecular microbiology* **15**: 1049-1053.
19. Dineen, S.S., Villapakkam, A.C., Nordman, J.T., and Sonenshein, A.L. (2007) Repression of *Clostridium difficile* toxin gene expression by CodY. *Molecular microbiology* **66**: 206-219.
20. Dixon, T.C., Meselson, M., Guillemin, J., and Hanna, P.C. (1999) Anthrax. *N Engl J Med* **341**: 815-826.
21. Ezzell, J.W., and Welkos, S.L. (1999) The capsule of *Bacillus anthracis*, a review. *Journal of applied microbiology* **87**: 250.
22. Fouet, A., and Mock, M. (1996) Differential influence of the two *Bacillus anthracis* plasmids on regulation of virulence gene expression. *Infection and immunity* **64**: 4928-4932.

23. Friebe, S., van der Goot, F.G., and Burgi, J. (2016) The Ins and Outs of Anthrax Toxin. *Toxins (Basel)* **8**.
24. Galinier, A., and Deutscher, J. (2017) Sophisticated regulation of transcriptional factors by the bacterial phosphoenolpyruvate: sugar phosphotransferase system. *J Mol Biol* **429**: 773-789.
25. Gao, P., Pinkston, K.L., Bourgogne, A., Cruz, M.R., Garsin, D.A., Murray, B.E., and Harvey, B.R. (2013) Library screen identifies *Enterococcus faecalis* CcpA, the catabolite control protein A, as an effector of Ace, a collagen adhesion protein linked to virulence. *Journal of bacteriology* **195**: 4761-4768.
26. Guidi-Rontani, C., Weber-Levy, M., Labruyere, E., and Mock, M. (1999) Germination of *Bacillus anthracis* spores within alveolar macrophages. *Molecular microbiology* **31**: 9-17.
27. Hadjifrangiskou, M., Chen, Y., and Koehler, T.M. (2007) The alternative sigma factor sigmaH is required for toxin gene expression by *Bacillus anthracis*. *Journal of bacteriology* **189**: 1874-1883.
28. Hadjifrangiskou, M., and Koehler, T.M. (2008) Intrinsic curvature associated with the coordinately regulated anthrax toxin gene promoters. *Microbiology (Reading, England)* **154**: 2501-2512.
29. Haines, B.W., Klein, F., and Lincoln, R.E. (1965) Quantitative Assay for Crude Anthrax Toxins. *Journal of bacteriology* **89**: 74-83.
30. Hammerstrom, T. (2012). Functional Characterization of AtxA, the *Bacillus anthracis* Virulence Regulator. Ph.D. Univeristy of Texas Graduate School of Biomedical Sciences.
31. Hammerstrom, T.G., Horton, L.B., Swick, M.C., Joachimiak, A., Osipiuk, J., and Koehler, T.M. (2015) Crystal structure of *Bacillus anthracis* virulence regulator AtxA and effects of phosphorylated histidines on multimerization and activity. *Molecular microbiology* **95**: 426-441.

32. Hammerstrom, T.G., Roh, J.H., Nikonowicz, E.P., and Koehler, T.M. (2011) *Bacillus anthracis* virulence regulator AtxA: oligomeric state, function and CO(2) -signalling. *Molecular microbiology* **82**: 634-647.

33. Han, C.S., Xie, G., Challacombe, J.F., Altherr, M.R., Bhotika, S.S., Brown, N., Bruce, D., Campbell, C.S., Campbell, M.L., Chen, J., Chertkov, O., Cleland, C., Dimitrijevic, M., Doggett, N.A., Fawcett, J.J., Glavina, T., Goodwin, L.A., Green, L.D., Hill, K.K., Hitchcock, P., Jackson, P.J., Keim, P., Kewalramani, A.R., Longmire, J., Lucas, S., Malfatti, S., McMurry, K., Meincke, L.J., Misra, M., Moseman, B.L., Mundt, M., Munk, A.C., Okinaka, R.T., Parson-Quintana, B., Reilly, L.P., Richardson, P., Robinson, D.L., Rubin, E., Saunders, E., Tapia, R., Tesmer, J.G., Thayer, N., Thompson, L.S., Tice, H., Ticknor, L.O., Wills, P.L., Brettin, T.S., and Gilna, P. (2006) Pathogenomic sequence analysis of *Bacillus cereus* and *Bacillus thuringiensis* isolates closely related to *Bacillus anthracis*. *Journal of bacteriology* **188**: 3382-3390.

34. Hoffmaster, A.R., and Koehler, T.M. (1999) Control of virulence gene expression in *Bacillus anthracis*. *Journal of applied microbiology* **87**: 279-281.

35. Hoffmaster, A.R., Ravel, J., Rasko, D.A., Chapman, G.D., Chute, M.D., Marston, C.K., De, B.K., Sacchi, C.T., Fitzgerald, C., Mayer, L.W., Maiden, M.C., Priest, F.G., Barker, M., Jiang, L., Cer, R.Z., Rilstone, J., Peterson, S.N., Weyant, R.S., Galloway, D.R., Read, T.D., Popovic, T., and Fraser, C.M. (2004) Identification of anthrax toxin genes in a *Bacillus cereus* associated with an illness resembling inhalation anthrax. *Proceedings of the National Academy of Sciences of the United States of America* **101**: 8449-8454.

36. Hondorp, E.R., Hou, S.C., Hause, L.L., Gera, K., Lee, C.E., and McIver, K.S. (2013) PTS phosphorylation of Mga modulates regulon expression and virulence in the group A *Streptococus. Molecular microbiology* **88**: 1176-1193.

37. Horton, R.M., Hunt, H.D., Ho, S.N., Pullen, J.K., and Pease, L.R. (1989) Engineering hybrid genes without the use of restriction enzymes: gene splicing by overlap extension. *Gene* **77**: 61-68.
38. Ivanova, N., Sorokin, A., Anderson, I., Galleron, N., Candelon, B., Kapatral, V., Bhattacharyya, A., Reznik, G., Mikhailova, N., Lapidus, A., Chu, L., Mazur, M., Goltsman, E., Larsen, N., D'Souza, M., Walunas, T., Grechkin, Y., Pusch, G., Haselkorn, R., Fonstein, M., Ehrlich, S.D., Overbeek, R., and Kyrpides, N. (2003) Genome sequence of *Bacillus cereus* and comparative analysis with *Bacillus anthracis*. *Nature* **423**: 87-91.
39. Iyer, R., Baliga, N.S., and Camilli, A. (2005) Catabolite control protein A (CcpA) contributes to virulence and regulation of sugar metabolism in *Streptococcus pneumoniae*. *Journal of bacteriology* **187**: 8340-8349.
40. Jelacic, T.M., Chabot, D.J., Bozue, J.A., Tobery, S.A., West, M.W., Moody, K., Yang, D., Oppenheim, J.J., and Friedlander, A.M. (2014) Exposure to *Bacillus anthracis* capsule results in suppression of human monocyte-derived dendritic cells. *Infection and immunity* **82**: 3405-3416.
41. Joyet, P., Derkaoui, M., Bouraoui, H., and Deutscher, J. (2015) PTS-Mediated Regulation of the Transcription Activator MtlR from Different Species: Surprising Differences despite Strong Sequence Conservation. *J Mol Microbiol Biotechnol* **25**: 94-105.
42. Joyet, P., Derkaoui, M., Poncet, S., and Deutscher, J. (2010) Control of *Bacillus subtilis mtl* operon expression by complex phosphorylation-dependent regulation of the transcriptional activator MtlR. *Molecular microbiology* **76**: 1279-1294.
43. Kaiser, J.C., and Heinrichs, D.E. (2018) Branching Out: Alterations in Bacterial Physiology and Virulence Due to Branched-Chain Amino Acid Deprivation. *MBio* **9**.

44. Kaiser, J.C., Omer, S., Sheldon, J.R., Welch, I., and Heinrichs, D.E. (2015) Role of BrnQ1 and BrnQ2 in branched-chain amino acid transport and virulence in Staphylococcus aureus. *Infection and immunity* **83**: 1019-1029.

45. Kaiser, J.C., Sen, S., Sinha, A., Wilkinson, B.J., and Heinrichs, D.E. (2016) The role of two branched-chain amino acid transporters in *Staphylococcus aureus* growth, membrane fatty acid composition and virulence. *Molecular microbiology* **102**: 850-864.

46. Kaspar, R.L., and Robertson, D.L. (1987) Purification and physical analysis of *Bacillus anthracis* plasmids pXO1 and pXO2. *Biochem Biophys Res Commun* **149**: 362-368.

47. Kee, J.M., Oslund, R.C., Perlman, D.H., and Muir, T.W. (2013) A pan-specific antibody for direct detection of protein histidine phosphorylation. *Nat Chem Biol* **9**: 416-421.

48. Kinoshita, E., Kinoshita-Kikuta, E., Takiyama, K., and Koike, T. (2006) Phosphate-binding tag, a new tool to visualize phosphorylated proteins. *Mol Cell Proteomics* **5**: 749-757.

49. Klee, S.R., Ozel, M., Appel, B., Boesch, C., Ellerbrok, H., Jacob, D., Holland, G., Leendertz, F.H., Pauli, G., Grunow, R., and Nattermann, H. (2006) Characterization of *Bacillus anthracis*-like bacteria isolated from wild great apes from Cote d'Ivoire and Cameroon. *Journal of bacteriology* **188**: 5333-5344.

50. Koehler, T.M. (2002) *Bacillus anthracis* genetics and virulence gene regulation. *Current Topics in Microbiology and Immunology* **271**: 143-164.

51. Koehler, T.M. (2009) *Bacillus anthracis* physiology and genetics. *Mol Aspects Med* **30**: 386-396.

52. Krypotou, E., Scortti, M., Grundstrom, C., Oelker, M., Luisi, B.F., Sauer-Eriksson, A.E., and Vazquez-Boland, J. (2019) Control of bacterial virulence through the peptide signature of the habitat. *Cell Rep* **26**: 1815-1827 e1815.

53. Levy, H., Glinert, I., Weiss, S., Sittner, A., Schlomovitz, J., Altboum, Z., and Kobiler, D. (2014) Toxin-independent virulence of *Bacillus anthracis* in rabbits. *PLoS One* **9**: e84947.

54. Lyons, C.R., Lovchik, J., Hutt, J., Lipscomb, M.F., Wang, E., Heninger, S., Berliba, L., and Garrison, K. (2004) Murine model of pulmonary anthrax: kinetics of dissemination, histopathology, and mouse strain susceptibility. *Infection and immunity* **72**: 4801-4809.

55. Majerczyk, C.D., Sadykov, M.R., Luong, T.T., Lee, C., Somerville, G.A., and Sonenshein, A.L. (2008) *Staphylococcus aureus* CodY negatively regulates virulence gene expression. *Journal of bacteriology* **190**: 2257-2265.

56. Makino, S., Sasakawa, C., Uchida, I., Terakado, N., and Yoshikawa, M. (1988) Cloning and CO2-dependent expression of the genetic region for encapsulation from *Bacillus anthracis*. *Molecular microbiology* **2**: 371-376.

57. Marrero, R., and Welkos, S.L. (1995) The transformation frequency of plasmids into *Bacillus anthracis* is affected by adenine methylation. *Gene* **152**: 75-78.

58. Martin-Verstraete, I., Charrier, V., Stulke, J., Galinier, A., Erni, B., Rapoport, G., and Deutscher, J. (1998) Antagonistic effects of dual PTS-catalysed phosphorylation on the *Bacillus subtilis* transcriptional activator LevR. *Molecular microbiology* **28**: 293-303.

59. Miller, J.H. (1972) Experiments in molecular genetics. *Cold Spring Harbor Laboratory Press*: 352-355.

60. Mitchell, A., Tam, C., Elli, D., Charlton, T., Osei-Owusu, P., Fazlollahi, F., Faull, K.F., and Schneewind, O. (2017) Glutathionylation of *Yersinia pestis* LcrV and Its Effects on Plague Pathogenesis. *MBio* **8**.

61. Pflughoeft, K.J., Sumby, P., and Koehler, T.M. (2011) *Bacillus anthracis sin* Locus and Regulation of Secreted Proteases. *J. Bacteriol.* **193**: 631-639.

62. Poncet, S., Milohanic, E., Maze, A., Abdallah, J.N., Ake, F., Larribe, M., Deghmane, A.E., Taha, M.K., Dozot, M., De Bolle, X., Letesson, J.J., and Deutscher, J. (2009a) Correlations between carbon metabolism and virulence in bacteria. *Contributions to microbiology* **16**: 88-102.
63. Poncet, S., Soret, M., Mervelet, P., Deutscher, J., and Noirot, P. (2009b) Transcriptional activator YesS is stimulated by histidine-phosphorylated HPr of the *Bacillus subtilis* phosphotransferase system. *The Journal of biological chemistry* **284**: 28188-28197.
64. Raevuori, M. (1976) Effect of Sorbic Acid and Potassium Sorbate on Growth of *Bacillus cereus* and *Bacillus subtilis* in Rice Filling of Karelian Pasty *European Journal Applied Microbiology* **2**: 205-213.
65. Raynor, M.J., Roh, J.H., Widen, S.G., Wood, T.G., and Koehler, T.M. (2018) Regulons and protein-protein interactions of PRD-containing *Bacillus anthracis* virulence regulators reveal overlapping but distinct functions. *Molecular microbiology*.
66. Read, T.D., Peterson, S.N., Tourasse, N., Baillie, L.W., Paulsen, I.T., Nelson, K.E., Tettelin, H., Fouts, D.E., Eisen, J.A., Gill, S.R., Holtzapple, E.K., Okstad, O.A., Helgason, E., Rilstone, J., Wu, M., Kolonay, J.F., Beanan, M.J., Dodson, R.J., Brinkac, L.M., Gwinn, M., DeBoy, R.T., Madpu, R., Daugherty, S.C., Durkin, A.S., Haft, D.H., Nelson, W.C., Peterson, J.D., Pop, M., Khouri, H.M., Radune, D., Benton, J.L., Mahamoud, Y., Jiang, L., Hance, I.R., Weidman, J.F., Berry, K.J., Plaut, R.D., Wolf, A.M., Watkins, K.L., Nierman, W.C., Hazen, A., Cline, R., Redmond, C., Thwaite, J.E., White, O., Salzberg, S.L., Thomason, B., Friedlander, A.M., Koehler, T.M., Hanna, P.C., Kolsto, A.B., and Fraser, C.M. (2003) The genome sequence of *Bacillus anthracis* Ames and comparison to closely related bacteria. *Nature* **423**: 81-86.
67. Rediers, H., Rainey, P.B., Vanderleyden, J., and De Mot, R. (2005) Unraveling the secret lives of bacteria: use of in vivo expression technology and differential fluorescence induction promoter

traps as tools for exploring niche-specific gene expression. *Microbiology and molecular biology reviews : MMBR* **69**: 217-261.

68. Richardson, A.R., Somerville, G.A., and Sonenshein, A.L. (2015) Regulating the intersection of metabolism and pathogenesis in Gram-positive bacteria. *Microbiol Spectr* **3**.
69. Ristroph, J.D., and Ivins, B.E. (1983) Elaboration of *Bacillus anthracis* antigens in a new, defined culture medium. *Infection and immunity* **39**: 483-486.
70. Saile, E., and Koehler, T.M. (2002) Control of anthrax toxin gene expression by the transition state regulator abrB. *Journal of bacteriology* **184**: 370-380.
71. Saile, E., and Koehler, T.M. (2006) *Bacillus anthracis* multiplication, persistence, and genetic exchange in the rhizosphere of grass plants. *Appl Environ Microbiol* **72**: 3168-3174.
72. Scarff, J.M., Raynor, M.J., Seldina, Y.I., Ventura, C.L., Koehler, T.M., and O'Brien, A.D. (2016) The roles of AtxA orthologs in virulence of anthrax-like *Bacillus cereus* G9241. *Molecular microbiology* **102**: 545-561.
73. Schmalisch, M.H., Bachem, S., and Stulke, J. (2003) Control of the *Bacillus subtilis* antiterminator protein GlcT by phosphorylation. Elucidation of the phosphorylation chain leading to inactivation of GlcT. *The Journal of biological chemistry* **278**: 51108-51115.
74. Schuch, R., Pelzek, A.J., Kan, S., and Fischetti, V.A. (2010) Prevalence of *Bacillus anthracis*-like organisms and bacteriophages in the intestinal tract of the earthworm Eisenia fetida. *Appl Environ Microbiol* **76**: 2286-2294.
75. Shivers, R.P., and Sonenshein, A.L. (2004) Activation of the *Bacillus subtilis* global regulator CodY by direct interaction with branched-chain amino acids. *Molecular microbiology* **53**: 599-611.

76. Solano-Collado, V., Lurz, R., Espinosa, M., and Bravo, A. (2013) The pneumococcal MgaSpn virulence transcriptional regulator generates multimeric complexes on linear double-stranded DNA. *Nucleic acids research* **41**: 6975-6991.

77. Somarajan, S.R., Roh, J.H., Singh, K.V., Weinstock, G.M., and Murray, B.E. (2014) CcpA is important for growth and virulence of *Enterococcus faecium*. *Infection and immunity* **82**: 3580-3587.

78. Stenz, L., Francois, P., Whiteson, K., Wolz, C., Linder, P., and Schrenzel, J. (2011) The CodY pleiotropic repressor controls virulence in Gram-positive pathogens. *FEMS Immunol Med Microbiol* **62**: 123-139.

79. Strauch, M.A., Ballar, P., Rowshan, A.J., and Zoller, K.L. (2005) The DNA-binding specificity of the *Bacillus anthracis* AbrB protein. *Microbiology* **151**: 1751-1759.

80. Stulke, J., Arnaud, M., Rapoport, G., and Martin-Verstraete, I. (1998) PRD--a protein domain involved in PTS-dependent induction and carbon catabolite repression of catabolic operons in bacteria. *Molecular microbiology* **28**: 865-874.

81. Stulke, J., Martin-Verstraete, I., Zagorec, M., Rose, M., Klier, A., and Rapoport, G. (1997) Induction of the *Bacillus subtilis ptsGHI* operon by glucose is controlled by a novel antiterminator, GlcT. *Molecular microbiology* **25**: 65-78.

82. Tao, L., Chattoraj, P., and Biswas, I. (2012) CtsR regulation in *mcsAB*-deficient Gram-positive bacteria. *Journal of bacteriology* **194**: 1361-1368.

83. Thorne, C.B., and Belton, F.C. (1957) An agar-diffusion method for titrating *Bacillus anthracis* immunizing antigen and its application to a study of antigen production. *Journal of General Microbiology* **17**: 505-516.

84. Tippetts, M.T., and Robertson, D.L. (1988) Molecular cloning and expression of the *Bacillus anthracis* edema factor toxin gene: a calmodulin-dependent adenylate cyclase. *Journal of bacteriology* **170**: 2263-2266.

85. Tortosa, P., Declerck, N., Dutartre, H., Lindner, C., Deutscher, J., and Le Coq, D. (2001) Sites of positive and negative regulation in the *Bacillus subtilis* antiterminators LicT and SacY. *Molecular microbiology* **41**: 1381-1393.

86. Trevino, J., Liu, Z., Cao, T.N., Ramirez-Pena, E., and Sumby, P. (2013) RivR is a negative regulator of virulence factor expression in Group A *Streptococcus*. *Infection and immunity* **81**: 364-372.

87. Tsvetanova, B., Wilson, A.C., Bongiorni, C., Chiang, C., Hoch, J.A., and Perego, M. (2007) Opposing effects of histidine phosphorylation regulate the AtxA virulence transcription factor in *Bacillus anthracis*. *Molecular microbiology* **63**: 644-655.

88. Uchida, I., Makino, S., Sekizaki, T., and Terakado, N. (1997) Cross-talk to the genes for *Bacillus anthracis* capsule synthesis by atxA, the gene encoding the trans-activator of anthrax toxin synthesis. *Molecular microbiology* **23**: 1229-1240.

89. van Schaik, W., Chateau, A., Dillies, M.A., Coppee, J.Y., Sonenshein, A.L., and Fouet, A. (2009) The global regulator CodY regulates toxin gene expression in *Bacillus anthracis* and is required for full virulence. *Infection and immunity* **77**: 4437-4445.

90. Welkos, S., Little, S., Friedlander, A., Fritz, D., and Fellows, P. (2001) The role of antibodies to *Bacillus anthracis* and anthrax toxin components in inhibiting the early stages of infection by anthrax spores. *Microbiology* **147**: 1677-1685.

91. Wilson, A.C., Hoch, J.A., and Perego, M. (2009) Two small c-type cytochromes affect virulence gene expression in *Bacillus anthracis*. *Molecular microbiology* **72**: 109-123.

Vita

Naomi Bier-Reizes was born in Bnei Braq, Israel to Rabbi Moshe and Bluma Bier. Naomi took an unconventional path in her education and left high school at the age of 15. After receiving a general education diploma from the state of Maryland she enrolled in Baltimore City Community College in 2005. She later transferred to University of Maryland Baltimore County to receive a Bachelors of Science degree in biology in 2011. Starting in May 2012, she enrolled in The University of Texas MD Anderson Cancer Center UTHealth Graduate School of Biomedical Sciences.

Permanent address:

11131 Pembridge Dr

Houston, TX 77071